DOCTOR OF PHILOSOPHY

Developing a simulation-based approach to collision risk of tidal energy converters and marine wildlife

Horne, Nicholas

Award date:
2021

Awarding institution:
Queen's University Belfast

Developing a simulation-based approach to Collision Risk of Tidal Energy Converters and Marine Wildlife

Nicholas Horne

BSc (University of Portsmouth), MSc (University of Aberdeen)

A thesis submitted in fulfilment of the requirements for the degree of Doctor of Philosophy

School of Natural and Built Environment

The Queen's University of Belfast

June 2021

Abstract

Tidal energy has the potential to form an important part of renewable energy production, helping to reach global targets, such as those outlined in the Paris Agreement. The predictable nature of tides offers a reliable supply of renewable energy, making tidal energy converters (TECs) a desirable source of electrical generation. However, the drive for sustainable development and the legislative protection of species and habitats means that, in most countries, the environmental impacts of TECs must be quantified before consent for an installation is granted. There are several environmental issues raised regarding TECs, however, one major concern is the risk of an animal fatally colliding with the moving parts of a TEC i.e. collision risk. Collision risk was identified as an issue before the first grid-connected TEC was installed in 2008. Now, over 10 years later, it is still a major barrier in the consenting process. To address collision risk, modelling is used to predict the likely number of animals to collide with a TEC in a given time period, and the results from these models are presented to allow informed licencing decisions by regulators. Several collision risk models have been used in previous environmental assessments, however, they all have limitations. Firstly, they cannot estimate risk for novel device designs such as a tidal kite or cross-flow devices. Secondly, they are limited in their ability to incorporate additional information, such as through altering input parameters or post-processing of results. Previously, a simulation-based approach to estimating collision risk was developed for a tidal kite using open-source 3D modelling software. By simulating the 3D shapes of a TEC, an animal, and their movement, the approach allows for all aspects of the model to be controlled and therefore has the potential to be developed to address many different aspects of collision risk modelling.

Here, the development of a simulation-based approach to collision risk was undertaken with the aim of producing robust collision risk estimates between animals and tidal energy convertors. Developments such as (i) producing collision risk probabilities for any device design, (ii) altering various animal parameters, such as angle of approach and different body size, and (iii) extracting the speed of collisions and where they occur on the body of the animal to estimate mortality were undertaken. Also, (iv) streamlining of the model was performed to reduce computational time and (v) results from the simulation-based approach were compared against two collision risk models previously used in environmental impact assessment, reproducing the results of a collision risk assessment.

This work has resulted in the development of collision risk model using a simulation-based approach that can incorporate any type of TEC using the free open-source software Blender. I also demonstrated how variations in input parameters (animal size, speed, angle of approach) can be incorporated into the model with relative ease and how it can be used to post-process results from

the simulations to incorporate additional information on animal behaviour. I provided an example of how mortality estimates can be obtained from the model, based on collision speed and where on the animal the collision occurs. I also highlighted the complexities of collision risk modelling which identified that some relationships between parameters are non-linear. The efficiency of the model was also improved by decreasing the computational time needed for simulations to run. Finally, I demonstrated that the model produces similar results to two previously used collision risk models, the encounter rate and Band model, for a simple scenario when all conditions are matched, which provided reassurance in the validity of the approach. Overall, I have developed a model using a simulation-based approach that can be adapted and expanded to the needs of the user and therefore provides a state-of-the-art tool for producing collision risk estimates.

The work presented in this thesis significantly advances the modelling of collision risk between TECs and animals. The flexibility of the simulation-based approach allows for the best available data to be incorporated to produce robust and transparent collision risk estimates. Ultimately, this collision risk model is a step forward that was needed, as collision risk continues to be a barrier to the growth of the tidal energy industry.

Acknowledgements

First and foremost, I would like to thank Dr Louise Kregting for her unwavering support and guidance. For being able to cut through my ramblings and help me write some sensible science. Also, a huge thanks to Dr Ross Culloch for the huge amount of help you have given me throughout this PhD and your invaluable expertise. I would also like to thank my other supervisors, Prof Ben Wilson, Dr Andrew Dale, and Dr Jon Houghton.

A massive thanks also to Dr Pal Schmitt for his amazing technical, mathematical, and computational skills but also for having the ability to cheer me up simply by moaning about administration. Thanks a million, Dr Paddy Joyce for helping me move to Portaferry and holding my hand through the first few months. To Emma, Manus, Lawrence, Tash, Elin, Neil, Fergal, and the rest of the folk at Portaferry Marine Lab, thank you so much for all the great times, chats, pub quizzes, BBQs, and the like, it is a great place to work, and your company has helped me greatly through the rigors of this PhD.

To my Mum, Dad, and the rest of my family, thanks for the lifelong support. From allowing me, as a 5-year-old, to correct random strangers in Zoo's, to letting me return to live at home in between the many degrees, you have been amazing, and I wouldn't be here without you.

Thank you to my funders, The Bryden Centre, and don't forget, the Bryden Centre project is supported by the European Union's INTERREG VA Programme, managed by the Special EU Programmes Body (SEUPB). Thanks to the support also from Marine Scotland Science for letting me visit, present, and discuss my work.

Finally, I want to thank Connie for keeping me going through these years. You have been there when I have been at my worst and have helped me push through many barriers and hard times. I would not have achieved this (and would not still have a functioning brain) if you had not come into my life. Congratulations, you now get to know me without the stress of a PhD going on – buckle up.

And finally, finally, thank you to Indie. A walk or a game of fetch really did help clear the head when writing made me want to cry, you are a hero!

Contents

Chapter 1: General Introduction

1.1 Drivers of the Tidal Energy Industry

The overwhelming evidence for climate change (IPCC, 2014) has led to global agreements to limit greenhouse gas emissions. One agreement that is driving policy in many countries is the Paris Agreement, which aims to ensure global temperatures do not rise above 1.5^{o}C of pre-industrial levels (McCollum et al., 2018). To achieve this goal a rapid transformation of the energy grid is required to reduce dependency on fossil fuels and increase global renewable energy production (McCollum et al., 2018). Renewable energy production has risen considerably by 440% between 2009 and 2019 (BP, 2020) with industries such as wind and solar making up most of the renewable energy generation (BP, 2020). However, there are untapped marine energy resources, such as tides, that could also be used as part of the energy grid (Borthwick, 2016). The predictable nature of tides offers a reliable supply of renewable energy, making tidal energy converters (TECs) a desirable source of electrical generation (Zhou et al., 2017). There are a range of tidal turbine designs for extracting energy from fast-flowing tides (Fig. 1.1), such as horizontal axis tidal turbines (HATT) (MeyGen, 2014), crossflow turbines (ORPC, 2016), tidal kites (Zambrano, 2016) and vertical axis turbines (GKinetic, 2021).

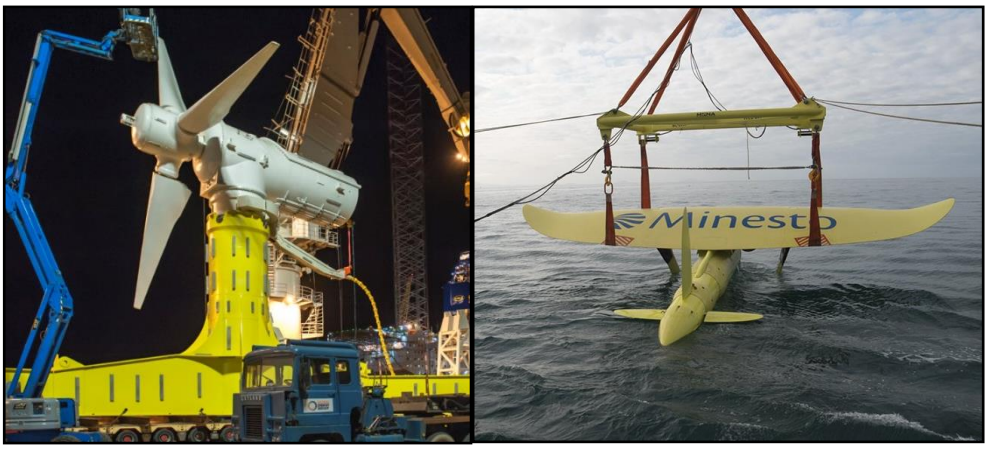

Figure 1.1 Two different tidal energy converters, Simec Atlantis' AR1500 Horizontal axis tidal turbine (left) and Minesto's DG500 Tidal Kite, which operates by 'flying' in a figure-of-eight using the wing and tail rudders seen in the image, this movement drives a turbine underneath the wing to produce energy (right).

In addition to the Paris Agreement, The United Nations (UN) Sustainable Goals, which aim to balance the need for renewable development with the need to protect the environment, have been outlined for the 193 member states within the UN (UN, 2015). Three of the 17 goals that are particularly relevant to the future of the tidal energy industry are:

Goal 8: Promote sustained, inclusive and sustainable economic growth, full and productive employment and decent work for all.

Goal 13: Take urgent action to combat climate change and its impacts.

Goal 14: Conserve and sustainably use the oceans, seas and marine resources for sustainable development.

These goals can guide the tidal energy industry in two ways. Firstly, the incentive to increase production of renewable energy which will help investment in the industry and secondly, the need to consider the most appropriate and proportionate way in which to conserve and sustainably use the marine environment when installing and operating TEC arrays.

1.2 Tidal Stream Environment

Tidal stream environments are dynamic and important habitats for many species. The movement of the tide through constrained channels, such as between two bodies of land (e.g. Bay of Fundy (Durand et al., 2008)) or between land and an island (e.g. Pentland Firth (Easton et al., 2012)) can create an energetic system with a range of complex hydrodynamic features. High-flow speeds between 2-4ms^{-1} may be generated at the peak of the tide which can create turbulent features such as boils and eddys (Slingsby et al., 2021). These characteristics can make tidal stream environments attractive to many species as the conditions may render prey easier to catch (Benjamins et al., 2015). Many marine species that occupy these regions, including marine mammals (Felleman et al., 1991; Hastie et al., 2016), seabirds (Waggitt et al., 2017) and diadromous fish (Levy and Cadenhead, 1995) are protected by legislation such as the Endangered Species Act in the US (Krahn et al., 2002) and the EU Habitats Directive (European Commission, 2007). To ensure that legislation is adhered to, commercial construction of developments in the marine environment often requires licensing by a regulator (Simas et al., 2009).

1.3 Environmental Concerns of Tidal Energy Converters

In countries where regulatory bodies oversee marine commercial developments, one aspect of the application stage is likely to involve assessing environmental impacts. In the case of TECs, an environmental impact assessment (EIA) may be required to quantify the risk to receptors of interest, and this would ultimately inform regulators in their decision making process on whether to consent the project and on what conditions (Glasson et al., 2019). Broadly, there are four main stages to an EIA, each of which are required as part of the process; however, these may vary slightly depending on the regulator and the size of the development, for example (Glasson et al., 2019):

1. Scoping – This first stage is used to identify what impacts may be of concern and whether an EIA is required.

2. Prediction – what are the likely impacts on the environment, are any impacts likely to be significant and are there mitigation measures that could be applied.

3. Statement – Environmental Impact Statement (EIS) that allows for a review of the findings and a decision to be made.

4. Mitigation and Monitoring – Any mitigation or monitoring measures that will be applied and/or assessed. Auditing of predictions may take place.

As of 2020, globally, there has been a little over 36MW of TEC installations (Ocean Energy Europe, 2020). While several short term (with respect to number of days of impact) environmental stressors have been identified for the installation and decommission stages of TEC developments, it is the operational stage, and the long-term impacts that are often given more attention in the EIAs. Some key issues regularly raised are: impacts on the benthos (Kregting et al., 2016), altering of the hydrodynamics (Shields et al., 2011), changes to the biogeochemistry (Schuchert et al., 2018), production of electromagnetic fields (Gill et al., 2012), noise pollution (Wilson et al., 2017) and potential barrier effects with respect to animal movement (Sparling et al., 2018b). A risk that was identified as a major concern during the initial stages of exploring the feasibility of commercial TECs (Keenan et al., 2011) and is still a major barrier for consent of TECs at present (Copping et al., 2020b) is collision risk i.e. the risk of animals colliding with the moving parts of a TEC.

Several installed tidal projects have undergone extensive EIAs where uncertainty around collision risk has been the major concern (Copping et al., 2020b; Keenan et al., 2011; MeyGen, 2014). An example of this is for the world's first grid-connected full scale tidal turbine, SeaGen, which was installed in 2008 in Strangford Lough, Northern Ireland. Understanding and quantifying collision risk was paramount for the SeaGen development, largely due to it being within a protected area for harbour seals (*Phoca vitulina*) and being the first project of its kind (Keenan et al., 2011). To mitigate the risk of collision, live monitoring of sonar to detect the presence of animals (i.e. seals) around the TEC was required and, where an animal came within 50 m of the turbine, the turbine was shut-down, temporarily stopping energy production (Keenan et al., 2011). Another tidal project, MeyGen, in the Pentland Firth in Scotland, undertook an EIA for a planned installation of 86 HATTs for an installed capacity of 398MW, with installation planned for 2014 (MeyGen, 2014). However, due to the presence of a declining population of harbour seals in proximity to the development, collision risk estimates were deemed too high and the project has been initially consented for 6 devices, pending further investigation into collision risk (McKie, 2013). Since this decision, there has been significant efforts undertaken to address the knowledge gaps surrounding collision risk and the MeyGen development (Band et al., 2016; Gillespie et al., 2020; Hastie et al., 2018; Onoufriou et al., 2019; Thompson et al., 2016).

One important element for refining collision risk estimates at the population level (as required for an EIA) is the density of animals in the vicinity of the TECs (Band et al., 2016). At the MeyGen site, telemetry tagging was undertaken to improve estimates of seal density close to the proposed locations for the TECs and results from the study indicated a collision risk estimate that was 72% less than the original collision risk estimate produced from the EIA (Thompson et al., 2016). However, the study stated the estimate of 103 seals per year for the 86 TEC array was still very high for a declining seal population and understanding two additional behavioural parameters, avoidance, and evasion, was identified as important with respect to producing a more accurate collision risk estimate. Avoidance is defined as the animal avoiding the area of a TEC or multiple

TECs, e.g. the seal hearing the device from a distance and avoiding the area of the TECs (Wilson et al., 2006). Evasion is defined as the animal evading a direct collision with a single device, for example an animal almost colliding with the blade but taking an evasive manoeuvre to escape the collision (Batty and Wilson, 2010). Quantifying these behaviours is an extremely difficult task but some work has investigated this through playback experiments, i.e. playing the sounds of a TEC through an underwater speaker and monitoring animal presence (Hastie et al., 2018) and through telemetry tagging (Onoufriou, 2020) which both indicated avoidance behaviour. New technologies are also being developed to be able to detect evasion and avoidance behaviour by tracking the 3D movement of animals close to TECs using active sonar (Hastie et al., 2019b) and passive acoustics (Gillespie et al., 2020). The findings from these studies have shown great promise, however, despite considerable investment in trying to address these knowledge gaps to better inform our understanding of collision risk, over 10 years on, this issue continues to be a major barrier for the tidal energy industry and, unless significant progress is made in understanding risk, it will continue to hinder the expansion of the industry (Copping et al., 2020b).

1.4 Estimating Collision Risk

Quantifying collision risk of animals with a TEC is complex, and estimates of risk are often produced with limited data (Copping et al., 2020b; Wilson et al., 2006) which often leads to conservative and precautionary estimates. Monitoring actual collisions is a difficult task (Polagye et al., 2020), and if they do occur, they are believed to be rare events. However, for many animal populations, especially those in decline, a small number of collisions could have population level effects (MeyGen, 2014). Therefore, in these cases, it is important that we have accurate and informative collision risk estimates as uncertainty in parameters (e.g. population density, mortality estimates) will require conservative predictions to be made. Quantifying collision risk is typically undertaken by predicting the number of animals colliding with the TEC over a given time period (e.g. year), i.e. collision risk modelling (CRM) and collecting data to validate and further improve the model estimate.

Data collection for estimating collision risk is a difficult task that can be time consuming and expensive. A key factor in determining collision risk is likely the behaviour of animals around TECs, however monitoring the movement of animals underwater, in the vicinity of the moving parts of a TEC, is challenging (Gillespie et al., 2020; Hastie et al., 2019b). With each new tidal development, new information and techniques become available from the post-installation monitoring, that will be important in informing new collision risk estimates. Some methods already exist that can monitor the behaviour of animals in close proximity to devices, including sonar tracking (Hastie et al., 2019b), passive acoustic tracking (Gillespie et al., 2020) and, if water clarity allows, video monitoring (Polagye et al., 2020). These techniques are useful in monitoring devices after installation and/or performing research on animal behaviour in response to devices. However, there are also often many assumptions made from the data collected for estimating collision risk.

For example, telemetry tagging of animals is used to estimate the density of animals in the area of the TEC and generalises the diving behaviour of the population to estimate how many seals are likely to transit the swept area of the TEC (MeyGen, 2014). Furthermore, there is evidence of variation in behaviour across different sites for many different animals, including seabirds (Waggitt et al., 2017) and seals (Onoufriou, 2020), therefore caution should be exercised when extrapolating data from the results of studies from other installations. While progress is being made to improve methods to directly observe animals near TECs (Gillespie et al., 2020; Hastie et al., 2019b), uncertainty remains around collision risk estimates and often, due to lack of empirical data, precautionary estimates have to be made using CRMs (Copping et al., 2020b).

To date, there have been two CRMs commonly employed to produce collision risk estimates for EIAs for TECs: the Band model and Encounter Rate Model (ERM) (Scottish Natural Heritage, 2016). These models both use a formulaic approach to estimate collision risk from the density of animals in the vicinity of the device, the speed of animal and device, and the time period being investigated (Scottish Natural Heritage, 2016). The main difference between these models is how the risk is calculated; the Band model calculates the number of transits through the swept area of the rotor, whilst the ERM calculates the volume swept by each blade over time. Two probabilistic CRMs also exist that estimate risk (Copping and Grear, 2018; Hammar et al., 2015), which both estimate the probability of a series of events occurring that would lead to an animal coming into contact with a device resulting in mortality. Another model (Rossington and Benson, 2020) is an extension of the Band model using an agent-based modelling approach to simulate the movement of fish which incorporates the hydrodynamics of the area and produces a collision risk estimate using the Band model equations.

All these models can only address collision risk for horizontal axis tidal turbines (HATT) which have made up the majority of installed TECs so far (Zhou et al., 2017). However, TEC designs are not restricted to HATTs, such that a range of designs exist, including crossflow turbines (ORPC, 2016), tidal kites (Zambrano, 2016), and vertical axis turbines (GKinetic, 2021). Therefore, an approach is needed to provide robust estimates of collision risk for all TEC designs. To estimate collision for a tidal kite, a simulation-based approach to collision risk was developed, funded by the EU Horizon 2020 Powerkite project (Schmitt et al., 2017). The approach made use of 3D modelling software to produce the movement of both an animal and TEC over time and estimate the probability of a collision occurring.

Whilst the models mentioned above have been instrumental in producing collision risk estimates they are limited in their ability to incorporate additional and/or alter parameters. For example, they are unable to incorporate differing angles that animals may approach TECs and cannot estimate information such as the location of the collision on the body of the animal or the speed at which the animal and device collide. By simulating a realistic 3D scenario of two objects colliding, a simulation-based CRM has the potential to be an extremely useful tool for the tidal energy industry

to produce more comprehensive estimates of risks by producing detailed results including the speed and location of each collision on both the animal and device. These could then be used alongside empirical data, such as information on the likely speeds of collision that may cause fatal injury to an animal (Onoufriou et al., 2019). By advancing this modelling approach, more robust collision risk assessments could be produced that would incorporate empirical data as and when it becomes available. This would complement efforts to gather new empirical data on collision risk and TECs and would greatly aid the consenting process and benefit the development of the tidal energy industry.

1.5 Aims of Thesis

The overall aim of this thesis was to develop an expansive collision risk modelling tool that is able to make robust estimates between animals and tidal energy convertors. Chapter 2 outlines how the simulation-based approach can produce collision risk probabilities for any device design. Chapter 3 outlines how the model can be used to alter various animal parameters, such as angle of approach and different body size. In Chapter 4, I further develop the model to extract the speed of collisions and where they occur on the body of the animal and develop methods for using the information to estimate mortality. Streamlining of the model was performed in Chapter 5 with the aim of reducing the computational time to run an assessment. In Chapter 6 I replicated a simple scenario from an existing EIA that used the Band model to provide reassurance that the models provided comparable results. Finally, Chapter 7 brings together the work in chapters 2 – 6 to outline the flexibility of this simulation-based approach to CRM and discusses the potential for further development to aid the consenting of TECs.

Chapter 2: Incorporating different tidal energy device designs into 4D collision risk simulations allowing increased flexibility for industry.

This work has been published as:

Horne, N., Culloch, R., Schmitt, P., & Kregting, L. (2019, September). Incorporating different tidal energy device designs into 4D collision risk simulations allowing increased flexibility for industry. In *European Wave and Tidal Energy Conference*.

Abstract

The marine renewable energy industry has created a wide variety of device designs including horizontal and vertical axis tidal turbines. One key issue in consenting the devices is the risk of animal collision with the infrastructure. Current efforts in addressing collision risk use simplified analytical solutions to calculate probabilities over the swept area of a horizontal axis tidal turbine. However, this method is not appropriate for every device as there are a multiple different tidal energy device designs being tested including tidal kites and cross-flow turbines. The 4D collision risk model is a simulation-based platform which, to date, has investigated a novel tidal energy kite, with a figure-of-eight trajectory, and its collision risk with an object. This earlier work demonstrated the effectiveness of this model to assess differences in collision risk due to variations in the device configuration. In a step change of this work, we simulate the collision risk probabilities of three tidal devices: a horizontal axis turbine, a cross-flow turbine and a tidal kite. Here we demonstrate the flexibility and ease in which this 4D model can be adapted to any device type giving the user the ability to quantify a wide range of scenarios which could therefore be of use to developers, consultants and regulators for project design, assessments, and licencing.

2.1 Introduction

Tidal energy has the potential to be a key contributor to global renewable energy targets in tackling climate change, as the predictability of the tidal cycle makes this an attractive option for many countries looking to expand their renewable energy sources (Zhou et al., 2017). Growth in the industry has led to the development of multiple tidal device designs, however there is still a lack of understanding on how marine fauna interact with these devices. A key issue raised in the consenting process of tidal energy converters (TECs) is the risk of animal collision. To date, there has been no evidence of collisions occurring, however, there has been limited monitoring for collisions and, where TECs have been installed, mitigation protocols, such as shut-down procedures (Keenan et al., 2011), have been in place.

Collision risk with renewable energy devices has been an ongoing concern since the 1980s, where studies investigating the occurrence of bird strikes with onshore wind energy devices counted the number of carcasses around wind turbines (Byrne, 1983) . Byrne (1983) only monitored this for five days, but in order to understand collision risk over the life of a turbine, a theoretical modelling approach was required, and so the Band model was developed (Band, 2000). The Band model (2000), uses a formulaic approach to calculate a collision rate over a period of time (Eq.2.1).

Eq. 2.1 $$CRM = D \times B \times CR \times v \times pcoll$$

Collision risk over a period of time (CRM) is calculated using the mean risk of a collision during a single transit ($pcoll$), animal speed (v), the number of rotors (B), cross-sectional area (CR) and animal density (D). A collision is simply classified as an animal coming into contact with a device

and does not necessarily equal a fatality. In the Band model the mean risk of a collision during a single transit, $pcoll$ (Eq.1) is calculated using the device's blade characteristics and a simplified animal shape. Calculating the blade profile of a horizontal axis turbine is possible with this equation but with a device such as the Minesto DeepGreen kite the blade profile of the device is not suitable to be used in the calculation. Since its development the Band model has been adapted to assessing collision risk around horizontal axis TECs (Scottish Natural Heritage, 2016).

In 2007 the Encounter Rate Model (ERM) was developed by Wilson *et al* (B Wilson et al., 2006) which also uses a formulaic approach to calculate the risk of collision between TECs and animals. The difference between the two models is that the Band model calculates risk from the number of animal transits through the rotor whereas the ERM focuses on volume per unit time swept by each blade (Scottish Natural Heritage, 2016). Despite their differences they both use a physical model of the rotor, the animal body size and swimming activity to calculate the probability of collision.

These models are well suited for horizontal axis tidal turbines, which are the design-type in which the majority of modelling investigations have been carried out on (Copping et al., 2017; Hammar et al., 2015; Wilson et al., 2006); which is unsurprising, as they are both similar designs to wind turbines and the first grid connected full scale tidal turbine, SeaGen (Fig. 2.1).

Figure 2.1. SeaGen Tidal Turbine installed in Strangford Lough, Northern Ireland. The first commercial scale grid connected tidal turbine in the world. In the image the two twin-bladed rotors (white parts) have been raised above the water so they can be accessed from the pile (red part). During operation the two rotors are lowered into the water and turn to produce energy from the passing tide.

Since the installation of SeaGen in 2008, further development of horizontal axis turbines such as the Atlantis AR1500 (Fig. 2.2) have led to increased complexity in design. Modelling efforts assume a single blade profile with a mean speed of rotation for assessing collision risk, however many horizontal axis turbines can change the pitch of the blades and rotate the rotor to face the incoming tide (Simec Atlantis, 2019). Not all devices are horizontal axis tidal turbines, designs such as the

tidal kite, Archimedes screws, vertical axis and paddle devices have been proposed (European Marine Energy Centre, 2019). In North America, the ORPC TidGen device (a cross-flow turbine using a Gorlov helical design to harness tidal power) is being tested and installed, and in the United Kingdom the Minesto DeepGreen tidal kite is being tested. These two device designs have a complexity of design that cannot be captured in collision risk models, to-date.

In 2017, Schmitt *et al* (2017) presented a simulation-based approach to collision risk modelling to offer a solution for assessing unique tidal energy devices. The 4D model (3D space over time) assessed collision probabilities between the quarter-scale Minesto DeepGreen kite and an object (based loosely on an adult harbour seal), using a uniform distribution of objects passing throughout the swept area of the device. This work also investigated how altering parameters that influenced the device flight path affected collision probabilities. The model was developed within the software, freeCAD (Juergen Riegel Werner Mayer, 2017) which is an open-source computer aided design software that can be run using the coding language, python.

Figure 2.2. Model representation of Atlantis AR1500 horizontal axis tidal turbine installed in the Pentland Firth, Scotland.

The work presented herein extends the 4D model using the software package Blender (Blender Online Commuinity, 2018), which is an open-source game design software. Blender is similar to FreeCAD as it is computer aided design software that uses the coding language python, but with additional flexibility allowed by the game-engine for detailed inputs (e.g angle of approach) and fast, accurate real time physical space for simulations. To demonstrate that multiple different TECs can be simulated using the 4D model approach, this paper builds on Schmitt *et al* (2017), and presents three hypothetical case studies using different TECs: a tidal kite, a cross-flow turbine and a horizontal axis tidal turbine (HATT).

2.2 Methods

2.2.1 Model Development

Within Blender, three 3D shapefiles were created to represent the devices being simulated in this paper: a tidal kite (Fig. 2.5), a cross-flow turbine (Fig. 2.6) and a horizontal axis turbine (Fig. 2.7). The devices were created with both static parts (e.g. foundation) and moving parts (e.g. rotor) and were modelled in two files (static and moving). The moving parts then required the motion to be configured to match the movement of the device. This was done using the game-engines motion input which can give an object different motion, such as linear and rotational velocity.

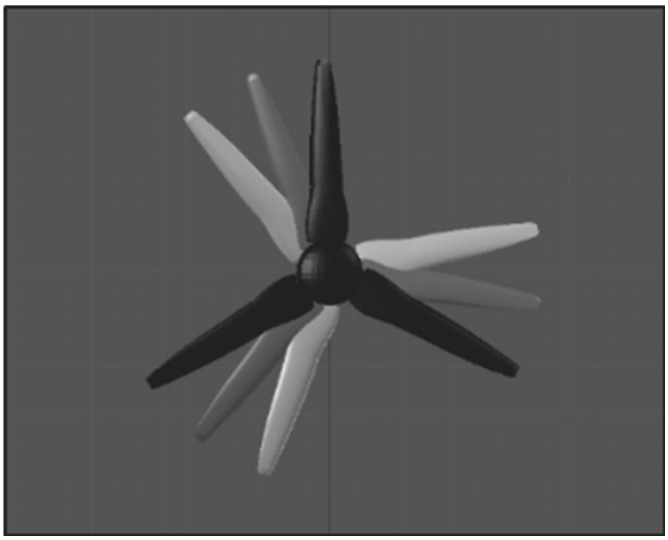

Figure 2.3. Example of a turbine rotor starting positions with time lag of 0 (black), 1 (dark grey) and 2 (light grey).

For a single simulation the starting position of the device's moving parts will affect the chances of a collision occurring. Therefore, to get a probability of a collision, multiple simulations must be run over the time it takes for one full transit of a device's moving part(s), for example, one full rotation of a turbine rotor. Each simulation must have a different device starting position of the,which is input into a simulation via a time lag; an example of three different time lags can be seen in Figure 2.3. Each device requires time lags to be set according to the time taken for the completion of one full transit of the device's moving parts.

2.2.2 Tidal Kite

The 3D shapefile for the tidal kite used in Schmitt *et al* (2017) was adapted for use in Blender. The simulation was run for a quarter scale model with a 12m wingspan based on the 3kW Minesto DeepGreen Kite (Fig. 2.4) currently being tested in Strangford Lough, UK. The figure of eight flight path requires a set of three equations to produce a rotation vector for each timestep of a simulation. A detailed description of these equations can be found in Schmitt *et al* (2017). The flight path for these simulations are presented in Table 1 and the 3D shapefile used, is shown in Figure 2.5.

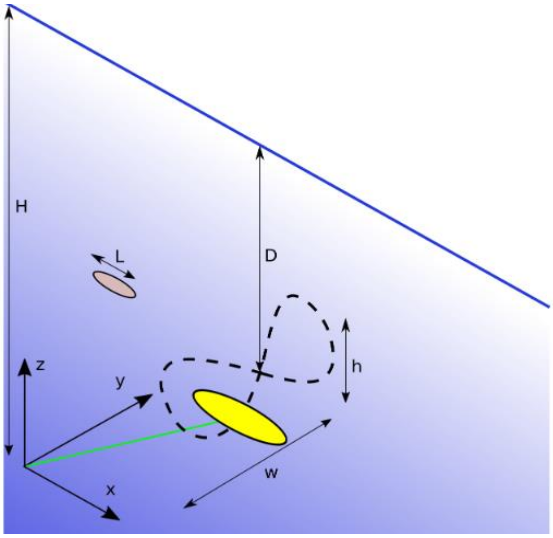

Figure 2.4. Schematic illustration of the tidal kite (yellow), tether (green) and flight path (dashed line) with main variables as defined in Table 2.1 and coordinate system as used in the simulations. The grey elliptic symbol represents the animal under risk of collision. The foundation is located at the origin.

Table 2.1. Flight path parameters for tidal kite simulations with the relevant parameters identified in Figure 2.4 in parentheses.

Parameter	**Input**
Water Depth (D)	30m
Figure width (w)	10m
Figure height (h)	3m
Figure period	8s
Tether Length	20m
Kite wingspan	3m

The tether and kite are defined as two separate shapefiles in order to differentiate collisions between them. Animal starting positions for an area of 14m wide and 20m high were used with 50 time lags over 8 seconds (the time taken for a full rotation) as per Schmitt *et al* (2017), creating 15,750 simulations.

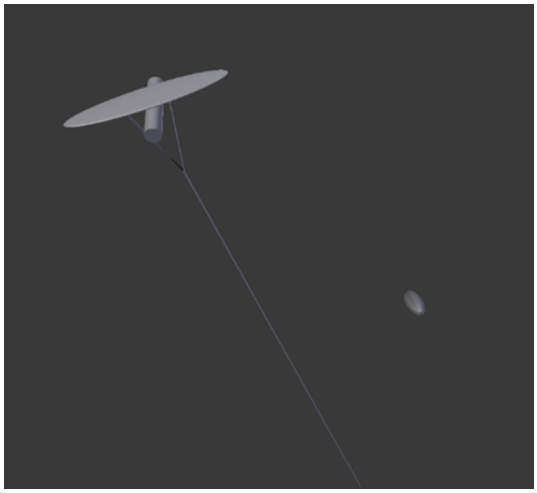

Figure 2.5. Screenshot from Blender of the tidal kite 3D shapefile and the ellipsoid object of the seal in the simulations presented.

2.2.3 Cross-flow Turbine

The cross-flow turbine was adapted from a free Gorlov helical design wind energy device 3D shapefile (CG Trader, 2014) and the device base and overall design was built to represent a device similar to the 150kW ORPC TidGen® device. The structure was based upon Figure 2.6 from Viehman (Viehman, 2016) with the static parts (base) of the device as a separate shapefile from the moving parts (rotor), parameters used can be seen in Table 2.2.

Table 2.2. Parameters used for design and simulation of cross-flow turbine

Parameter	**Input**
Number of rotors	4
Rotor diameter	2.8m
Rotor Width	4m
Power output	150kW
Tip speed ratio	2

The rotational speed for the rotor part of this device was run using a tidal speed of $3ms^{-1}$ and with a tip-speed ratio of 2 (Bachant and Wosnik, 2015). This meant that the rotational speed of the device was 2.129 radians per second. Animal starting positions were run for a 35m wide and 11m high area and with 50 time lags over the 2.9321 seconds taken for one full rotation of the rotor, creating 19,250 simulations. Lags were not tested further, as 50 time lags is accurate enough over the longer time period of the tidal kite (Schmitt et al., 2017).

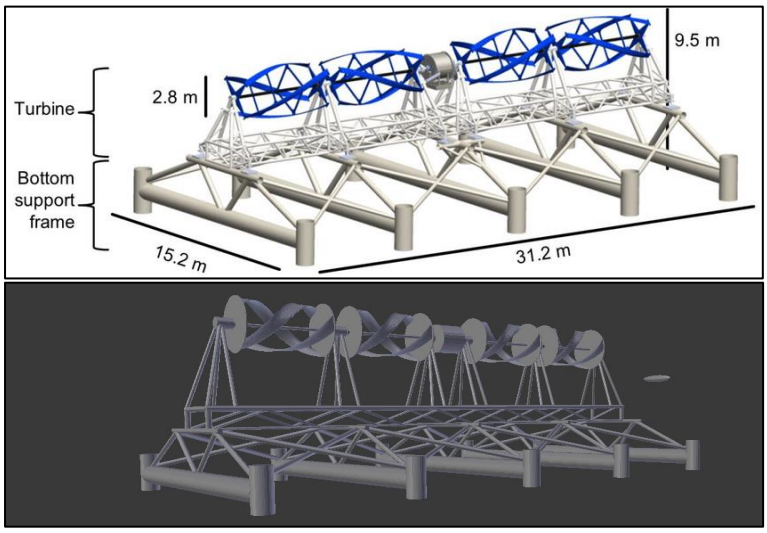

Figure 2.6. Ocean Renewable Power Company's TidGen ® Power System. Turbine image provided by ORPC (Top), Device structure was taken from the diagram in Viehman (Viehman, 2016) and a screenshot from Blender of the 3D shapefile created from the design with the ellipsoid object of the seal for scale purposes (Bottom).

2.2.4 Horizontal Axis Tidal Turbine

The horizontal axis tidal turbine used was adapted from a free 3D shapefile (375 Designs, 2014) and adapted to have characteristics similar to the 1500kW Atlantis AR1500 device (Atlantis Resources, 2016). The device characteristics are displayed in Table 2.3.

Table 2.3. Input parameters for the design and simulation of a horizontal axis turbine, based on available information on the AR1500 (Atlantis Resources, 2016).

Parameter	**Input**
Number of blades	3
Rotor diameter	18m
Hub size	2.4m
Turbine length	12m
Power output	1500kW
RPM	14

The Atlantis AR1500 is described as rotating at 14RPM equating to 1.466 radians per second, which was used as the rotational speed for these simulations. The animal starting positions were

simulated over an area of 35m wide and 20m high. 50 time lags over the 4.29s period for a full rotation were used for each animal starting position, creating 48,050 simulations. Lags were not tested further as 50 lags was accurate enough over the longer time period of the tidal kite (Schmitt et al., 2017).

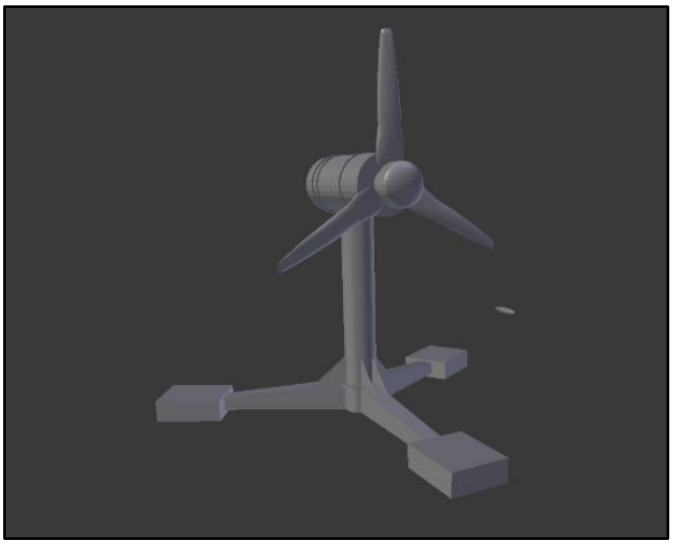

Figure 2.7. Screenshot of 3D shapefile of the horizontal axis turbine design, the ellipsoid object of the seal can be seen for scale purposes.

2.2.5 Simulations

The animal shape is created from an ellipsoid representing the dimensions of an adult harbour seal, length of 1.41m and width 0.3m, based on recommendations from Scottish Natural Heritage (Scottish Natural Heritage, 2016). This was used for all devices and the swim speed of the seal object was 1.8ms^{-1} for all simulations.

The simulations in this paper are run with a 1m by 1m grid of fixed animal starting positions, set to be wider than the width and height of the area the device occupies during operation. For each animal starting position a set of time lags are set in order to obtain a probability of collision for each point on the device. These steps create the configuration for a set of simulations for a single device (Fig. 2.8).

Figure 2.8. Schematic of model configuration required to run a set of simulations. Time lag is where the device starting position is varied to estimate risk for any device starting position in order to get a probability of collision, an example of 3 time lags can be seen in figure 2.3.

2.2.6 Analysis

The probability of a collision occurring from each animal starting position was calculated from the number of collisions at an animal starting position divided by the number of lags (i.e. 50 in this case). This was then used to display the collision percentage at each position, and the output was displayed using ggplot2 (Wickham, 2016) in R (R Core Team, 2009).

The collision probability used in the Band model ($pcoll$; Eq.1) refers only to the swept area of the turbine and therefore, to be consistent with this approach, herein, only the moving parts of the devices were used to calculate the chance of collision. In order to calculate the percentage chance of a collision in the swept area of each simulated device, the following calculation is used on the output data:

$$P\text{SweptA} = NColl/\left(\frac{NCollPos}{Nlags}\right) \times 100 \quad (2)$$

Where $NColl$ is the number of collisions and $NCollPos$ is the number of positions at which at least one collision occurred for all time lags tested. $Nlags$ is the number of time lags for each animal starting position. All post processing of the data generated was implemented in R.

The value produced for $P\text{SweptA}$ in each case is equivalent to the Band model $(pcolll; Eq.1)$ and therefore the values described are referring to the probability of collision from a single transit and would be scaled up to a number of collisions over a time period using information on the time period, number of animals in the area of the device, and the area swept by the device's moving parts.

2.3 Results

2.3.1 Tidal Kite

Figures 2.9 & 2.10 present the distribution of collisions from the tidal kite simulations, displaying the collisions of the seals with the kite (Fig. 2.9) and the entire structure (Fig. 2.10), both through the shading and size of the points, where darker and larger points indicate a higher chance of collision. Figure 2.9 shows the figure of eight movement, passing through the centre twice in a single rotation, resulting in a higher percentage of collisions as compared to the outer edges of the flight path.

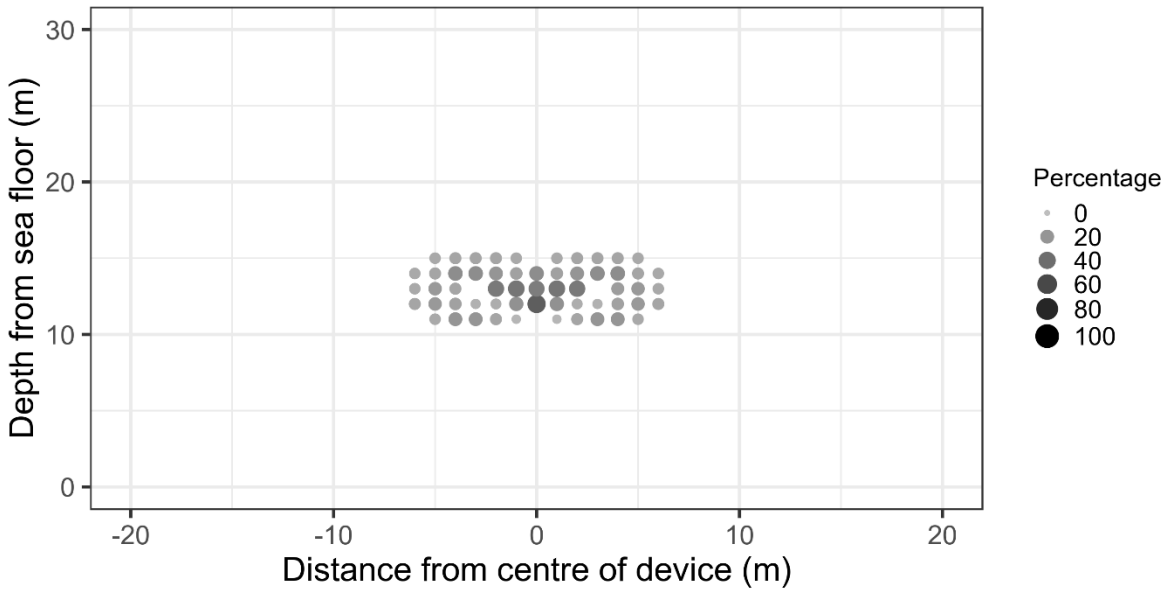

Figure 2.9. Percentage chance (%) of a collision at each animal starting position between an animal and the kite only. Darker shades and larger dots indicate a higher chance of collision (Number of simulations = 15,750).

Figure 2.10 shows collision percentages for both the tether and the kite, note that at the base of the tether, the area of the device with little to no movement, there is a 100% chance of collision. The tidal kite had a $PSweptA$ of 20.6%, which was calculated using the collisions with both the kite and tether, as both are moving.

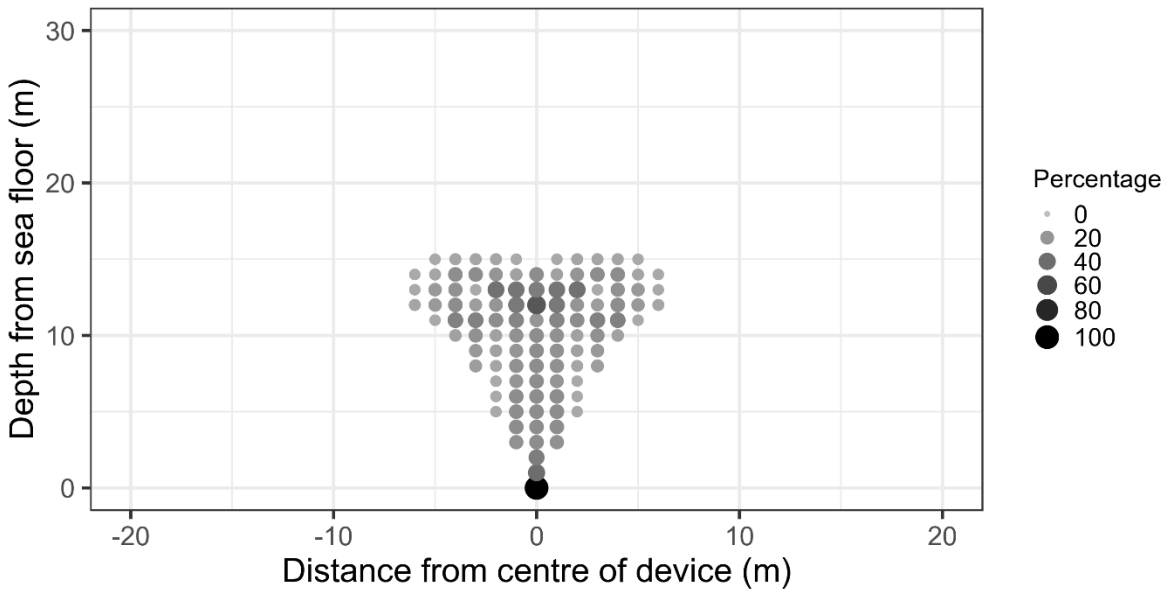

Figure 2.10. Percentage chance (%) of a collision at each animal starting position between an animal and the whole tidal kite device. Darker shades and larger dots indicate a higher chance of collision (Number of simulations = 15,750).

2.3.2 Cross-flow turbine

Figures 2.11 & 2.12 present the distribution of collisions from the cross-flow device simulations. It displays the collisions with the rotor and the entire structure, both through the shading and size of the points. Figure 11 shows the collision percentages over the swept area of the device, i.e. the moving parts of the device.

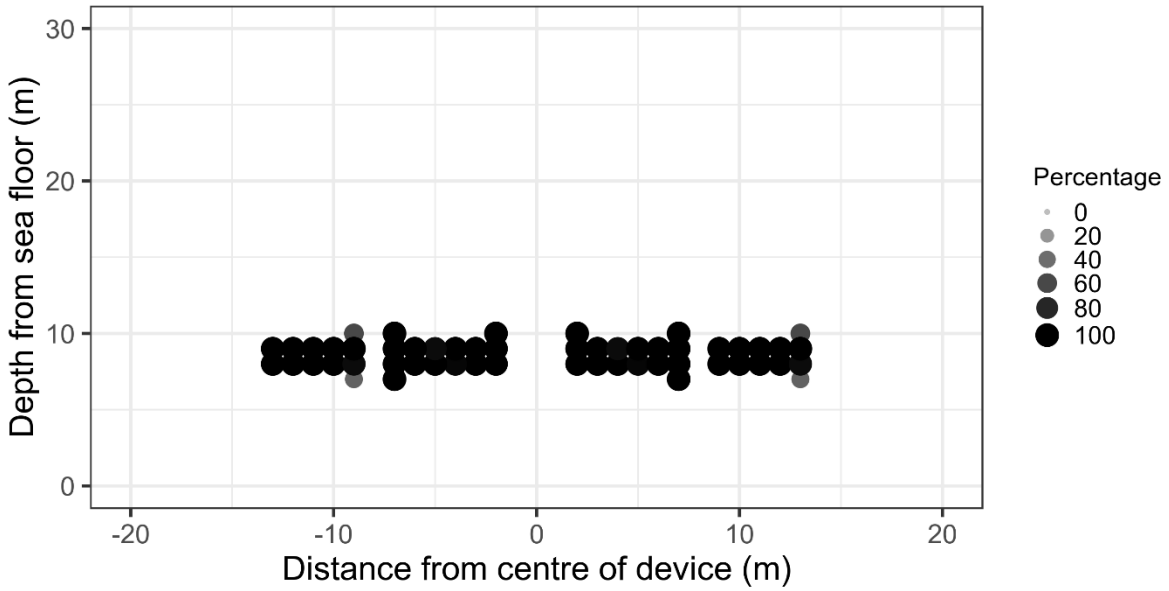

Figure 2.11. Percentage chance (%) of a collision at each animal starting position between an animal and rotor only. Darker shades and larger dots indicate a higher chance of collision (Number of simulations = 19,250).

Figure 2.12 shows the collision percentages for the whole device (i.e. moving and static parts, the latter of which has a 100% chance of collision). A $PSweptA$ of 96.0% for the cross-flow device was calculated for the rotor (i.e. excluding the static part of the device). This was done as the rotor is the moving only part of the device, and is therefore the only component contributing to the swept area.

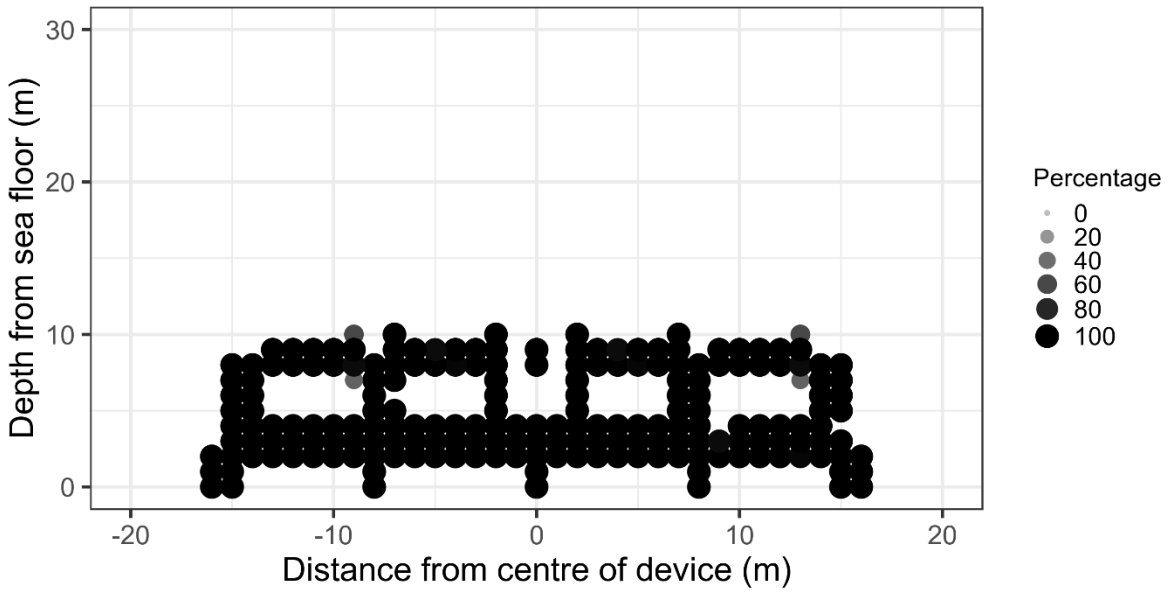

Figure 2.12. Percentage chance (%) of a collision at each animal starting position between an animal and whole cross-flow device. Darker shades and larger dots indicate a higher chance of collision (Number of simulations = 19,250).

2.3.3 Horizontal Axis Tidal Turbine

Figures 2.13 & 2.14. present the distribution of collisions from the HATT simulations. It displays the collisions with the rotor and the entire structure both through the shading and size of the points. Figure 2.13 shows the collision percentages over the swept area of the device (i.e. for the parts of the device that are moving). Whereas Figure 2.14 shows collision percentages for the entire device (i.e. the moving and static parts of the device, the latter of which has a 100% chance of collision). A $PSweptA$ of 81.4% for the HATT was calculated for the rotor (i.e. excluding the static part of the device). This was done as the rotor is the only moving part, and is therefore the only component contributing to the swept area.

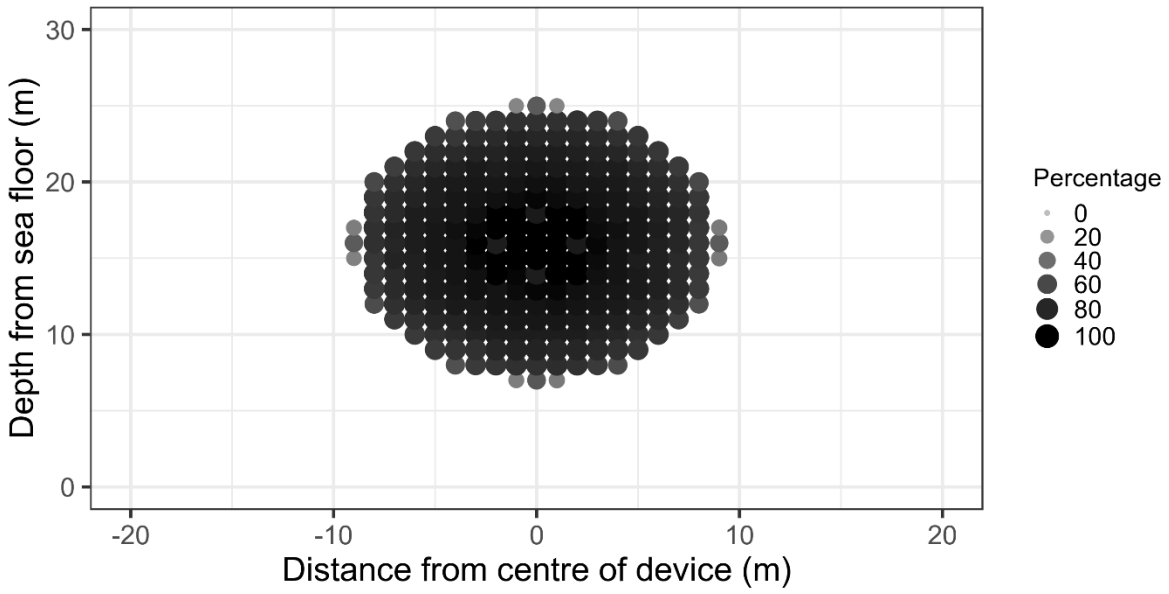

Figure 2.13. Percentage chance (%) of a collision at each animal starting position between an animal and the rotor. Darker shades and larger dots indicate a higher chance of collision (Number of simulations = 48,050).

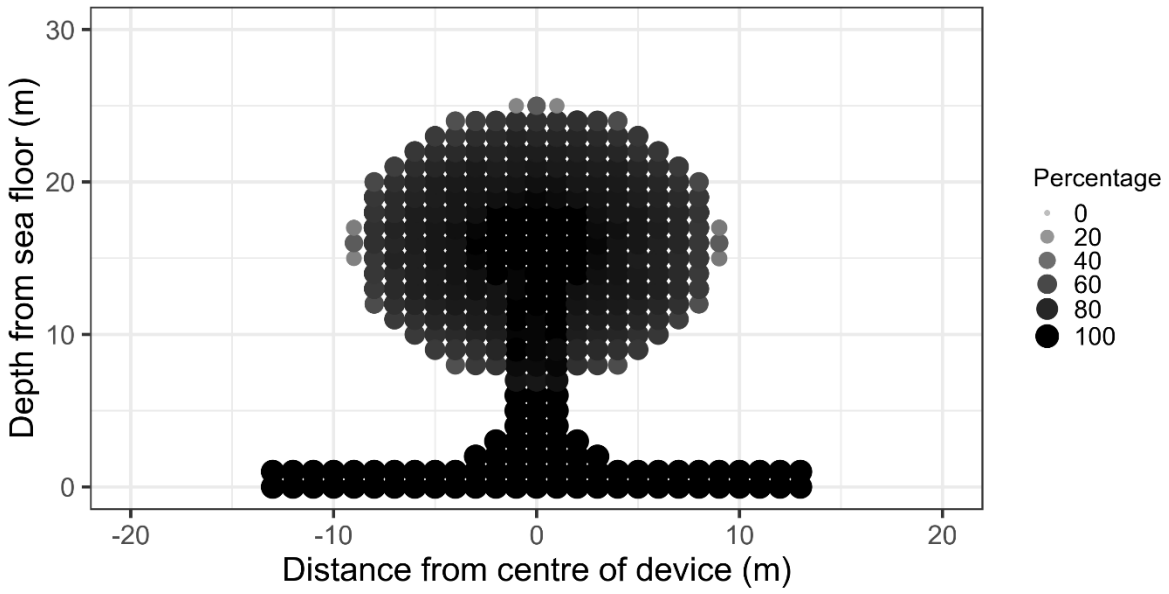

Figure 2.14. Percentage chance (%) of a collision at each animal starting position between an animal and whole horizontal axis turbine. Darker shades and larger dots indicate a higher chance of collision (Number of simulations = 48,050).

2.4 Discussion

We have demonstrated the application of a 4D simulation-based approach to collision risk modelling that can tackle the issue of different TEC designs. Using these basic scenarios to

demonstrate the application of this approach does make comparisons somewhat irrelevant without consideration to area occupied and the potential influence of environmental and ecological factors, for example. It should also be noted that, as can be seen in Eq. 2.1 the cross-sectional area of the device must be taken into account to understand overall collision risk. For example, the tidal kite has a flightpath that is a figure of eight 10m wide and 3m in height and therefore the cross-sectional area would give a larger collision risk when implemented to Eq. 2.1.

The calculated $PSweptA$ for each device are directly comparable to $pcoll$ (Eq. 2.1), with the additional benefit being that the simulation-based approach is capable of quantifying collision risk for novel device designs, such as those that cannot be calculated using the currently applied modelling methods. The simulations presented in this paper are based on a uniform distribution and do not incorporate ecological (with the exception of the size and shape of the object being based on an adult harbour seal) or environmental data, both of which are well documented as being important for better informing collision risk models (Wilson et al., 2006). These parameters could be integrated into this simulation-based approach, either as part of the simulation or during post-processing. For example, using empirical studies on the likelihood of fatality through collision risk (Thompson et al., 2015) as collisions on different points of the device may be less severe than others (e.g. the hub of the HATT vs the rotor tips), Blender offers a flexible and powerful system in which information such as speed of a collision could be extracted (Chapter 4); this, could then be used to take a step further, with respect to estimating the proportion of collisions that are fatal, as seen in Chapter 4.

Being an emerging industry, TECs are continuously changing. Although most devices currently installed are horizontal axis turbines, other devices such as Minesto's sea kite are being installed in the UK and further afield (e.g. two 100kW devices have been sold for installation in the Faroe Islands (Minesto, 2019a)). Even as these devices are being installed improvements to the technology and design continue to progress at a rapid rate, for example, Minesto have announced a new improved wing design (Minesto, 2019b). In the development stages 3D shapefiles are used in testing and advertising (Offshore Renewable Energy Catapult, 2016). As these files already exist it is straightforward for developers to use these shapefiles, which can be quickly and easily implemented into this simulation-based modelling framework, as we have demonstrated here. This could potentially allow for more flexibility during the process of informing the EIA for turbine design/parameters, for example, variations in flightpath parameters of the tidal kite may reduce impact on a protected species.

This paper serves to illustrate the flexibility of this simulation-based approach, whilst providing an insight into the potential for incorporating parameters of interest into collision risk assessment (e.g. size and swim speed of animals; Chapter 3), which would give different collision risk estimates. Furthermore, this approach could be used to assess sensitivities in parameters and the uncertainties, the outputs of which could then be used to provide recommendations on the areas

in which targeted research is needed in order to reduce uncertainty around the most influential parameters in collision risk modelling.

Chapter 3: Collision risk modelling for tidal energy devices: A flexible simulation-based approach

This work has been published as:

Horne, N., Culloch, R. M., Schmitt, P., Lieber, L., Wilson, B., Dale, A. C., ... & Kregting, L. T. (2021). Collision risk modelling for tidal energy devices: A flexible simulation-based approach. *Journal of Environmental Management*, *278*, 111484.

Abstract

The marine renewable energy industry is expanding as countries strive to reach climate targets as set out in the Paris Agreement. For tidal energy devices, the potential risk for animals to collide with a device, particularly its moving parts such as rotor blades, is often a major barrier in the consenting process. Theoretical work surrounding collision risk has commonly made use of a formulaic modelling approach. However, whilst providing a platform to assess conventional horizontal axis tidal turbines, the frameworks applied lack the flexibility to incorporate novel device designs or more complex animal movement parameters (e.g. dive trajectories). To demonstrate the novel simulation-based approach to estimating collision probabilities a hypothetical case study was used to demonstrate how the approach can assess the influence that variations in ecological and behavioural data had on collision probabilities. To do this, a tidal kite moving in a 3D figure-of-eight trajectory and a seal-shaped object were modelled and variations to angle of approach, speed and size of the animal were made. To further improve the collision risk estimates, results of the simulations were post-processed by integrating a hypothetical dive profile. The simulations showed how variation in the input parameters and additional post-processing influence collision probabilities. Our results demonstrate the potential for using this simulation-based approach for assessing collision risk, highlighting the flexibility it offers by way of incorporating empirical data or expert elicitation to better inform the modelling process. This framework, where device type, configuration and animal-related parameters can be varied with relative simplicity, on a case-by-case basis, provides a more tailored tool for assessing a diverse range of interactions between marine renewable energy developments and receptors. In providing a robust and transparent quantitative approach to addressing collision risk this flexible approach can better inform the decision-making process and aid progress with respect to developing a renewable energy industry in a sustainable manner. Therefore, the approach outlined has clear applications that are relevant to many stakeholders and can contribute to our ability to ensure we achieve sustainable growth in the marine renewable energy industry as part of a global strategy to combat climate change.

3.1 Introduction

The marine renewable energy industry is expanding as countries strive to reach climate targets as set out in the Paris Agreement (McCollum et al., 2018), whilst also aiming to achieve the Sustainable Development Goals, as outlined by the United Nations (UN, 2015). In regions with sufficiently rapid and energetic tidal flows, such as in waters around the UK, US and Canada, tidal energy offers a predictable renewable energy source (Zhou et al., 2017). In many countries, the construction of any major marine infrastructure project requires the potential ecological impacts to be quantified and, where deemed necessary, monitored (Simas et al., 2009). Approved mitigation plans also need to be in place, prior to the regulator providing consent for the development (Moura et al., 2010). Sites identified for tidal energy converters (TECs) tend to be relatively close to shore and, as one would expect, in tidally dynamic and energetic environments. These areas are often

important to a wide range of protected species (Benjamins et al., 2015; Copping et al., 2016). Therefore, any potential impacts to protected populations following the construction and/or operation of proposed developments must be considered as part of an environmental impact assessment (EIA) (Moura et al., 2010). In progressing the tidal energy industry, one of the barriers to consent is the risk of animal collisions with TEC(s) (Wilson et al., 2006). However, given the logistical challenge of gathering animal behaviour data close to TEDs, a modelling approach is often adopted, and the assessment typically follows the precautionary principle. Consequently, the construction of large-scale arrays of TECs remains in the planning stage, in part due to the increased perceived risk to protected species through potential impacts, namely collision risk.

Collision risk models (CRMs) estimate the impact of collisions to a relevant population or management unit for the receptor of concern. A number of models exist to estimate collision risk; including the commonly used Band model (Band, 2000; Band et al., 2016) and encounter rate model (ERM) (Wilson et al., 2006), with two more recent examples, one proposed by (Copping and Grear, 2018) and another, using an agent-based approach, (Rossington and Benson, 2020). All of these models use a geometric model of the rotor, as well as animal shape and movement to calculate a theoretical risk of collision. These models were designed for horizontal axis tidal turbines (HATT), however other device designs have, and are, being developed, including cross-flow turbines (ORPC, 2016), floating turbines (Orbitall Marine, n.d.) and tidal kites (Zambrano, 2016); the motion and shape of these devices differ to HATTs (Chapter 2). Consequently, the geometric nature of these models means that they are not capable of estimating collision risk for these novel TECs, which can often have more complex movement patterns, particularly in the case of a tidal kite (Fig. 1) (Booth et al., 2015; Schmitt et al., 2017).

A simulation-based approach was developed to estimate the collision risk for tidal kites using computer-aided-design software, FreeCAD (FreeCAD., 2017), built on previous collision risk approaches by incorporating the simulation of the three-dimensional (3D) figure-of-eight movement of the TEC (Schmitt et al., 2017). Schmitt *et al* (2017) used a uniform distribution of an approaching object (based on the basic morphology of a swimming seal) over many simulations to calculate a collision probability with the TEC and tether. Further development of this simulation-based approach has been made using Blender (Blender Online Community, 2018), an open-source game-engine software, to demonstrate how collision risk can be assessed, with ease, for a variety of TEC designs including a crossflow turbine (Chapter 2). Blender offers advantages over FreeCAD, such as an integrated collision detection system, and the ability to incorporate additional parameters of interest, such as changing the angle of approach.

The current suite of collision risk models is limited with respect to the user's ability to incorporate the best available information and scientific evidence into the model framework, in order to provide

a robust estimate of collision risk, and the associated uncertainties. A robust estimate would increase confidence in assessments and better assist regulators in making informed decisions regarding the consenting of marine renewable energy projects. For example, previously used collision risk models are unable to alter ecological inputs, such as angle of approach, where the Band model assumes an animal adopts a single horizontal approach to the device (Scottish Natural Heritage, 2016) and the ERM assumes an equal probability of approach from any angle (Wilson et al., 2006). In reality, the angle of approach may differ for different receptors of interest (Wilson et al., 2006). In addition, the equations used in these models assume linear relationships between ecological inputs (such as size and speed of animals) with the risk of collision, which is unlikely to accurately represent the true complexity of the situation. Lastly, these models have a limited capacity for incorporating additional spatio-temporal empirical data, such as the dive profiles of animals. The simulation-based approach can help overcome such problems by allowing the user to alter input parameters such as the animal size, speed and angle of approach. Moreover, it is possible to include additional behavioural data, such as dive profiles, during post-processing, to further refine collision risk estimates.

The objective of this paper is to demonstrate how variations in input parameters (animal size, speed, angle of approach) can be incorporated into the simulation-based approach with relative ease. Furthermore, we outline the method for post-processing results from the simulations to incorporate additional information on animal behaviour (dive profile). For this, we apply hypothetical scenarios using a seal-shaped object and a tidal kite to address the following questions: 1) How does varying the animal speed, size and angle of approach affect collision risk probabilities and 2) how does the incorporation of a dive profile further refine collision risk probabilities. By addressing these questions, we provide a worked example of how the simulation-based approach can allow for a comprehensive assessment of collision risk, which is often required for assessing the potential ecological impacts of tidal energy projects.

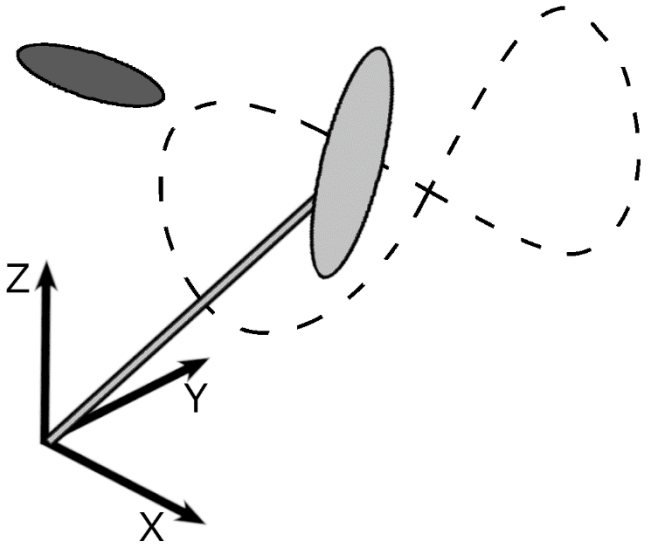

Figure 3.1. Tidal kite schematic showing a wing and tether (light grey) undertaking a 3-D figure-of-eight movement (black dashes). The dark grey ellipsoid represents a seal-shaped object moving towards the tidal kite. Note: The co-ordinate system uses XYZ axis; where X is the direction of the tidal flow, Y is the horizontal distance normal to the flow direction and Z represents the distance from the seabed.

3.2 Methods

3.2.1 Model Development

The simulated tidal kite was produced from a 3D shapefile of the device, previously described in Chapter 2. The shapefile was a representation of the Minesto kite with a tether length of 20 m and a wingspan of 3 m. The movement of the kite was simulated in Blender (version 2.79b) using three angles of rotation around the base of the device to create a figure-of-eight motion. The formulae used to calculate these angles are described in Schmitt *et al* (2017) and were transcribed into a python script for use in Blender; this code essentially controlled the movement of the kite during simulations. To ensure the reliability of results and that there were no issues with the re-coding, results for identical scenarios were compared between Blender and the original model in FreeCAD, which showed a satisfactory margin of error of <1 %.

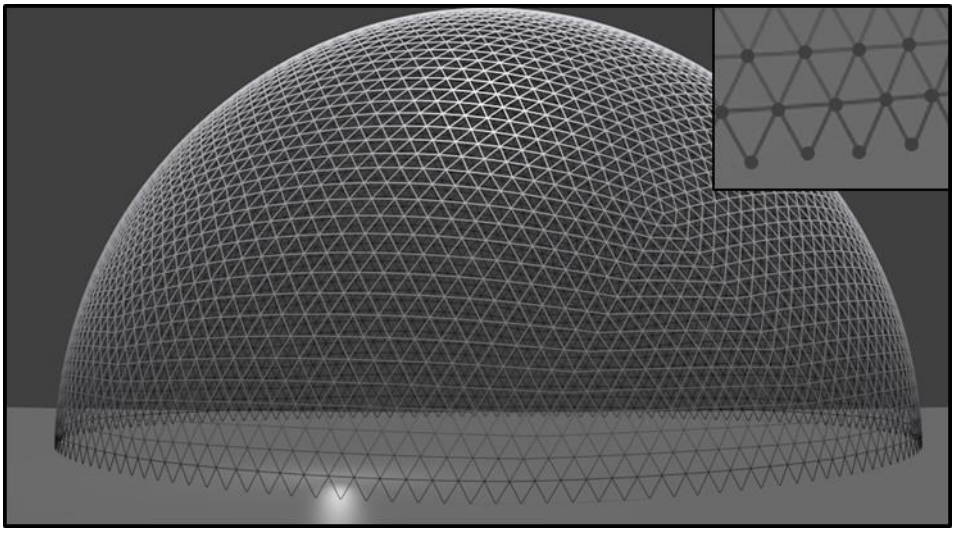

Figure 3.2. An example of an icosphere created in Blender with the upper right panel showing a close-up of the starting positions (dots) of the seal-shaped objects.

Previous simulations were run for a seal-shaped object moving horizontally and parallel to the flow direction (Horne et al., 2019; Schmitt et al., 2017). However, the investigation of arbitrary directions of travel posed a problem, since starting positions must be assigned in such a way that all directions of animal movement are considered. To address this, starting positions were distributed on the surface of an icosphere, with a radius larger than the kite's swept area and centred on the base of the kite's tether. An icosphere, made up of equilateral triangles, was used to create a dome of possible starting positions of the animal (Fig. 3.2). The positions where the lines of the triangles met, were used as the starting positions for seal-shaped object approaches during simulations (Fig. 3.2). The number of starting positions were determined by the number of subdivisions used to create the dome. The more subdivisions, the more complex (higher resolution) the sphere, where a single subdivision results in a sphere with 12 starting positions, two subdivisions create 42 positions, and so on. The number of subdivisions and the radius of the sphere combined determine the distance between each starting position. After creating the sphere, all points from one half were removed to create a dome so that starting positions could originate from no lower than the seabed. For the scenarios tested here, the radius of the icosphere was 21 m with six subdivisions, which resulted in 5,106 starting positions with 0.9 m distance between each neighbouring position.

3.2.2 Input of Ecological Parameters

The values for the ecological parameters, speed, size and angle of approach, were chosen to represent feasible scenarios in the way a seal could hypothetically approach a turbine. The speed of the animal was set using a value for linear velocity and was defined before every simulation. Two different speeds were tested, one, representing the mean swim speed of an adult harbour seal (*Phoca vitulina*) (1.8 ms^{-1}; Scottish Natural Heritage, 2016) which is referred to as the 'slow' speed (Table 3.1). A second speed of 4 ms^{-1} was chosen to represent a seal travelling in a fast

flowing tidal stream, such as that of the Narrows tidal channel in Strangford Lough, Northern Ireland, UK (Kregting and Elsäßer, 2014) or the Bay of Fundy, Canada (Durand et al., 2008).

An ellipsoid object was used to represent the shape of a harbour seal and the dimensions used in the simulations were representative of an adult seal (L= 1.41 m, W=0.3 m) (Scottish Natural Heritage, 2016) and a pup (L=0.8 m, W=0.2 m) (Cottrell e*t al.*, 2002). To change between the two, the length (L) and width (W) of the seal-shaped object was altered before each run, where required. Two manipulations to the dimensions of the shapefile were used to display the flexibility of the system, however any animal shape or size could be incorporated as a 3D shapefile.

The angle of approach for each seal-shaped object was created using yaw and pitch parameters which were input before each simulation (Fig. 3.3). Yaw is the orientation in the X-Y plane, clockwise relative to the flow direction (Fig. 3.1), whereas pitch is the orientation in the vertical plane of motion, relative to horizontal. For the scenarios tested herein, the orientation of the seal is the same as the direction of travel i.e. the seal-shaped objects travelled headfirst however, if required, any orientation can be incorporated with ease. Two different inputs for angle of approach were tested, one where the seal travelled downstream toward the device, parallel to the seabed (Fig. 3.3a), referred to as the 'flat' trajectory (Table 3.1) and the other where the seal travelled downstream toward the device with a 45˚ downward trajectory (Fig. 3.3b) referred to as the 'downward' trajectory (Table 3.1).

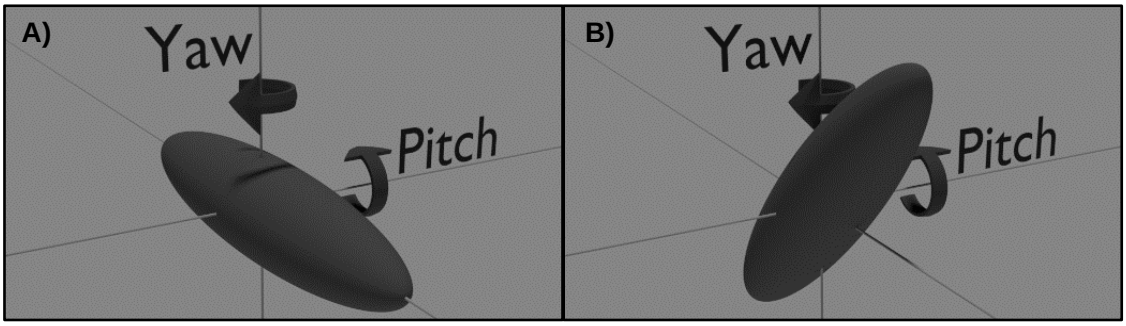

Figure 3.3. The yaw (Y) and pitch (P) of the seal-shaped objects for the baseline case (Y=0, P=0) (A) and alternative case (Y=0, P=45) (B).

3.2.3 Simulations

Simulations were run on a Dell OptiPlex 7060 with an Intel Core i5-8500 and 16GB RAM using the step-by-step conceptual outline in Figure 4. The device shapefile was imported into Blender and the python script controlling device movement was then configured. The animal shape file was then imported, and the starting position of the animal set. Eight different scenarios were tested (Table 3.1) and collisions were deemed to occur if the seal-shaped object collided with any part of

the tidal kite (e.g. wing and/or tether; Fig. 3.1). These scenarios were set up using three combinations of the input parameters: swim speed, size and angle of approach.

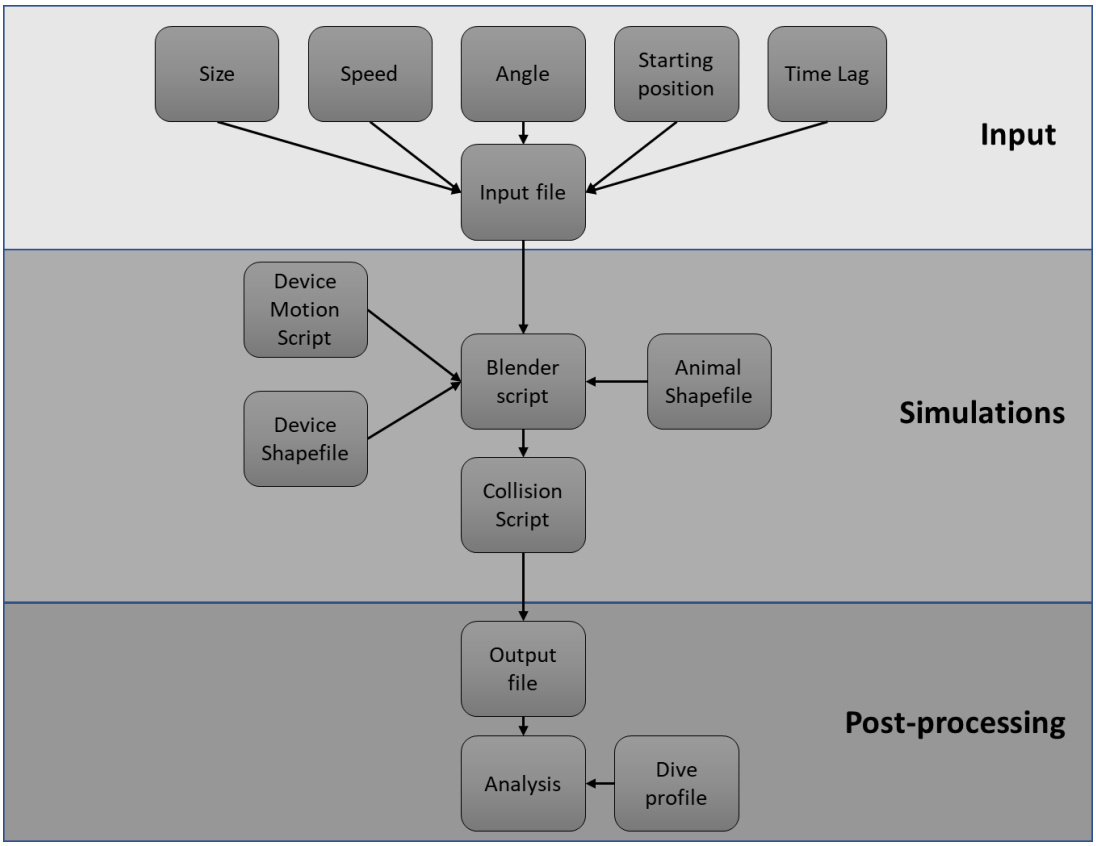

Figure 3.4. The key processes used in the simulation-based approach, outlining the three discrete steps: creating the input parameters and associated files, running the simulations, and the post-processing step (if additional empirical data are available to further refine collision risk estimates).

Whether the animal collided with the kite or passed unhindered depended on both the relative timing of the animal and the device movement in the simulations. Therefore, to evaluate collision probabilities, animals that were released from the same starting position, were varied at time lags distributed evenly between 0s and 8s (the time taken for one complete figure-of-eight movement of the kite). Resolution of this lag had to be sufficient to capture the true probability of a collision, which was defined as the number of collisions at a position divided by the overall number of seal-shaped objects released from that position (i.e. number of lags). The required resolution could not be established *a priori* and had to be determined by performing convergence studies. For this, it was logical to assume that larger and slower animals would run a higher risk of collision than smaller, faster ones. Therefore, smaller and faster moving animals would need a greater number of lags to resolve the fewer instances of collisions. Consequently, the fast (4 ms^{-1}) and small (pup) seal-shaped object on a downward trajectory was used to perform the convergence study.

The reliability of the simulations were tested using the method outlined in (Eça and Hoekstra, 2014), which is used in numerical modelling to assess the convergence behaviour of simulations and the grid size required for simulations to be accurate. Following this method, an R score of less than 1 indicates that convergence had been achieved; in this case, convergence was achieved at 100 lags (R=0.495). Therefore, the scenarios used herein were run with 100 lags (which equated to a gap of 0.08 s between each time lag). Consequently, for each of the eight scenarios tested, 510,600 individual simulations were required (i.e. 5,106 starting positions with 100 lags per position).

3.2.4 Analysis

All data processing, error checking and analysis was performed in R (R Core Team., 2019). Outputs from each scenario were matched to the corresponding input file, which created a database for each simulation run. Firstly, the number of collisions at an individual starting position were divided by the number of time lags (n=100) to create a collision probability for each starting position (Table 3.1).

As simulations were run using a dome of starting positions to allow a wide range of scenarios to be tested, the positions of collisions must be translated from 3D to 2D positions for an average collision probability to be calculated. This was achieved by removing the axis in alignment with the direction of travel (i.e. the direction of tidal flow; X-axis (Fig. 3.1) to project the results in the YZ plane (Fig. 3.5)). To translate the downward trajectory scenarios into 2D, the positions had to be rotated so that they aligned with at least one axis. The axis chosen was the same axis that the flat (0°) scenarios were run in to allow for a direct comparison. Therefore, new positions were calculated by rotating the 3D vectors by the trajectory (45°) to align them with the flat (0°) scenarios. After this conversion, positions no longer maintained equal distances between points (Fig. 3.5b); to account for this, inverse distance weighting (IDW) (Pebesma, 2004), which uses the distance between each point to average the values over 2D space, was used. The overall collision probability was then calculated, using the 2D vectors and the collision probability for each individual position.

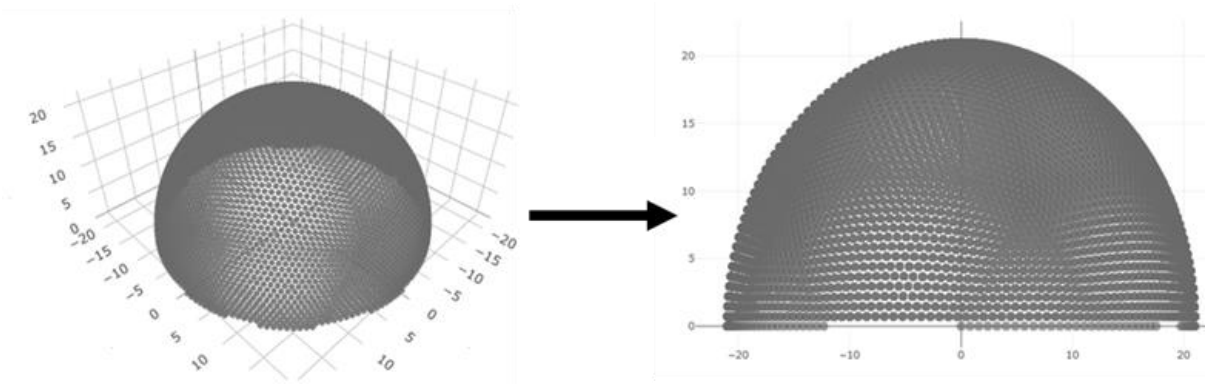

Figure 3.5. The transformation from 3D **A)** to 2D **B)** starting positions. Note that at the edges of the 2D plot the points are closer together (higher density).

3.2.5 Dive Profiles

The influence of a hypothetical dive profile on the probability of collision was investigated during post-processing. For this, a 'U-shaped' dive profile was used, based on data presented by Thompson *et al* (2016) for a telemetry tagged adult harbour seal. A time-depth distribution, at 1 m intervals throughout the water column along the z-axis, was incorporated as a post-processing step, using R. Therefore, rather than assuming an unrealistic uniform distribution throughout the water column (Fig. 3.5; z axis), incorporating information on the dive profile (i.e. the proportion of time spent at a given depth throughout the water column) can provide improved estimates of collision risk. Both the hypothetical and the uniform (equal probability for each 1 m interval) dive profiles were tested for a single scenario: a slow-moving, flat trajectory, adult seal. Updated collision risk probabilities were calculated by multiplying the collision probability for each starting position by the probability for that depth interval. After applying the dive profiles, the IDW methods outlined above were used to calculate the overall collision probability.

3.3 Results

3.3.1 Ecological Inputs

Varying the ecological inputs (i.e. the size of animal, speed and angle of approach) did change the collision probabilities (CP), with the highest chance of collision occurring for a slow (1.8 ms^{-1}) downward trajectory adult (CP=0.214) (Table 3.1), as compared to a fast (4 ms^{-1}) pup on a downward trajectory, which had the lowest collision probability (CP=0.037) (Table 3.1).

Table 3.1. Results of the different input scenarios. The three-letter code in the scenario column refers to the ecological inputs used: the first letter represents the approach speed; 4 ms^{-1} (**F; fast**) or 1.8 ms^{-1} (**S; slow**).,the second letter refers to the angle of approach; with a flat (**F**) or downward (**D**) trajectory, while the third letter refers to the size of the seal; adult (**A**) or pup (**P**). **Positions** are the number of starting positions in which at least one collision occurs. **Collisions** are the total number of collisions across those positions and **CP** is the collision probability calculated using inverse distance weighting.

Scenario	Speed	Angle	Size	Positions	Collisions	CP
FFP	4 ms^{-1}	Flat	Pup	174	875	0.0583
SFA	1.8 ms^{-1}	Flat	Adult	224	4,477	0.2004
FFA	4 ms^{-1}	Flat	Adult	224	2,501	0.1155
SFP	1.8 ms^{-1}	Flat	Pup	177	1,520	0.0898
FDP	4 ms^{-1}	Down	Pup	317	1,117	0.0371
SDA	1.8 ms^{-1}	Down	Adult	353	7,587	0.2140
FDA	4 ms^{-1}	Down	Adult	353	4,435	0.1293
SDP	1.8 ms^{-1}	Down	Pup	333	2,176	0.1293

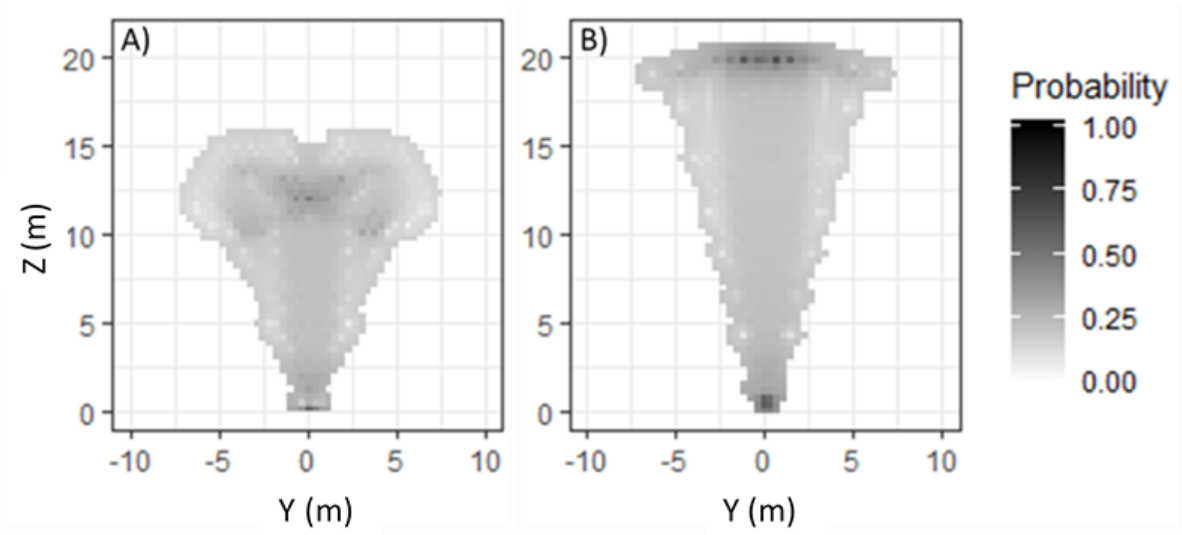

Figure 3.6. The 2D distribution of the probability of collisions for two of the eight scenarios tested **A)** Slow, Flat, Adult (SFA) and **B)** Slow, Downward, Adult, (SDA). The other four scenarios are presented in the supplementary material (supplementary material, Fig. 1). The shading of the points relates to the probability of collision for that point (with darker shading indicating a higher probability of collision).

Across all scenarios, the highest collision probabilities occurred at the static base of the device (Fig. 3.6; supplementary material, Fig. 1). There was a larger distribution of collisions over the z-dimension for the downward trajectory scenario (Fig. 3.6b), as compared to the flat trajectory scenario (Fig. 3.6a), whereby approximately 5 m is added on the z-axis (Fig. 3.6b). The increase in the possible area for collisions is due to the movement of the tidal kite, whereby, at the largest 2D projected swept area, it operates at approximately 45°, meaning that the device will be

perpendicular to the 45° trajectory of the animal (resulting in an increase in the available surface area for collisions).

Small changes can be seen when comparing across speed of movement or size of an animal. For example, a slow-moving adult on a flat trajectory (SFA) (CP = 0.2004; Table 3.1) showed a higher CP throughout the swept area, as compared to a fast-moving pup on a flat trajectory (FFP) (CP = 0.0898; Table 3.1). More broadly, and as expected, a faster animal had an overall lower CP (Table 3.1), where the mean CP was 0.086 (sd = 0.044) and 0.150 (sd = 0.059) for scenarios incorporating fast and slow seals, respectively. Similarly, larger seals, on average, were more likely to collide with the kite, as compared to their smaller counterparts. In this case, the mean CP for an adult and a pup was 0.165 (sd = 0.050) and 0.079 (sd = 0.040), respectively. However, when comparing CPs for flat trajectories against 45° downward trajectories, results were not as definitive. While three of the four downward trajectory scenarios showed a higher CP, as compared to the flat trajectory equivalents (i.e. the same speed and size), in the case of the fast and downward moving pup (FDP), a lower collision probability was observed (CP = 0.0371; Table 3.1) as compared to the flat trajectory (CP = 0.0583; Table 3.1).

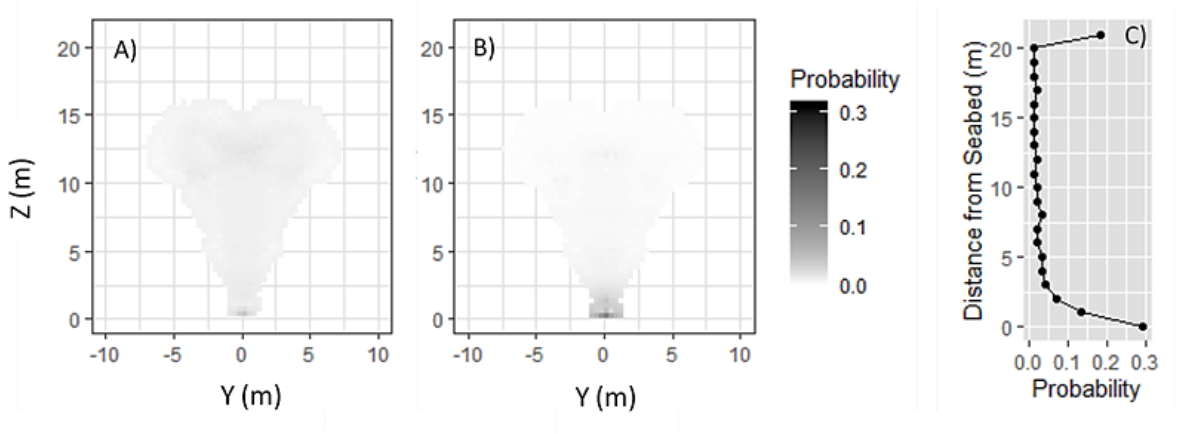

Figure 3.7. 2D distribution of collision probabilities with the shading showing the probability of collision for each location (with darker colours indicating a higher probability of collision). **A)** the probability distribution for a uniform time depth profile **B)** the probability distribution when the hypothetical dive profile presented in **C)** is employed in post-processing.

3.3.2 Dive Profiles

The collision scenarios represent only a single transit probability without any information on the animal's distribution throughout the water column. By incorporating a uniform dive profile, giving an animal an equal chance of being at any depth, the CP for a slow moving, flat trajectory adult is reduced from 0.214 (Table 3.1) to 0.009. By incorporating a hypothetical dive profile to this scenario, the CP is reduced further, to 0.007. Figure 3.7 displays the distribution of collisions for the uniform time depth distribution (Fig. 7a) and when the hypothetical dive profile is included (Fig. 3.7b) during post-processing. Comparison of the two distributions highlighted that the majority of

collisions where the dive profile has been employed occur near the base of the device, which is intuitive, given that the base was static and this was the location within the water column where the animal has the highest probability of occurrence (Fig. 3.7c).

3.4 Discussion

This flexible, simulation-based approach to collision risk assessment allows the incorporation of device specifications and information on the ecology and behaviour of the receptor(s) of interest. These input parameters can be changed with ease when more empirical data become available, for example, or if the user wants to assess thresholds or the potential impact of variations in the l input parameters, as demonstrated herein. Consequently, the simulation-based approach can be used to provide more detailed, transparent, and robust collision risk probabilities, and can therefore contribute to our ability to ensure we achieve sustainable growth in the marine renewable energy industry as part of a global strategy to combat climate change.

The approach has potential advantages over other collision risk models, such as the ERM and Band model, which use only a horizontal approach (equivalent to the flat trajectory tested herein) and a uniform distribution of trajectories (Scottish Natural Heritage., 2016). As demonstrated here, CPs can be affected considerably by the angle of approach, where the 45° downward trajectory scenarios showed a larger distribution of collisions, due to the movement characteristics of the tidal kite. Efforts to incorporate varying angles of approach for wind turbines and birds have been made using mathematical equations similar to those in the ERM and Band model (Holmstrom et al., 2011). However, this approach has not been used when assessing TEDs, and it is similarly limited in its ability to estimate collision risk with novel turbine designs. Given the development of different TEC designs, such as HATTs (MeyGen, 2014) and cross-flow turbines (ORPC, 2016), investigations into the angle of approach are likely to be important if we are to better understand the risk that different TEC designs pose to receptors of interest.

Another benefit of the simulation-based approach is that relationships between input parameters can be investigated. Herein, to provide a basic example of this, three input parameters; animal speed, size and angle of approach, were explored. In comparison, both the ERM and the Band model use simplified relationships with changes to inputs, where the equations used to calculate probabilities assume a linear relationship between impact probability and changes to speed or animal length. These assumptions may not be correct, as different parameters relative to the receptor of interest (e.g., shape, speed or angle of approach) and device characteristics (e.g., device type) could alter the relationship between these covariates. Therefore, the dynamic nature of the simulation-based approach means these relationships can be explicitly assessed and this can be done with a wide range of parameters for any device design (Chapter 2).

The ability to incorporate empirical data into collision risk estimates is a valuable attribute of this simulation-based approach. However, there are a growing number of studies showing that site-

specific variations in the environment and associated animal behaviour are characteristic within these high energy environments (Hastie et al., 2016; Joy et al., 2018b; Lieber et al., 2018; Russell, 2016). Therefore, when applying this approach to a real-world scenario, it is likely that site-specific data, where available, would generate more robust and accurate estimates of collision risk. However, where few empirical data exist, as is often the case, then the simulation-based approach can be used to assess worst case scenarios. Within the thresholds of what are considered plausible, this would be true for both the receptor and the TEC (e.g. if a developer wanted to assess the potential ecological impacts at the design phase).

In this chapter, post-processing of results from simulation with hypothetical dive profiles demonstrated a method for incorporating more data into collision risk assessments. This method was chosen as it can take into account the detailed differences in depth profiles and how they will affect collision risk in a similar manner found in (Band et al., 2016)**.** However, the incorporation of dive data, and other data sources such as movement behaviour, could be undertaken in a more holistic manner. For example, simulation conditions could be produced from distributions using random sampling techniques that would produce a collision risk estimate that has multiple input distributions that would produce an estimate with confidence intervals derived from empirical data. This would offer a more holistic and informative estimate of risk.

Key behavioural considerations for understanding collision risk are avoidance (an animal avoiding the area of a device; 'far-field') and evasion (an animal evading being struck by the moving part of the device; 'near-field') (Wilson et al., 2006). In the case of marine mammals and TECs, there is a lack of empirical data on these behaviours, as such, assessments may opt to use the worst case scenario (where there is no avoidance or evasion) or, a range of avoidance rates, e.g. 10, 20, 50% of animals will avoid collisions (Scottish Natural Heritage, 2016). However, recent studies have shown that harbour seals changed their behaviour as a result of the SeaGen device, the first grid-connected operational TEC (Joy et al., 2018b; Sparling et al., 2018b). In this case, Sparling *et al* (2018) found that, during operation there was no barrier-effect caused by the device, however, there was a reduction in movement of GPS tagged seals passing the TEC during operation. Joy *et al* (2018), also using the GPS tag data from these seals, investigated the direction and speed of movement of the animals. Incorporating these data within the ERM, Joy *et al* (2018) estimated a 90% reduction in collision risk. As well as understanding behavioural changes around TECs, observing fine-scale underwater movement in close proximity (e.g. <50 m) would improve our understanding of collision risk (Wilson et al., 2006). Developments to quantify and better understand underwater movement of animals in these tidally energetic environments is being addressed through three different technologies; active acoustic monitoring (Hastie et al., 2019a; Lieber et al., 2014; Williamson et al., 2017), passive acoustic monitoring (Gillespie et al., 2020; Macaulay et al., 2017; Malinka et al., 2018) and through animal-borne loggers (Gabaldon et al., 2019; McKnight et al., 2019). These methods provide information on how animals move in three-

dimensional space, which will provide valuable empirical data, such as angle of approach, animal speed, dive profile, and avoidance and evasion behaviours, that can be used to better inform this simulation-based approach to collision risk models.

The simulation-based approach was developed to build on previous CRMs that have been employed to predict the risk to animals posed by tidal energy devices. However, the principles that underpin the simulation-based approach can be employed, with ease, to a wide range of systems and scenarios that predict wildlife collision risk such as wind turbines with birds and bats (Masden and Cook, 2016) or ship strikes with whales (Williams and O'Hara, 2010). Therefore, the application of this simulation-based approach to provide a quantitative assessment on which to address other management and conservation questions is extensive.

3.4.1 Conclusion

This proof-of-concept study demonstrates the feasibility of simulation-based approaches to quantifying collision risk probabilities that can incorporate the best available scientific evidence and, where lacking, expert elicitation, to provide robust and transparent outputs that can consider uncertainties (i.e. variations in the input parameters). The development of this approach is ongoing, aligned with the overall aim of creating a user-friendly and flexible collision risk assessment tool. The intention is to produce an end product that will be useful to developers and consultants when it comes to undertaking collision risk modelling for environmental assessments, and for informing regulators and their advisors when considering the potential impacts on receptors during the application phase of a development.

Chapter 4: Incorporating mortality estimates into a simulation-based approach to collision risk

4.1 Introduction

A key issue when considering potential environmental impacts of TECs is collision risk between the device(s) and animals; this has, and continues to be, a potentially significant barrier in consenting these devices (Copping et al., 2020a). Estimates of collision risk are calculated using collision risk models (CRMs) which are used to predict the potential risk at a population or management unit level (Scottish Natural Heritage, 2016). However, there is still a level of uncertainty in collision risk estimates, largely due to the difficulty in validating models by directly witnessing any potential collisions and the often limited information and data available on fine-scale behaviour of animals around devices (Band et al., 2016; Gillespie et al., 2020; Wilson et al., 2006). CRMs currently make use of empirical data such as those pertaining to device characteristics and animal size, to produce probabilities of collision (Scottish Natural Heritage, 2016). Broadly, the estimates produced by the CRMs currently employed calculate the probability of a single transit by an animal leading to a collision which is then scaled up to a population level or management unit estimate of impact. Also, multiple values (e.g. 50, 75, 90, 98%) are often applied to these CRM estimates for the assumed evasion and avoidance by the animals (MeyGen, 2014).

While it is recognised that monitoring fine-scale animal behaviour around TECs is key to understanding the likely number, speed, and location of collisions; nonetheless, it is at which relative speeds, and the point on the animal's body where collision occurs that will determine which collisions are likely to cause death. To my knowledge, there are only three published papers that have investigated consequences of a collision with TECs using animals post-mortem recovered from strandings (Carlson et al., 2012; Copping et al., 2017; Onoufriou et al., 2019). Carlson *et al* (2012) and Copping *et al* (2017) showed, using tensile testing of tissue samples, that for orca (*Orcinus orca*), collisions were unlikely to be fatal irrespective of where the strike occurred on the animal's body (Carlson et al., 2012) and for harbour seals (*Phoca vitulina*), demonstrated a range of scenarios where mortality was likely, such as collisions with a tip speed over 6.5ms^{-1} (Copping et al., 2017). However, for both Carlson *et al* (2012) and Copping *et al* (2017) the physiology was modelled by simulating tissue structure to estimate the likelihood of severe injury and therefore did not consider any injuries that may occur to the organs or bone structure of the animal.

Using harbour and grey seal (*Halichoerus grypus*) carcasses and striking them at the sea surface with a tidal turbine blade attached to a small vessel, Onoufriou *et al* (2019) investigated at which relative speed and where on the seal's body severe trauma would likely occur, based on pathological examination of the carcasses post-collision. They predicted that pathological effects likely to cause mortality occurred at speeds greater than 5.1ms^{-1} (95% C.I. = 3.2-6.6 ms^{-1}). The results from these experiments were then used to refine a collision risk assessment by calculating the percentage of time the blade spent over 5.1 ms^{-1}. However, those calculations were based on 2D modelling that did not consider the 3D shape of the animal and the relative speed that occurs

from two moving objects colliding, therefore potentially underestimating the likelihood of mortality. Furthermore, the issue of concussion was unable to be investigated by Onoufriou *et al* (2019), which is important, due to the potential for lower collision speeds to cause concussion, resulting in marine mammals drowning, which would inflate the number of fatal collisions. Consequently, having a collision risk model with the ability to extract the location of a strike on the body of the animal, as well as the relative speed of collision, would be a valuable tool.

Here I further develop the simulation-based approach that can estimate collision risk for any TEC (Chapter 2) and incorporate ecological parameters (Chapter 3) to offer a method for estimating the probability of mortality in collision risk assessments. The approach applies a game design software, Blender (Blender Online Commuinity, 2018) and makes use of the wide variety of functions within the software to simulate collisions. For example, it uses the collision detection system to obtain additional information when a collision occurs, such as the speed and location of a collision on both the device and animal. By extracting the speed for each collision, outputs from the simulations can be used to determine the likelihood of mortality occurring and, in doing so produce a distribution of data from which the risk of mortality can be assessed.

This chapter aims to demonstrate how the simulation-based approach can be used to incorporate mortality estimates into a collision risk assessment. By simulating a horizontal axis turbine and a seal, a method is outlined for a) extracting collision speed, b) extracting the location of collision on the animal and c) applying the information on collision speed and location of collision to produce probabilities of mortality.

4.2 Methods

4.2.1 Simulations

Blender, an open-source 3D modelling and game-design software, was interfaced using a python script to setup and run simulations. The movements of an animal and TEC were simulated in 3D space, which was repeated over many simulations to calculate a collision probability (CP) over the swept area of the TEC. The simulations presented herein are of a seal moving horizontally downstream towards a rotating three-bladed horizontal-axis tidal turbine (HATT). The seals starting positions were set to ensure a uniform distribution of 0.5m intervals over a 22m by 23m area that covered the full swept area of the HATT, (i.e. the size of the rotor blade, 18m). The TEC was based on the dimensions and characteristics of the Siemens Atlantis AR1500 HATT and was simulated using the same 3D shapefile for the 18m diameter rotor blade previously used in Chapter 2. The seal was based on the dimensions of an adult harbour seal (Length = 1.41m, Width = 0.34m) (Scottish Natural Heritage, 2016). See Chapters 2 & 3 for full details of the model formation.

The effect of two factors on the collision speed were investigated: the approach speed of the animal and the rotational speed, in rotations per minute (RPM), of the device rotor. Three biologically

feasible approach speeds, equivalent to the animal's speed over ground were used. Low speed (0.5ms^{-1}) to represent an animal moving against the tidal current, a behaviour which has been recorded occurring in Strangford Lough (Joy et al., 2018b). Medium speed (1.8ms^{-1}) based on the Scottish Natural Heritage guidance for the mean swim speed of a harbour seal to be used in a CRM (Scottish Natural Heritage, 2016). High speed (4.0ms^{-1}) where a seal is moving with the tidal flow (Joy et al., 2018b). Two rotational speeds were chosen to represent the cut-in speed, at a tidal flow of approximately 1.0ms^{-1}, where the HATT begins rotating and reaches speeds of 8RPM and the operational speed of around 3.4ms^{-1}, rotating at approximately 14RPM (MeyGen, 2014). The RPMs associated with the cut-in and operational speeds were used to calculate the rotations in radians per second (RPS); the unit used to set the rotational speed of objects within Blender, which is calculated as:

Eq. 4.1 $$\boldsymbol{RPS = \frac{RPM \times 2\pi}{60}}$$

Where the number of times the blade completes a 360^{o} rotation ($\boldsymbol{2\pi}$) in one minute ($\boldsymbol{RPM}$) divided by the number of seconds in a minute ($\boldsymbol{60}$) produces the radians per second ($\boldsymbol{RPS}$) (Eq. 4.1). 211,500 simulations were run; these consisted of 21,150 starting positions with 100 time-lags per starting position. Time-lags, detailed further in Chapter 2, are used to calculate a probability for each starting position and, in undertaking a convergence study (Chapter 3), 100 time-lags were deemed sufficient for the scenarios tested here.

A python script was developed to extract the collision speed, point of contact on the animal and the location of the centre of the animal shape for each collision that occurs during the simulations. By subtracting the location of the centre of the animal shape from the point of contact, the point of collision on the animal was produced. These results, in addition to the original input parameters for each individual simulation, are output to a CSV file for further analysis. Each line of the CSV file corresponds to an individual collision and contains the collision speed, the point of contact on the TEC and animal, and an individual ID number for the simulation that corresponded to the input parameters for that individual simulation. The ID number of the simulations were used to match the results to the input file to generate a file that contained all the information for each scenario.

4.2.2 Analysis

4.2.2.1 Collision Speed

Using R (R Core Team, 2020) the collision speed was explored to demonstrate the difference between the cut-in speed scenarios and the operational speed scenarios. Collision speed over the device was also investigated by plotting the distribution of collision speeds for the points of collision. These plots were produced in R using ggplot2 (Wickham, 2016).

4.2.2.2 Collision Position

If a collision occurred on the head of an animal, this potentially could mean a higher probability of mortality (e.g. through concussion and subsequent drowning). To demonstrate how this issue can be addressed using the simulation-based approach, the point of contact on the animal was also classified as either ‘head’ or ‘torso’ by subtracting the animal location from the point of collision. From head to tail, a point 0.4m from the nose of the animal was chosen to define the difference between collision with the head (<0.4m) and torso (>0.4m). The distinction between head and torso collisions were then used to calculate probabilities with different precautions included, for example, determining all head collisions as fatal irrespective of the speed of collision.

4.2.2.3 Mortality Thresholds

In order to investigate how speed of collision affects collision risk, a variety of thresholds were applied to calculate mortality probabilities (MP). For example, a collision speed threshold could be set to $4ms^{-1}$ meaning any collision over that speed would be determined fatal. Multiple hypothetical collision speed thresholds (from 0 to $7ms^{-1}$) were applied to all scenarios to investigate how different thresholds influenced mortality probabilities.

In addition to applying a collision speed threshold, the position on the animal that a collision occurs was incorporated into the mortality probability estimate by classifying all head collisions as fatal and applying collision speed thresholds only to collisions with the torso. Graphical outputs were produced using R and ggplot2 across all the scenarios tested.

4.3 Results

4.3.1 Collision Speed

For each of the rotational speeds (RPMs) and seal approach speeds, distributions of collision speeds are presented (Fig. 4.1). The lowest collision speed for each scenario occurred at the hub (centre) of the device and increased linearly towards the tip of the blades (Fig. 4.1; black arrows). When comparing distributions, the cut-in scenarios (Fig. 4.1; left) showed slower collision speeds, as compared to the operational speed scenarios, which had collision speeds as high as $17ms^{-1}$ (Fig. 4.1; right).

The distribution of collision speeds varied with scenario, where some had a more even spread of collision speeds (Fig. 4.1f) and some had a more distinct peak (Fig. 4.1a). An even spread represents collisions occurring evenly across the device rotor, whilst the scenarios that have peaks in their distribution have collisions occurring more often near either the hub of the device (Fig. 4.1c) or at the fast-moving tips of the blades (Fig. 4.1d).

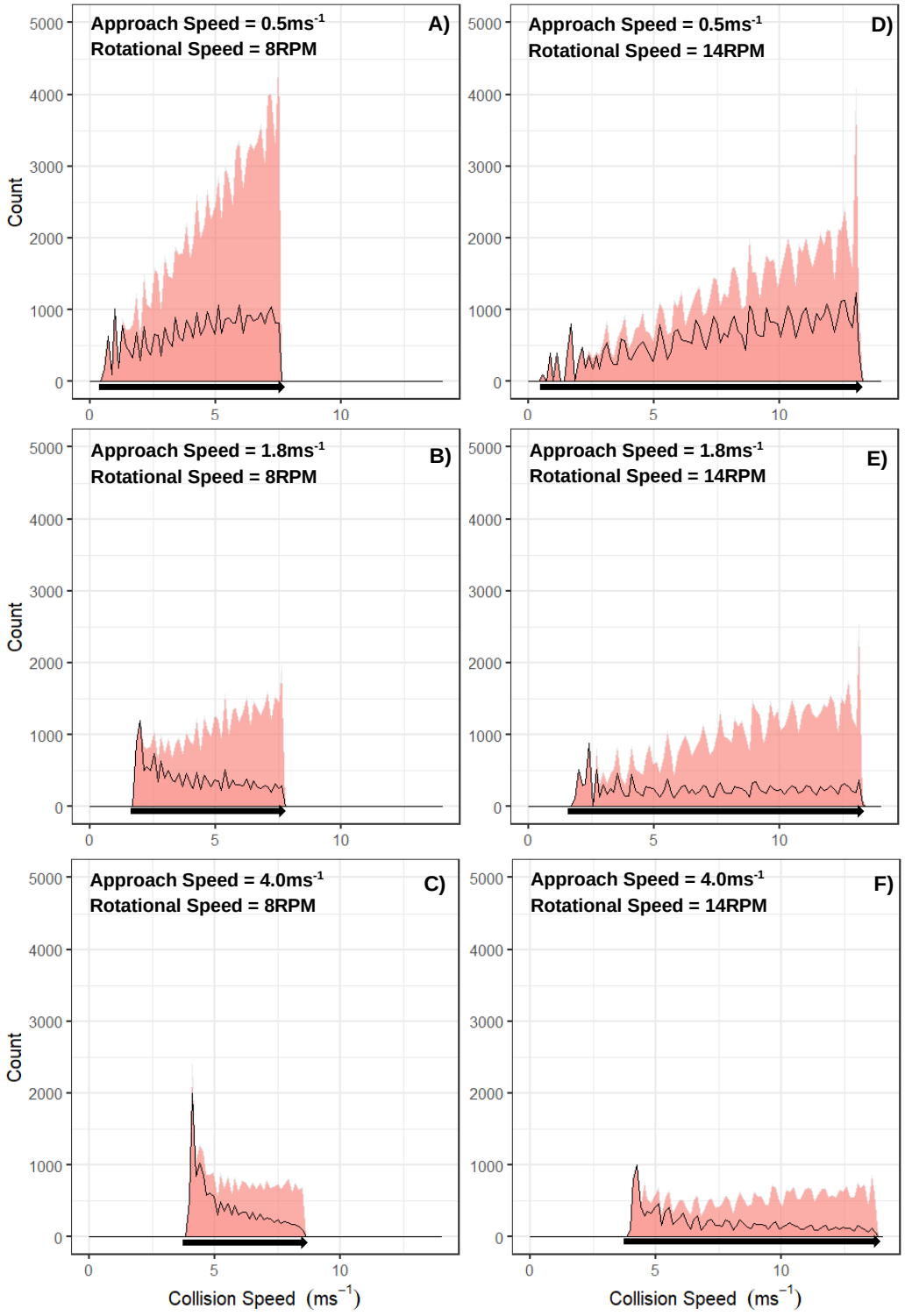

Figure 4.1. Area plots displaying the total number of collisions (area) and the number of times (count) varying collision speeds (ms^{-1}) (X-axis) occurred. The area under the black line are collisions with the head and the area above are collisions with the torso of the animal. Each graph represents a different scenario with approach and rotational speeds displayed on the corresponding graphs and the black arrows on the x-axis represent how the speed of collision increases from the hub to the tip of the blade (tip of the arrow).

4.3.2 Point of Contact

The point of contact is the position on the seal that the collision occurred, and this was assessed for accuracy by plotting the distribution from a side on view of the seal (Fig. 4.2). The collision positions on the X-axis, which represents the head to tail dimension of the seal, were deemed to be within reasonable bounds (error < 0.09%).

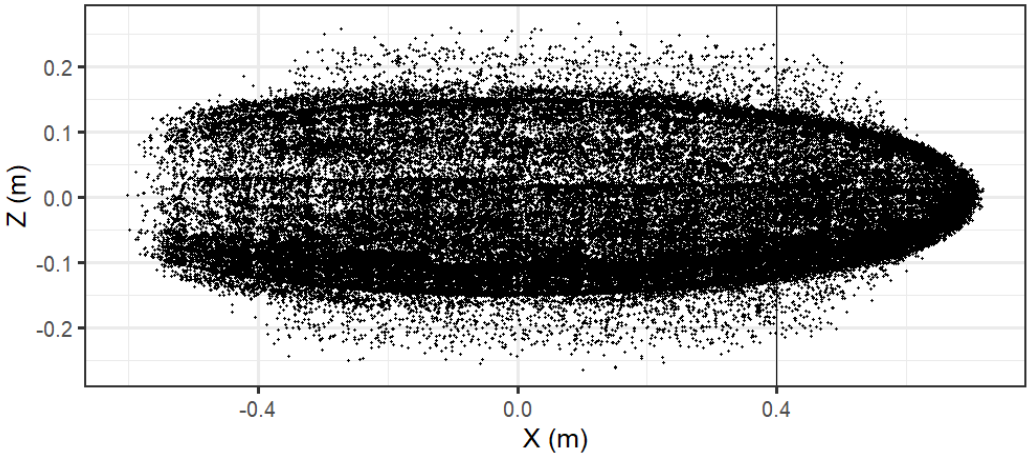

Figure 4.2. Points of collisions on the seal from a side on view, the X-axis displays the length of the seal object from head to tail and the Z-axis is the virtual width of the seal from dorsal to ventral. The threshold for head/torso collisions is displayed by the black line at 0.4m on the X-axis.

Over the range of scenarios, the number of collisions that occurred to the head of the animal compared to the torso changed dependent on both the approach (A) and rotational speed (R) (Table 4.1). A faster moving animal resulted in fewer collisions, whilst for most cases a faster device RPM resulted in more collisions. The mid-speed scenarios for both rotational speeds showed a lower percentage of head collisions when compared to the low and high approach speeds (Table 4.1). This indicated a non-linear pattern between animal speed, and the percentage of collisions with the head or torso. For example, when looking at the operational speed (Table 4.1; R2), the low-speed scenario (A1) had 53.0% of collisions with the head which dropped to 26.1% for the mid-speed scenario (A2). However, this trend did not continue, as for the high-speed scenario (A3), the percentage of head collision rose to 36.3%, indicating a more complex relationship between animal speed, RPM, location of collisions and the number of collisions. Also, it can be seen in Figure 4.1 that the collisions with the head (area below the black line) make up a lower proportion of collisions the higher the speed (or further towards the blade tip) that collisions occur.

Table 4.1. The total number of collisions in each scenario, and the % of those that were to the head or torso of the seal. The scenarios refer to the codes, where A1R1 represents the scenario for the slowest approach speed (A1) and the cut-in rotational speed (8RPM) (R1).

Scenario	Rotational Speed	RPM	Approach Speed	Speed	Head	Torso	Total
A1R1	Cut-in	8	Low	0.5ms^{-1}	33.8%	66.2%	103576
A2R1	Cut-in	8	Mid	1.8ms^{-1}	35.1%	64.9%	47688
A3R1	Cut-in	8	High	4.0ms^{-1}	51.2%	48.8%	27020
A1R2	Operational	14	Low	0.5ms^{-1}	53.0%	47.0%	102459
A2R2	Operational	14	Mid	1.8ms^{-1}	26.1%	73.9%	77773
A3R2	Operational	14	High	4.0ms^{-1}	36.3%	63.7%	38835

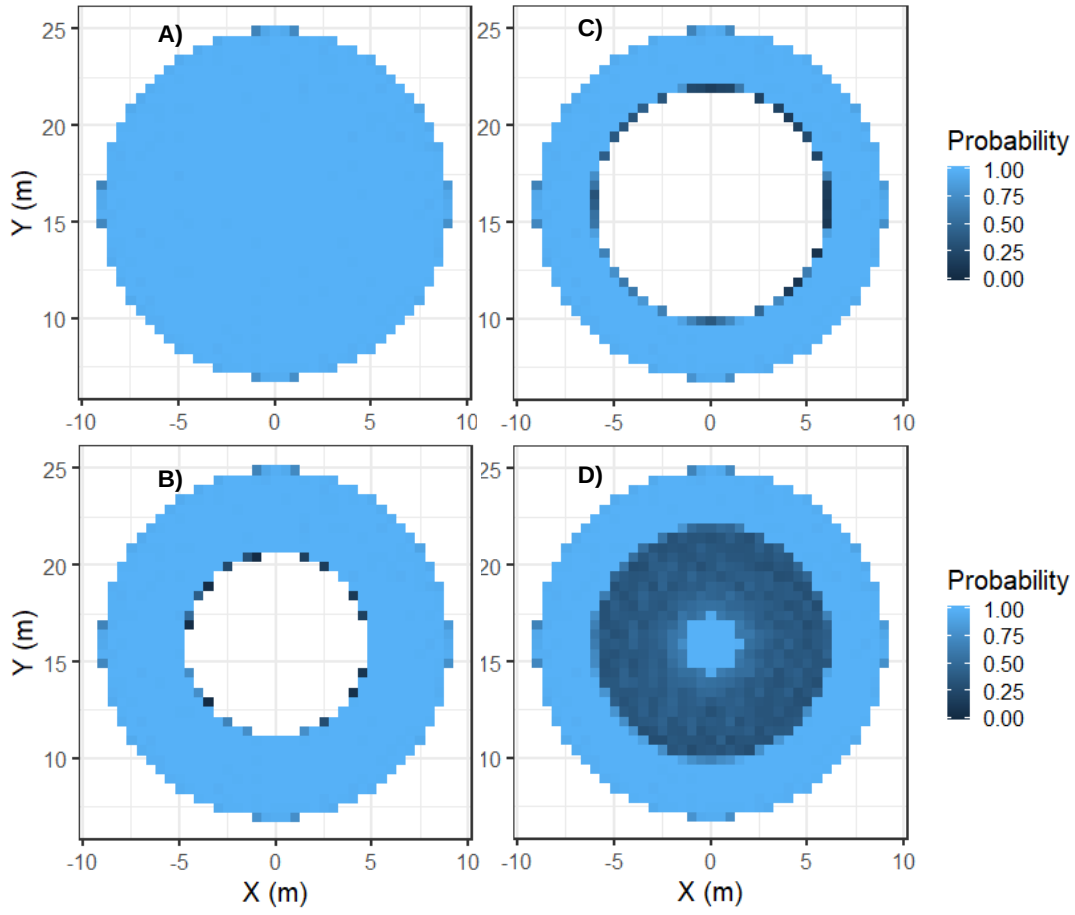

Figure 4.3. Probability of fatal collisions over the swept area of the device for scenario A1R1 for probabilities calculated with a) no collision speed threshold set (i.e. all collisions are fatal) b) above a collision speed threshold of 4.0ms^{-1} and c) above a collision speed threshold of 5.1ms^{-1} and d) all collisions with the head and collisions with the torso above a collision speed threshold of 5.1ms^{-1}.

4.3.3 Mortality Thresholds

The collisions near the hub of the device (i.e. the slower moving parts of the device) were not deemed fatal and were removed from calculations when a collision speed threshold was used (Fig. 4.3). Figure 4.3a shows a slow-moving animal (0.5ms^{-1}) with no collision speed threshold applied, which produced a uniform collision probability close to 1.0 across the entire swept area. However, when thresholds of 4.0ms^{-1} (Fig. 4.3b) and 5.1ms^{-1} (Fig. 4.3c) were applied, the low-speed collisions at the hub were deemed non-fatal, leading to a reduced mortality probability. When collisions with the head were deemed fatal regardless of the collision speed and only collisions with the torso were deemed fatal for speeds over 5.1ms^{-1}, this led to some collisions close to the hub being defined as fatal (Fig. 4.3d).

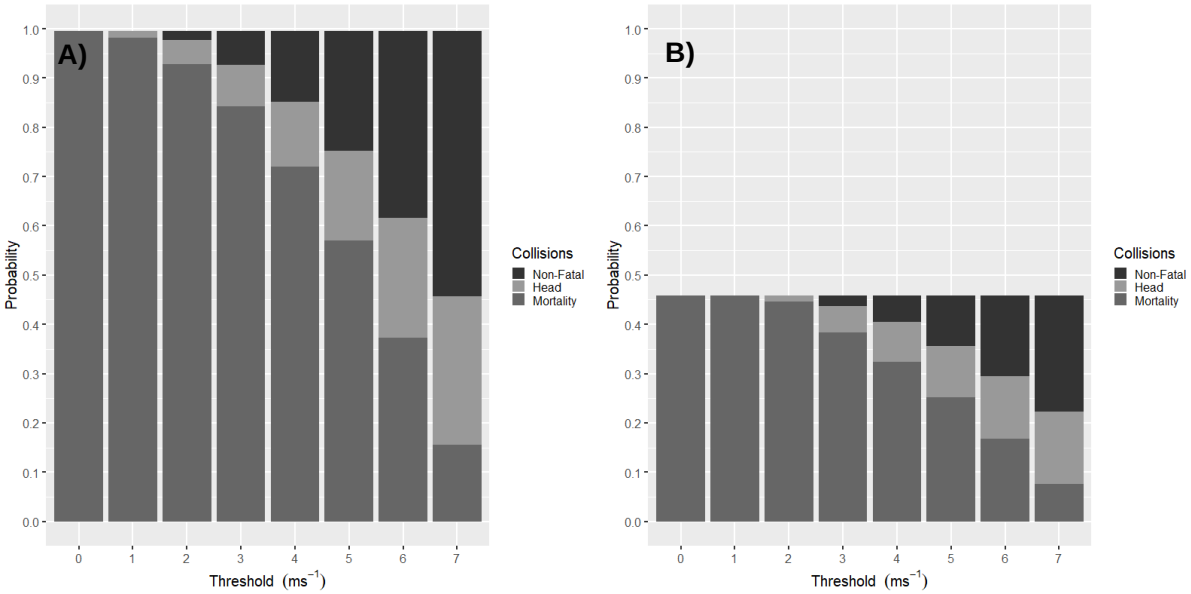

Figure 4.4. The probabilities for scenario a) A1R1 (low approach speed and cut-in rotational speed) and b) A2R1 (medium approach speed and cut-in rotational speed) with a variety of collision speed thresholds applied from 0 to 7ms^{-1}. The dark grey represents the mortality probability, which is classified as a collision that occurs at a greater speed than the threshold set, and the black represents the probability of an animal colliding at a speed lower than the threshold set and, therefore, is deemed to survive the collision. The light grey represents the probability that is made up of collisions above the threshold but where the collision was to the head of the animal.

A range of thresholds from 0ms^{-1} to 7ms^{-1} were used to examine what effect a variety of collision speed thresholds might have on the different scenarios (Fig. 4.4). The mortality probabilities in this regard were intuitive, as a less conservative threshold results in a reduced probability of mortality for each scenario. Furthermore, the change in scenario from a low approach speed (Fig. 4.4a) to the mid-speed (Fig. 4.4b) had a large effect on mortality probability before any thresholds were applied, a reduction in probability from 0.98 to 0.46. The way collision speed thresholds affect probabilities for different animal speeds can be demonstrated; for example, for a faster speed of approach (Fig. 4.4b), mortality probabilities were not affected by collision speed thresholds up to

2ms^{-1} due to the lowest collision speed being above 1.8ms^{-1} (i.e. the speed the animal was moving at); therefore, all collisions were deemed fatal.

By classifying all collisions with the head as fatal and only applying thresholds to the collisions with the torso, a higher mortality probability is calculated. For example, this increased the mortality estimate for A1R1 at 5ms^{-1} from 0.57 to 0.75 (Fig. 4.4a). Therefore, including all head collisions in the mortality probability estimate, irrespective of the collision speed threshold used, did provide a more conservative estimate. Furthermore, in these examples the conservative nature of this approach increases with collision speed, for example, for A1R1 at 3ms^{-1} the head collisions account for 0.08 of the mortality estimate whilst at a threshold of 7ms^{-1} they account for 0.30 of the mortality estimate.

4.4 Discussion

Improving our ability to estimate if mortality occurs when an animal collides with a tidal energy convertor (TEC) is an important step forward for collision risk assessments. This chapter demonstrated the first collision risk model (CRM) that can extract speed at the point of collision and where the location of the collision occurs on the body of the animal and on the device. This information can be used to predict whether collisions are fatal. In addition, the CRM also allows for the incorporation of other parameters including those relating to animal ecology and behaviour (e.g. dive patterns, Chapter 3) and different TEC designs (e.g. tidal kites, Chapter 2). Therefore, this model allows us to assess the uncertainty for given scenarios. For example, herein, I have demonstrated variation in mortality probabilities depending on collision speed thresholds and point of impact on the animal. Where earlier CRMs produced one value of collision risk, the plots produced by the simulation-based approach can be useful to advisors and regulators when considering realistic scenarios for assessing the potential impact on a protected population, for example, proportionate to the risk.

Variations to animal speed and device rotational speed affected the collision speed and where on the body of the animal collisions occurred. An increase in approach speed of the animal did not necessarily result in higher relative collisions speeds. For example, an animal is less likely to collide near the tip of the blade, the fastest moving part of the device, when it is approaching at faster speeds. Conversely, when the device is rotating faster, it increases both the collision speed, but also the probability of a collision occurring. The relationship between mortality and collision speed is complex, as changes to parameters (e.g. approach speed) will effect both the speed of collisions but also the number of collisions occurring.

Where the collision occurred on the body of the animal varied depending on the speed of the animal and the device. It may be expected that the point of contact on the animal would follow a simple rule, such as an increase in animal speed reduces the percentage of collisions with the head. However, the mid approach speed (1.8ms^{-1}) for both rotational speeds showed the lowest

percentage of collisions with the head whereas the low (0.5ms^{-1}) and high (4ms^{-1}) approach speeds showed a higher percentage of collisions with the head. This non-linear relationship is seen because the point of collision on the animal will depend on the speed of the animal, the speed of the device and where on the device collisions occur. When the seal is moving slowly (0.5ms^{-1}), the chance of a head collision is increased as the time taken to pass by the rotating blade is longer (Fig. 4.5a). Device speed is important here, as a faster moving blade will be more likely to strike the head of a slow-moving animal as the animal cannot pass enough of the rotating blade in time. However, when the animal had a faster (1.8ms^{-1}) approach speed, the proportion of head collisions reduced, as before colliding, the head of the animal could pass the rotating blade more often (Fig. 4.5b). However, the fastest approach speed (4.0ms^{-1}) led to a reduced number of collisions near the tip of the blade as the animal was moving faster than one full rotation of the blade and so it would no longer collide (Fig. 4.5). This produced more collisions near the hub (Fig. 4.1) which can be observed in Figure 4.1c, where the collision speeds for the 4.0ms^{-1} scenario showed a tall peak near 4.0ms^{-1} indicating a higher proportion of collisions near the hub, which will only occur with the head of the seal.

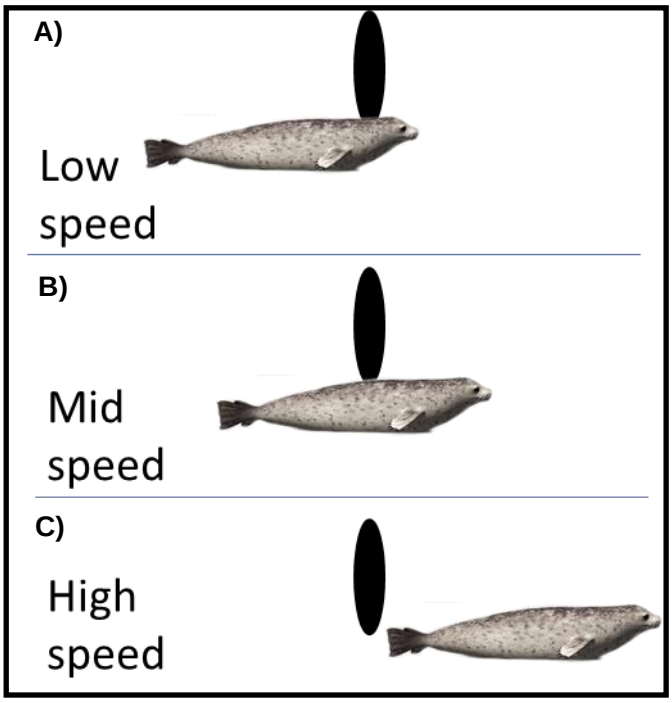

Figure 4.5. Diagram displaying three potential interactions between a rotating blade (black ellipsoid) and a seal that are likely to occur due to changes in animal approach speed. **A)** Displays a common occurrence with low approach speed, where the animal is moving so slowly that most collisions occur with the head. **B)** Demonstrates how at mid speed the seal is often moving fast enough for the head to pass the rotating blade before a collision occurs with the torso. **C)** Represents how at a high speed many more collisions are missed except for collisions near the hub of the device, which is most often with the head of the animal.

Here, we addressed the issue of concussion by determining all head collisions as fatal. The potential for animals to perform some evasive action (e.g. evading a direct strike from a blade) is

not considered in CRMs. Based on the scenarios used here, a large proportion of collisions often occur close to the hub of the device at low collision speeds. If evasive action is presumed, the animal could evade collision entirely, or collision could occur with the torso, rather than the head (as the animal would move its head away during evasive action) and, if that the collision is close to the hub the relative speed would be low and would have a low chance of being fatal. However, there would also be the possibility that evasive action could take the animal into the path of the faster moving tip, but still with this the animals speed towards the device would be lowered also, as it is no longer swimming directly towards the blades and therefore could still cause a reduction in collision speed and with a less sensitive part of the animal. Therefore, this could, offer a reduction in the chances of mortality as head collisions, speed of collision and the probability of collision could all be affected by the addition of evasive actions. The addition of any evasive action to collision risk modelling would, however, require additional empirical information on fine-scale animal behaviour.

Hypothetical collision speed thresholds, that were loosely based on empirical investigations of severe trauma (Onoufriou et al., 2019), were used to demonstrate how the simulation-based approach can be used to provide probabilities of collision and mortality over a range of speeds. This is a significant development to the traditional CRM approaches, which typically produce a single output value (i.e. number of animals colliding), over one or very few scenarios (MeyGen, 2014; Scottish Natural Heritage, 2016). Furthermore, the 2-dimentional nature of those approaches may underestimate collision speeds as they consider all collisions to occur perfectly perpendicular (i.e. a blade moving perpendicular to a seal) and use only the speed of the blade in the calculations. However, the blade and seal are 3D bodies that are actively moving, therefore when colliding they create a resultant force that is a combination of their two velocities, which is used to calculate the speed used throughout.

The ability to consider multiple scenarios based on empirical evidence or expert opinion, offers considerable advantages to industry and regulators. This will allow an increased ability to understand how uncertainty may impact upon the outputs from the CRM, and, in turn the perceived risk to a protected population or Management Unit. For example, the 95% confidence intervals around collision speed for harbour and grey seal mortality (3.2-6.6ms^{-1}) calculated by Onoufriou *et al* (2019), could be used to estimate a degree of uncertainty for the mortality estimate. This lower bound of the confidence interval (3.2ms^{-1}) could also be used in a precautionary manner for a vulnerable population, or where there is little information on status. The ability to adapt this approach to consider different scenarios is important, as often key parameters are location specific, for example, status of population (Thompson et al., 2019), behaviour of animals (e.g. dive behaviour) (Onoufriou, 2020), importance of the area (e.g. feeding ground, haul out sites, breeding colonies) (Benjamins et al., 2015), seasonal and diurnal variations in presence/occurrence (Allegue, 2017). Therefore, in an area where little is known about the ecology of a population, but

numbers are low or in decline, a more precautionary approach to the collision speed threshold could be employed, and this could be updated as and when more information becomes available.

Research, such as the fine-scale monitoring of marine mammals around TECs (Gillespie et al., 2020; Hastie et al., 2019a), may provide the best opportunity to refine estimates by incorporating site specific data in to the model. In the absence of empirical data, it is important that we continue to develop a framework of collision risk modelling that can facilitate a better understanding of the potential risk of collision and mortality by providing information on uncertainties and confidence intervals around these estimates. This approach, as demonstrated, can be adapted to incorporate new empirical data (or expert opinion) with ease as and when it becomes available.

Chapter 5: Fast & Flexible: streamlining a simulation-based approach to collision risk assessments.

This work has been accepted for publication as:

Horne, N., Schmitt, P., Culloch, R., Wilson, B., Dale, A C., Houghton, J D R., & Kregting, L. (2021). Fast & Flexible: streamlining a simulation-based approach to collision risk assessments. In *European Wave and Tidal Energy Conference*.

Abstract

It is critical that tools for assessing potential environmental impacts are, amongst other things, fit to reduce uncertainty and provide sufficient confidence to permit decisions. To address collision risk between marine mammals and tidal energy devices a simulation-based approach was developed to create a robust system that can adapt to any typical scenario and include novel device designs and ecological parameters. The approach here makes use of an open-source game-engine, Blender, to simulate a tidal energy device, the animal, and its movement in 3D to calculate collision probabilities. This free-to-use software offers an economical solution, however, the complexity of simulating a 3D environment, and adapting game-design software for the purposes of environmental questions poses challenges such as the time required for simulations to complete and the computing power required (e.g. number of CPU cores). The aim of this study was to streamline the simulation-based approach and outline a more efficient process so that the time to produce results is greatly reduced. Simulation runtime has been significantly reduced by employing increased parallelisation and enabling running the software on a high-performance computer. The end-to-end runtime was reduced by a factor of 17 to greatly improve efficiency. Further improvements to this simulation-based approach gives industry a greater number of options for robust quantification of collision risk and, consequently this work can aid regulators in making decisions during the consent, and post-consent phases of tidal energy developments.

5.1 Introduction

It is important that modelling tools for environmental assessments of marine renewables are comprehensive, cost-effective, and efficient. Collision risk, i.e. the risk of an animal colliding with the moving parts of a tidal energy converter (TEC), remains a key environmental concern to the growth of the tidal energy industry (Copping et al., 2020b). Estimating collision risk has been an issue since the first device was installed (Keenan et al., 2011) and can still hinder the consenting of device(s) (Copping et al., 2020b). Understanding the collision risk posed by TECs is a complex issue due to several factors such as, firstly, the difficult conditions for monitoring environmental conditions (e.g. turbidity, flow speeds), secondly, the variability of species present in the area, and the differing behaviours of animals (e.g. dive behaviour, avoidance, evasion), thirdly, the variety of device designs (Chapter 2) and finally, the modelling of collision risk with limited data (Copping et al., 2020b). Estimating collision risk is therefore a difficult problem and requires a comprehensive modelling approach that can tackle the complexities of the issue whilst maximizing computational efficiency.

The simulation-based approach developed by Schmitt *et al* (Schmitt et al., 2017) simulates an animal and TEC in 4-dimensions (3D space and time) and can assess any device design (Chapter 2). It can also incorporate ecological data by varying input parameters, such as the animal's angle of approach to produce more informed collision risk estimates (Chapter 3). Furthermore, in terms of cost, it is a cost-effective tool, making use of the open-source game-engine software Blender

(Blender Online Commuinity, 2018). Depending on the complexity of the scenario, to obtain the desired results, thousands or even millions of simulations might need run to calculate collision risk probabilities. These take time.

In the model's present setup on a standard computer, it may take several days to run 3D simulations for a single scenario as the approach is making use of game-engine software and is computationally demanding. For example, one of the scenarios, outlined in Chapter 3, to simulate collision risk between a harbour seal and tidal kite for one swim speed with a set angle of approach required the running of over 500,000 simulations, taking approximately 5 days to complete. The simulations can be run in parallel to improve efficiency, however, the game-engine, despite its advantages, is not designed to be run without a graphical user interface (GUI).

Displaying 3D simulations uses a large amount of computing power which limits the computational efficiency of the model. While the model has been run previously, with a GUI, in parallel with up to eight simulations running simultaneously, if more simulations could be run in parallel, the time to completion may be reduced greatly. For the efficiency of the approach to be improved a solution is required to run the model without a GUI. In addition, the number of simulations the model can run in parallel needs to be tested to investigate the improvements to the efficiency of the approach.

This paper outlines a method for running the simulation-based approach in a streamlined setup. Efficiency was tested initially by running with and without a GUI on a standard computer. Secondly, the streamlining of the simulation-based approach was assessed with an increased number of simulations in parallel on a standard computer and a high-performance computer.

5.2 Methods

5.2.1 Simulations

The simulation-based approach runs a multitude of simulations of an animal and TEC moving in 3D space to produce collision probabilities. For example, an individual simulation consists of an animal starting off in a determined position and is given a direction and speed to travel that will pass by the TEC. The TEC is given movement based on operational conditions of that design, for example, rotation at a set rotations per minute (RPM) for a horizontal axis turbine for a set flow velocity. Full details of simulations can be found in Chapter 2 and 3.

In this study, to test the efficiency of the model in a consistent way, a simple case of one starting position, one speed of animal and one speed of device was tested. This allowed for a direct comparison of results, with respect to the time it took to complete the simulations using a standard computer and a high-performance computer (Table 5.1).

5.2.2 Scripting

To setup simulations, an input CSV file, provides the settings for each individual simulation. The input file has a user-defined number of ‘splits’, each creating new input files that can be used to run many simulations in parallel.

Table 5.1. Specifications of the devices used for testing of model efficiency.

Computer	**CPU Cores**	**Processors**
Laptop	8	1 Intel Core i7-7700HQ CPU 4 Core Processor
HPC	64	2 AMD EPYC 7282 16-Core Processor

For example, when running 1000 simulations with 5 splits, 5 input files would be needed each with the settings for 200 individual simulations and these could all be run simultaneously using a python script to control all aspects of the model.

To reduce the amount of computing power used by the model, Blender had to be run ‘headless’ i.e. without producing a graphical user interface (GUI). This was achieved by making use of a game-engine function ‘setRender’ that when set to false, stops the game-engine from rendering any complex 3D graphics. With this function added to the python script that runs the model, it was then possible to use a virtual frame buffer (VBF) to create a virtual system that acts, in the background, as a monitor that manages all display information produced by Blender. The type of VBF employed was Xvfb (David P. Wiggins, 2021) this was done using the Xvfb-run command before calling for Blender to run.

5.2.2.1 Headless vs GUI

To test the increase in efficiency from running the model headless, a comparison was run on a single computer, a standard laptop (Table 5.1), using 100 simulations. The time taken for simulations to complete (runtime) was recorded for 5 different numbers of splits (5, 10, 20, 25, 30) for the two methods, headless and GUI.

5.2.2.2 HPC vs Laptop

Further testing was undertaken by comparing the efficiency of the model using higher computing power. Two computers (Table 5.1) were tested, a laptop and high-performance computer (HPC), with the time taken for 1000 simulations to be run in the headless setup recorded. The number of simulations were increased to 1000 as six different numbers of splits were tested (5, 10, 20, 40, 80, 160).

5.3 Results

The model was run successfully across all comparisons for both the headless and GUI methods and on the two computers.

5.3.1 Headless vs GUI

Running the model headless consistently showed a reduction in runtime for a given number of splits. The shortest runtime for headless and GUI was 42 seconds for 20 splits, and 52 seconds for 25 splits, respectively (Fig. 5.1). At 30 splits the two methods both showed a large increase in time to completion, illustrating the computational burden of running a larger number of simulations simultaneously. This outlines that, at a point, increasing the number of splits will have a detrimental effect on the runtime, due to the CPU becoming overwhelmed and ceasing to operate effectively.

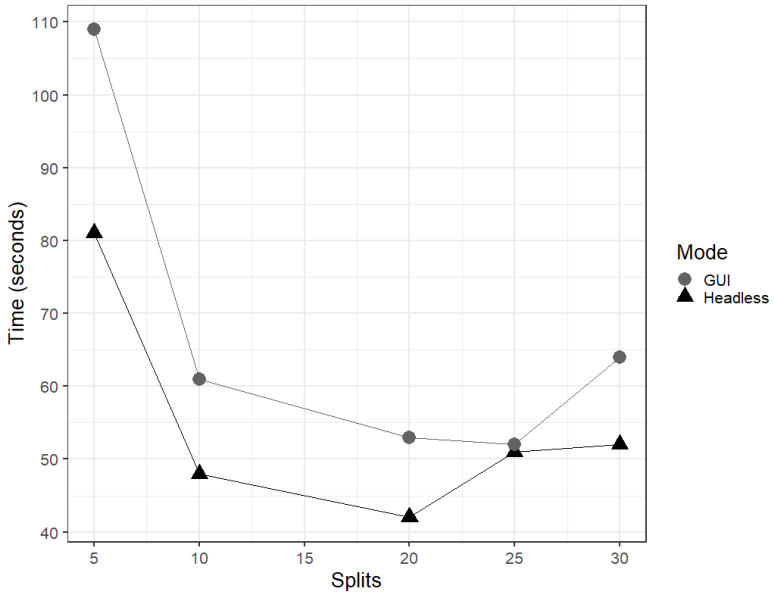

Figure 5.1. Time (seconds) to complete 100 simulations on the laptop for the five splits (5, 10, 20, 25, 30) for the model run headless (black, triangles) vs with a GUI (grey, circles). The number of splits represents how many times the 100 simulations are divided e.g. for 10 splits each split runs 10 simulations and for 20 splits each split runs 5 simulations.

5.3.2 HPC vs Laptop

Running the model on the HPC allowed an increased number of simulations to be run simultaneously. The HPC showed the greatest improvement in runtime with a consistent improvement from 5 (711 seconds) to 160 (41 seconds) splits (Fig. 5.2). The reduction in runtime on the HPC was less prominent as the number of splits increased, where the smallest decrease was from 80 splits to 160 splits (18 seconds) (Fig. 5.2), which indicated that any additional splits would be unlikely to increase the efficiency. On the laptop, runtime decreased as the number of splits increased, until 40 splits, thereafter, the runtime greatly increased (Fig. 5.2). Running 1000 simulations at 40 splits on the laptop, however, showed a decrease in runtime (Fig. 5.2) Overall,

the improvement in efficiency of running the model headless on a HPC reduced the runtime from 711s to 41s (Fig. 5.2).

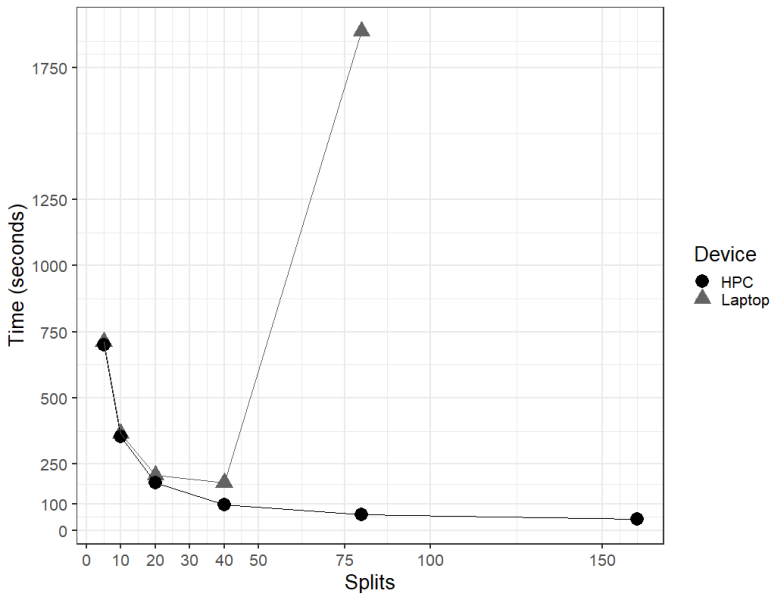

Figure 5.2. Time (seconds) to completion of 1000 simulations run on HPC (black, circles) and Laptop (grey, triangles) over 6 different splits (5, 10, 20, 40, 80, 160). The number of splits represents how many times the 1000 simulations are divided e.g. for 10 splits each split runs 100 simulations and for 100 splits each split runs 10 simulations.

5.4 Discussion

When the headless setup simulation-based approach was carried out on a high-performance computer the runtime was improved by a factor of 17. Previously, the simulation-based approach could take up to a week to run the 1000s of simulations required to produce a collision probability for a given scenario, such as the those demonstrated in Chapter 3. Now, these same results can be achieved in less than 12 hours. The 36,450 simulations that were used to produce comparable results to the ERM and Band model in Chapter 6 would have taken under an hour.

Removing the GUI from the model made a slight improvement to the runtime. The decrease in runtime was roughly 10s independent of the number of splits, with the notable exception of the 25-split case, where no improvement was found. The reason for this is unclear and under further investigation. The main advantage of running the model in a headless setup is that it simplifies the running of the model and removes any need for 3D rendering. The laptop on which the model was run had a graphics card and this may have contributed to how well it performed with a GUI, however the effect of removing the GUI may be greater on other hardware setups, such as those without a graphics card. This change could therefore make the model more accessible to those without high computing power, whilst still allowing a significantly improved runtime.

The model was able to be run 160 simulations simultaneously on the high-performance computer. The two computers performed similarly until 40 splits, where the time to completion differed slightly more, as the laptop was close to computational capacity and then after 40 splits the time to completion increased dramatically. The two computers performed similarly until 40 splits because, as long as the computer is not at computational capacity, the model must complete each simulation, which takes a set amount of time, and the main time difference between the two computers was due to the time to initiate Blender. This difference becomes more apparent when comparing the two tests. As the first test was run for 100 simulations and the second for 1000 simulations, the effect of initiating Blender accounted for a greater proportion of the runtime for the first test. Consequently, the most efficient number of splits for the model run headless on the laptop was 20 splits for the first test (Fig. 5.1) and 40 splits for the second test (Fig. 5.2). Therefore, when running a complete scenario that would require 100,000s of simulations, the number of splits possible is the most important factor in reducing the runtime.

The number of simulations run simultaneously was greatly improved, which has lowered the time it takes for the model to run. The high-performance computer used here showed little improvement at 160 splits, however there is potential for this to be improved further using more high-performance nodes. Since the simulations can be run entirely independent from each other and do not require the exchange of any information between processes, parallelisation is simple and not limited by inter-processor communication, as is usually the case for many other numerical simulation tools. Although the Blender game-engine in its proxy settings provides a flexible platform to model collision risk, it did have a long runtime to test different scenarios, especially when addressing complex issues such as changes to the angle of approach, speed, and size of the animal (Chapter 3). However, the streamlining of the simulation-based approach presented herein allows the many features of the model to be exploited without the burden of an excessively long time to produce results. Furthermore, with developments of this nature, a collision risk model can be made available that many users, such as consultants and researchers, can use without extensive understanding of coding, modelling or high-performance computing.

The simulation-based approach offers many advantages over other collision risk models. It provides a comprehensive tool that can test any device design (Chapter 2) and incorporate many different parameters (Chapter 3). These developments continue to demonstrate how the approach could be used in the future to provide highly comprehensive assessments of collision risk across a multitude of scenarios. The improved efficiency of the model now reduces the time burden of testing multiple scenarios and will facilitate more comprehensive collision risk assessments that will ultimately be able to provide measures of sensitivity and uncertainty through confidence intervals obtained from running multiple alternative scenarios. For example, important data sources, such as the speed of animal and device, could be tested to investigate uncertainty around the input values and the effect on collision risk estimates. This information could better inform

where effort should be focused on gathering empirical data on TECs and collision risk (Copping et al., 2020b; Gillespie et al., 2020; Onoufriou et al., 2019). Further improvements to this simulation-based approach gives users, such as environmental consultants, a greater number of options for robustly quantifying collision risk. As a consequence, this work can aid regulators in making decisions during the consent, and, where applicable, post-consent phases of tidal energy developments.

Chapter 6: Comparison of the simulation-based approach to other collision risk models

6.1 Introduction

Before a tidal energy converter (TEC) can be installed, an environmental impact assessment (EIA) is typically required to quantify the risk to receptors of interest, and ultimately aids regulators in whether to consent the project and on what conditions. To date there have been several TECs installed globally, each development undertaking an assessment of collision risk for receptors of interest (e.g. marine mammals) as part of an EIA (Keenan et al., 2011; MeyGen, 2014). The aim of the EIA is to understand risk and, if required, can be used to aid in risk mitigation and recommendations (Glasson et al., 2019). To give an estimate of the collision risk, in terms of a predicted number of animals per time period (e.g. year) collision risk modelling (CRM) is typically used (MeyGen, 2014; Scottish Natural Heritage, 2016). Previous chapters have focused on developing the simulation-based CRM that can estimate risk for any TEC (Chapter 2), alter input parameters (Chapter 3) and estimate mortality (Chapter 4). These developments allow the model to produce refined collision probabilities through simulations which is the probability of an animal colliding from a single transit through the swept area of the TEC. For the simulation-based approach to be incorporated routinely into TEC licencing procedures it must be placed in the context of a full collision risk estimate (number of animals per time period, e.g. year) such as those produced by other CRMs for EIAs.

To date, two CRMs are commonly used in research and EIAs, the Band Model and the Encounter Rate Model (ERM) (Scottish Natural Heritage, 2016). These models both use a formulaic approach to estimate collision risk by using the number of animals in the area of the device, the speed of animal and device, and the time period being investigated (Scottish Natural Heritage, 2016). The Band Model has been used for tidal energy developments since being adapted from its use in collision risk modelling of birds and wind turbines in 2000 (Band, 2000). The ERM, similarly, was adapted from a predator-prey model to assess tidal energy collision risk in 2006 (Wilson et al., 2006). The main difference between these models is how the risk is calculated; the Band model calculated the number of transits through the swept area of the rotor, whilst the ERM calculates the volume swept by each blade over time. Another subtle difference between the two models is how the Band model estimates risk for an animal approaching horizontally (perpendicular to the rotor) (Scottish Natural Heritage, 2016). The ERM however, estimates the risk from every angle uniformly (Wilson et al., 2006). These two models are limited to addressing collision risk for horizontal axis tidal turbines (HATT), which make up the majority of installed TECs so far (Zhou et al., 2017). However, TEC designs are not limited to HATTs, such that a range of designs exist, including crossflow turbines (ORPC, 2016), tidal kites (Zambrano, 2016), and vertical axis turbines (Hammar et al., 2013). Therefore, an approach is needed to provide robust estimates of collision risk of these TEC designs.

The development of the simulation-based approach offers a solution to the limitations of previous models. Where the previous chapters have focused primarily on the input parameters used to

produce the collision probabilities, other information, such as the number of animals in the vicinity of the device, must also be incorporated to scale the probability of collision risk to a meaningful estimate, e.g. number of animals colliding per year (Scottish Natural Heritage, 2016). With respect to the Band model, which is the most commonly used in EIAs, the probability of risk is calculated from a single transit, which in the Band model is named $pcoll$ (Scottish Natural Heritage, 2016), and therefore the remaining elements of the Band equations may be used to calculate a collision risk estimate from the collision probability produced by the simulation-based approach.

The objective of this chapter was to produce a collision risk estimate using the simulation-based CRM to compare to those results of the ERM and Band model. To do this, the collision risk estimate for harbour seals (*Phoca vitulina*) is produced using the Falls of Warness example outlined in the Scottish Natural Heritage Guidance Note on tidal energy collision risk (Scottish Natural Heritage, 2016). The predicted number of harbour seals colliding in a year with a TEC is calculated and compared to the Band model and ERM results for the same example.

6.2 Methods

6.2.1 Band Model Equations

The Band model equations offered a simple solution to calculate collision risk estimates using collision probabilities produced with the simulation-based approach. The collision probability, i.e. the probability of an animal colliding with the device from a single transit, is used in the Band model (Scottish Natural Heritage, 2016) when calculating collision risk and is represented as $pcoll$ here, I have adapted the equation to include $Collision\ probability$ which represents the value produced using the simulation approach as follows:

Eq. 6.1 $$C_{CRM} = D \times \pi(R + 0.5W)^2 \times v \times Collision\ probability$$

Where Eq. 6.1 calculates the no avoidance encounter rate per second (C_{CRM}) by multiplying the $Collision\ probability$ by the velocity of the animal (v), the swept area of the device ($\pi(R + 0.5W)^2$) and the density of animals at risk depth (D).

The second equation used as part of the Band model calculates the number of collisions in a time period without avoidance. It multiplies the no avoidance encounter rate (C_{CRM}) with the time period (t) and the proportion of time in operation ($1 - nop$) which produces the number of predicted collisions in a period without avoidance, for example the number of seals per year, which constitutes a collision risk estimate.

Eq. 6.2 $$Collisions\ in\ period\ without\ avoidance = C_{CRM}(1 - nop)t$$

The simulation-based approach can therefore be integrated into the two equations above to produce a collision risk estimate with the simple adaptation made to Eq. 6.1.

6.2.2 Falls of Warness Example

To allow direct comparison of results from the simulation-based approach with the Band model and the ERM, the Falls of Warness example was used for a harbour seal (Scottish Natural Heritage, 2016). This example is an assessment from the European Marine Energy Centre (EMEC) tidal test site on Orkney and used empirical data from wildlife surveys of the site from 2005-2014. The input parameters from the example (Table 6.1) were used in the setup of simulations, the remaining input parameters were then used with the simulation results using Eq. 6.1 and 6.2. Some parameters were used as an input into the simulations and in the adapted equations (Eq. 6.1). For example, animal approach speed is used as an input parameter for simulating an animal approaching the TEC, but it is also used in Eq. 6.1, as the speed of animals through the area is important in determining how many times animals will encounter the TEC.

Table 6.1. Inputs from the Falls of Warness example (SNH, 2016), the symbols, their units and values and their use in the model (i.e. using in the simulations, in Eq.1 and 2, or in both simulations and equation).

Input	Symbol	Unit	Value	Use
Animal length	L	m	1.41	Simulation
Number of blades	b	-	3	Simulation
Rotational speed	Ω	rpm	6.95	Simulation
Maximum blade width	Ω	m	1.5	Simulation
Blade profile	c/C	-	Table 2	Simulation
Blade pitch at tip	y	degrees	5	Simulation
Animal approach speed	v	ms^{-1}	1.82	Simulation/Equation
Animal width	W	m	0.34	Simulation/Equation
Rotor radius	R	m	12.5	Simulation/Equation
Animal density	D	animals m^{-3}	$3.33e^{-10}$	Equation
Time in period	t	s	$3.15e^{7}$	Equation
Non-operational period	nop	-	12.4%	Equation

6.2.3 Simulations

To run simulations for the Falls of Warness example, a rotor matching the device characteristics was developed. This was created using the blade information provided in Scottish Natural Heritage (2016), and included the rotor radius (e.g. blade length), the number of blades, maximum blade width and blade pitch at the tip (Table 6.1) as well as the blade profile (Table 6.2). An individual blade was produced using these specifications in FreeCAD (Juergen Riegel Werner Mayer, 2017) which was then imported into Blender (Blender Online Community, 2018) to be transformed into a rotor by multiplying the blade three times and joining them at the base.

The input files that provide the parameters for each simulation to be used in Blender were then created including the starting position of the animal, its length, width, and approach speed (Table 6.1). The animal angle of approach for these simulations was horizontal, i.e. perpendicular to the rotor, which is the same as in the Band model (Scottish Natural Heritage, 2016). To produce a collision probability, a 26m grid of 1m by 1m starting positions were used and 50 time-lags were used per starting position. Further details of grid size and time lags can be found in Chapter 2. This created 729 starting positions, meaning there were a total of 36,450 simulations run.

The collision probability was produced from the outputs of the model after simulations were completed using R (R Core Team, 2020). The collision probability was then used with Eq. 6.1 and Eq. 6.2 to produce a collision risk estimate in number of seals per year.

Figure 6.1. Diagram of a tidal turbine blade where the rotor with a radius R is the length of the blade, and r is a distance along the blade. A chord (c) is the width of the blade at a point with C being the maximum chord length.

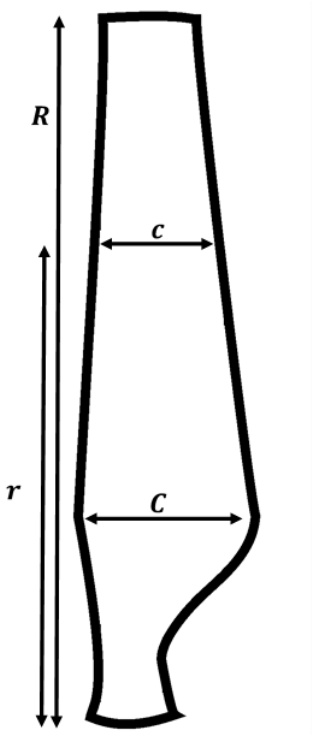

Table 6.2. Profile of the blade used in the Falls of Warness example, r/R is the position along the blade where the blade chord (c) is a proportion of the maximum blade chord (C).

r/R	c/C
0	0.690
0.050	0.730
0.100	0.790
0.150	0.880
0.200	0.960
0.250	1.000
0.300	0.980
0.350	0.920
0.400	0.850
0.450	0.800
0.500	0.750
0.550	0.700
0.600	0.640
0.650	0.580
0.700	0.520
0.750	0.470
0.800	0.410
0.850	0.370
0.900	0.300
0.950	0.240
1.000	0.000

6.3 Results

The simulation-based approach produced a collision probability of 0.3095 and when used within Eq. 6.1 produced a no avoidance collision rate of 9.46E-08 collisions per second. When Eq. 6.2 was incorporated the number of seals per year was estimated at 2.61.

When compared to the results for the ERM and Band model there was a -5.36% and -0.77% difference in the collision risk estimate, respectively (Table 6.3). Comparing the collision probability from the simulations to $pcoll$ calculated using the Band model the difference was -0.58%.

Table 6.3. Results from the simulations-based approach alongside the results for the Band model and ERM gathered from the Falls of Warness example in the Scottish Natural Heritage guidance note (Scottish Natural Heritage, 2016).

Result	**Simulation-based approach**	**Band model**	**ERM**
Collision probability ($pcoll$)	0.3095	0.3077	-
Collision rate per second of operation (no avoidance)	9.46E-08	9.39E-08	8.93E-08
Collision risk estimate (no avoidance)	2.61 seals per year	2.59 seals per year	2.47 seals per year
Percentage difference to simulation-based approach	-	-0.77%	-5.36%

6.4 Discussion

The results from this work indicate that the simulation-based approach results are comparable to two CRMs when using a basic scenario. The difference in results, when parameters are the same, were less than 1% and 6% different from the Band and ERM, respectively. The similarity of these results when using this basic scenario provides reassurance in the simulation-based approach, at least with respect to comparability to CRMs previously used in EIAs. While the previous models have provided collision risk estimates for EIAs (MeyGen, 2014), there are limitations to which parameters can be incorporated, whereas the simulation-based approach offers several advantages, as demonstrated in previous chapters.

The results from the simulation-based approach were closer to the Band model than ERM. This is likely due to the angle of approach being horizontal, which is the same as used in the Band model, whereas the ERM predicts collision risk from all angles equally (Scottish Natural Heritage, 2016). Neither of these methods are realistic as animals have varied behaviours and may favour certain approach angles, for example tagged black guillemots (*Cepphus grylle*) in the Pentland Firth

performed benthic dives 88% of the time and therefore would likely move in a trajectory close to vertical (Masden et al., 2013). Previous work using the simulation-based approach has provided a platform for altering the angle of approach (Chapter 3) and therefore can offer refinements to estimates. In addition, the swept area of the device would change if a more complex shaped device were incorporated like a tidal kite, which cannot be produced through the simple equations used in the Band model and ERM. To estimate risk in these scenarios, the results from the simulation-based approach could be used to calculate the swept area of the device with relative ease. The advantages of the simulation-based approach, such as altering inputs (Chapter 3) and estimating mortality (Chapter 4) allow for more refined collision risk estimates. These are incorporated in a flexible way and can be performed in a manner as requested by regulators; for example, mortality could be determined to occur above certain speeds of collision or with the head of the animal, irrespective of speed (Chapter 4). It is important that these additions to collision risk assessments are improved and updated upon the production of more data/information, for example with angle of approach being refined by data on the fine-scale movement of animals around TECs (Gillespie et al., 2020).

The simulation-based approach has been developed to offer an adaptable solution for collision risk assessments. The results produced are comparable to the Band and ERM and therefore provide reassurance in its use, especially as more information is incorporated into estimates and more complex scenarios are addressed. Uncertainty around collision risk estimates is a major barrier to the consenting of TECs and particularly so for arrays of devices (Copping et al., 2020b). It is therefore important for collision risk estimates to make best use of the data available to offer more robust estimates of risk. Studies are starting to gather more detailed information on animal behaviour around devices such as their fine-scale movement (Gillespie et al., 2020), response to noise of the device (Hastie et al., 2018) as well as movement in relation to the tidal flow in the area (Onoufriou, 2020). However, it is important to note the site-specific nature of this data (Benjamins et al., 2015; Onoufriou, 2020). Therefore, the simulation-based approach is an important and flexible tool for estimating collision risk where conservative estimates can be produced in the absence of site-specific data and refined as data become available.

Chapter 7: General Discussion

7.1 General Synthesis

The aim of this thesis was to develop a flexible, comprehensive, and robust approach for estimating collision risk between tidal energy converters and animals. I have developed this model using a simulation-based approach that can incorporate any type of TEC using the free open-source software Blender (Chapter 2). I have demonstrated how variations in input parameters (animal size, speed, angle of approach) can be incorporated into the model with relative ease (Chapter 3). I also outlined a method for post-processing results from the simulations to incorporate additional information on animal behaviour (Chapter 3). I provided an example of how mortality estimates can be obtained from the CRM, based on collision speed and where on the animal the collision occurs (Chapter 4). Whilst also highlighting the complexities of collision risk modelling by investigating the relationships between parameters, which identified that some relationships between parameters are non-linear (Chapter 4). The efficiency of the model was also improved by decreasing the computational time needed for simulations to run (Chapter 5). Furthermore, I demonstrated that the model produces similar results to the ERM and Band model for a simple scenario when all conditions are matched, which provided reassurance in the validity of the approach (Chapter 6). In demonstrating the flexible, comprehensive, and robust approach of the simulation-based model, I have also displayed the many advantages this approach has over the ERM and Band model (Chapters 2, 3 & 4). Overall, I have developed a model using a simulation-based approach that can be adapted and expanded to the needs of the user and therefore provides a state-of-the-art tool for producing collision risk estimates that can benefit several relevant stakeholders.

7.2 Advancing Collision Risk Modelling

The work presented in this thesis is a step change in the modelling of collision risk between TECs and animals. Other CRMs, such as the Band Model and ERM, produce a single value for collision risk. The simulation-based approach can produce several informative collision risk outputs including the speed of collisions, where on the animal a collision occurs (Chapter 4), and the distribution of collisions over the swept area of the TEC (Chapter 3) to provide highly informative estimates of collision and mortality probabilities (Chapter 4). Furthermore, being able to alter input parameters and produce detailed results that can be post-processed to incorporate further data sources (Chapter 3) means this approach can make best use of data as and when it becomes available.

Collision risk between TECs and animals is an issue for a wide range of species, including birds, fish, and marine mammals, therefore the flexibility of this CRM will be useful in tailoring estimates to different species. Within and amongst species there are many differences including size, shape, swim speeds (Wilson et al., 2006), their use of the tide (Hastie et al., 2016; Waggitt et al., 2017), and diving behaviour (Onoufriou, 2020). These differences can be easily incorporated by using different shapes and sizes of shape file that are a realistic representation of the animal whilst

different behaviours can be addressed by altering input parameters (Chapter 3). Also, for each species and/or TEC design, the angle of approach will likely be important for animals such as diving birds and/or novel designs such as the tidal kite (Chapter 3), which can also be readily included in the simulation-based approach. The flexibility of the simulation-based approach allows for the best available data to be incorporated to fit the needs of the end-user and produce robust and transparent collision risk estimates.

The various scenarios where collision risk modelling for tidal energy may be used are important to consider. Studies on animal behaviour in tidally energetic regions have shown a variety of behaviours (Onoufriou, 2019; Benjamins et al., 2017, 2016; Joy et al., 2018b; Sparling et al., 2018b; Waggitt et al., 2018). Many investigations have focused on the seal behaviour due to their protection and presence close to tidal developments in the Pentland Firth, Scotland (MeyGen, 2012) and Strangford Lough (Keenan et al., 2011). Tagging efforts in Strangford Lough during the operation of SeaGen have shown that seals often move against the tide in during fast flowing periods (Joy et al., 2018b) whilst also showing some level of avoidance to the device (Sparling et al., 2018b). Harbour porpoise are another species that has been studies extensively where research on harbour porpoise movement in tidal regions showed strong use of tidal currents (Benjamins et al., 2016). Much of the focus of new research on collision risk has centred around gathering more empirical data on animal behaviour around TECs (Gillespie et al., 2020; Hastie et al., 2019c, 2018; Joy et al., 2018). Technologies, such as passive acoustic monitoring (Gillespie et al., 2020; Malinka et al., 2018) and sonar tracking (Hastie et al., 2019b; Polagye et al., 2020), now enable the monitoring of animals passing through the swept area of tidal turbines. As this new information becomes available, the simulation-based approach will be well placed to incorporate the data and produce improved collision risk estimates. For example, empirical data from sonar or passive acoustic tracking of animals (Hastie et al., 2019b) could provide information on the angles and speeds that animals move close to TECs, which could be used to better inform the collision risk estimates using my model. As more data of this nature is produced, collision risk modelling would benefit from the development of a more holistic and realistic approach that could incorporate many data sources (and their inherent variability). This could be achieved using randomisation techniques, where each simulation has input parameters informed by empirically derived distributions and a random sample is taken from each distribution to set each input parameter. The resultant mean value and confidence intervals would therefore provide highly informative estimates of risk that can be aid in the licencing process.

Several EIAs for TECs have listed collision risk as a key concern (Keenan et al., 2011; Mcpherson et al., 2018; MeyGen, 2014). Over a decade, collision risk has been an area of active research with significant investment aiming to improve our understanding and reducing the uncertainty that comes with collision risk estimates. Despite these efforts this uncertainty is one aspect that is still acknowledged to be hindering the development of the industry (Copping et al., 2020b). A major

reason why the simulation-based approach was developed was to address the issue of estimating collision risk with novel device designs. This CRM has since been established as a versatile and useful approach with many advantages over other CRMs (Horne et al., 2021a, 2021b, 2019). Now, the simulation-based approach can not only be useful as a comprehensive tool for use in EIAs, but for investigating which parameters cause the greatest uncertainty in collision risk modelling.

7.3 Sensitivity Analysis

Accurately quantifying the risk of collision between TECs and animals is a complex problem with numerous parameters that may influence the estimated risk (Hammar et al., 2015; Wilson et al., 2006). The parameters involved can be broadly split into three categories: device, animal, and environment (Fig. 7.1). Figure 7.1 outlines some of the parameters that can influence collision risk, this is not an exhaustive list and does not consider the interactions between parameters. For example, the noise output of the device may be linked to the density of animals in the vicinity of the device, as a loud device may reduce the number of animals within the immediate area of the device (Hastie et al., 2018). Also, the approach speed of an animal and rotations per minute (RPM) of device depends on the tidal speed. Therefore, whilst it is important to understand the influence of each parameter on the results of the model separately, it is also important to investigate how they interact.

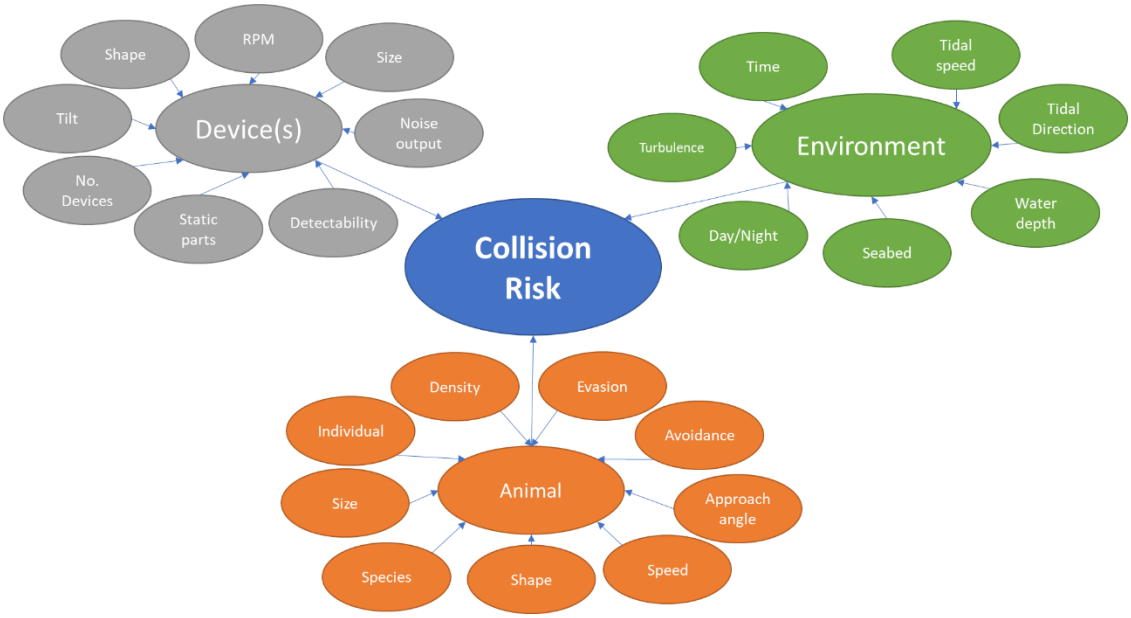

Fig. 7.1. Some of the parameters that may affect collision risk between TECs and animals, grouped across the three broad categories.

Sensitivity analysis, which is a method that measures how sensitive a result is to variations in each of the model parameters (Saltelli et al., 2008), would improve our understanding of the influence of parameters in collision risk modelling. For collision risk modelling, interactions between parameters, such as between animal speed and point of collision are likely to occur (Chapter 4) and non-linear trends are also likely to be present, such as those for angle of approach (Chapter

3). Therefore, global sensitivity analysis (GSA), which is able to assess these non-linear and interconnected relationships between parameters, would be a robust and appropriate method (Saltelli et al., 2008).

A pilot study was carried out to demonstrate how a GSA method could be applied to the inputs and outputs of the simulation-based approach to collision risk modelling (Appendix II). This was performed using the Sobol method of GSA which investigated how two inputs, tidal speed and animal density, influence collision risk estimates. The Sobol method assesses the sensitivity of the model output to the model inputs, put simply, to estimate sensitivities, the parameters being tested are varied, run through the model, and the variance of the results are analysed.

The pilot study unfortunately produced inconclusive results as it required a more detailed investigation, which will take several months for the simulations to run. However, in combination with the flexible nature of the simulation-based approach, the GSA could quantify and rank the most-to-least influential parameters. The outputs from this approach would be useful to researchers, developers, and consultants as the most influential parameters to collision risk may be different between locations, developments, and species. Also, data collection for EIAs can be an expensive and time-consuming process (Keenan et al., 2011; MeyGen, 2014). Therefore, understanding which data are most influential on collision risk models, and are the greatest sources of uncertainty, could guide future data collection efforts to improve collision risk assessment.

7.4 Future Work

For the tidal energy industry to contribute significantly to the global renewable energy production, arrays of devices are required (Zhou et al., 2017). Currently, collision risk modelling for arrays has involved modelling for a single TEC and is multiplied by the number in the array. This approach assumes the risk to be the same across each individual TEC, which is unlikely, as several factors, such as animal response to TECs and animal movement past the TEC, will likely differ for each TEC. Consequently, this may produce overly precautionary estimates. A solution that may offer some promise for understanding collision risk of arrays of TECs is the combined use of an agent-based model (ABM) and the simulation-based approach to collision risk. ABMs, such as the one being developed for the Pentland Firth (Chudzinska et al., 2021) makes use of a wide range of information to simulate the movement of animals in an area. An ABM can include an array of TECs in the area and predict, using telemetry data from tagged individuals, the behaviour of animals around the devices including their response to the TECs, such as from sonar and passive acoustic methods (Gillespie et al., 2021; Hastie et al., 2019a). This could allow a holistic approach, where a starting position, animal size, speed, angle of approach could be generated from the ABM and a simulation, using these data, is run to see where a collision occurs. This could then be run to produce an estimate for collision and mortality probabilities over a year, for example, that could also include an estimate of uncertainty. This would be a major step forward for estimating the

collision risk of arrays, and has wider uses, such as in the planning stage to investigate the effect of array configuration on key receptors.

7.5 Conclusions

To meet the net zero carbon targets such as those outlined in the Paris Agreement and the UN sustainable development goals, the renewable energy industry requires sustainable growth. As the tidal industry develops and different shapes of renewable energy devices are proposed, EIAs will need to give due consideration as to what impacts these variations from the typical single HATT devices may have on key receptors. The simulation-based approach offers a comprehensive predictive tool for assessing the risk of animals colliding with all types of TECs whilst incorporating a range of data sources. The principles that underpin the model can be easily adapted to a wide range of systems to predict wildlife collision risk, such as for wind turbines and birds (Masden and Cook, 2016), wave energy devices and marine life (Furness et al., 2012) and river flow devices and fish (ORPC, 2016). These industries all require similar consenting processes and will potentially interact with key receptors (e.g. birds, mammals, fish). Therefore, this CRM provides an optimal solution to address these issues using its flexible approach across the renewables industry, from wind in terrestrial and marine environments, to tidal and wave, all of which are critical in helping governments reach climate targets.

In conclusion, this tool is invaluable in providing transparent, flexible and comprehensive collision risk estimates. The simulation-based approach will be of interest to several relevant stakeholders, including regulators, their advisors, and consultants, due to its ability to incorporate empirical data and provide a clearer understanding of uncertainty. But also, to developers as this approach readily incorporates novel device designs and can be conveniently used at the planning stage to investigate, for example, the effects of array configuration on key receptors. The simulation-based approach, after more than three years of development, is at a place where it can be applied in an EIA context (as demonstrated through Chapters 2 – 6). The versatile and robust nature of this approach opens many avenues of exploration, such as sensitivity analysis. In exploring and developing these options I show further opportunities to better inform collision risk estimates and reduce knowledge gaps that are ultimately barriers to the tidal industry. Therefore, the expansion of the tidal industry will be aided by this research to support its role in combatting climate change.

References

375 Designs, 2014. Tidal Stream Turbine.

Alistair, J., Onoufriou, R., 2019. Harbour Seals (Phoca vitulina) in a Tidal Stream Environment: Movement Ecology and the Effects of a Renewable Energy Installation.

Allegue, H., 2017. Variability of harbour seal (Phoca vitulina) foraging behaviour during out-migrations of salmon smolts.

Atlantis Resources, 2016. AR1500 Tidal Turbine Brochure [WWW Document]. URL https://simecatlantis.com/wp/wp-content/uploads/2016/08/AR1500-Brochure-Final-1.pdf

Bachant, P., Wosnik, M., 2015. Characterising the near-wake of a cross-flow turbine. Journal of Turbulence 16, 392–410. https://doi.org/10.1080/14685248.2014.1001852

Band, B., 2000. Windfarms and birds: Calculating a theoretical collision risk assuming no avoiding action, Guidance Note Series, Scottish Natural Heritage.

Band, B., Sparling, C., Thompson, D., Onoufriou, J., Martin, E.S., West, N., 2016. Refining estimates of collision risk for harbour seals and tidal turbines. Scottish Marine and Freshwater Science 7, 133. https://doi.org/10.7489/1786-1

Batty, R.S., Wilson, B., 2010. Predicting the abilities of marine vertebrates to evade collision with tidal stream turbines . 3rd International Conference on Ocean Energy, 6 October, Bilbao 3–6.

Benjamins, S., Dale, A., van Geel, N., Wilson, B., 2016. Riding the tide: Use of a moving tidal-stream habitat by harbour porpoises. Marine Ecology Progress Series 549, 275–288. https://doi.org/10.3354/meps11677

Benjamins, S., Dale, A.C., Hastie, G., Waggitt, J.J., Lea, M.A., Scott, B., Wilson, B., 2015. Confusion reigns? A review of marine megafauna interactions with tidal-stream environments. Oceanography and Marine Biology: An Annual Review 53, 1–54. https://doi.org/10.1201/b18733

Benjamins, S., van Geel, N., Hastie, G., Elliott, J., Wilson, B., 2017. Harbour porpoise distribution can vary at small spatiotemporal scales in energetic habitats. Deep-Sea Research Part II: Topical Studies in Oceanography 141, 191–202. https://doi.org/10.1016/j.dsr2.2016.07.002

Blender Online Commuinity, 2018. Blender - a 3D modelling and rendering package.

Booth, C., Sparling, C., Wood, J., Tollitt, D., Scott-Heyward, L., Rexstad, E., Hultgren, Y., Johnsson, M., Knutzen, E., 2015. Advancing a key consenting risk for tidal energy: The risk of marine mammal collision for in-stream tidal energy, in: Proceedings of the 3rd Marine Energy Technology Symposium METS2015 April 27-29, 2015, Washington, D.C. p. 4.

Borthwick, A.G.L., 2016. Marine Renewable Energy Seascape. Engineering 2, 69–78. https://doi.org/10.1016/J.ENG.2016.01.011

BP, 2020. Statistical Review of World Energy.

Byrne, S., 1983. Bird Movements and Collision Mortality at a large horizontal axis wind turbine. Cal-Neva Wildlife Transactions 76–83.

Carlson, T., Elster, J., Copping, A.E., Jones, M., Watkins, M., Jepsen, R., Metzinge, K., Watson, B.E., 2012. Assessment of Strike of Adult Killer Whales by an OpenHydro Tidal Turbine Blade. Prepared for the U.S. Department of Energy by Pacific Northwest National Laboratory.

CG Trader, 2014. The-brandals, GORLOV Wind Turbine Free 3D model.

Chudzinska, M., Nabe-Nielsen, J., Smout, S., Aarts, G., Brasseur, S., Graham, I., Thompson, P., McConnell, B., 2021. AgentSeal: Agent-based model describing movement of marine central-place foragers. Ecological Modelling 440. https://doi.org/10.1016/j.ecolmodel.2020.109397

Copping, A.E., Grear, M., Jepsen, R., Chartrand, C., Gorton, A., 2017. Understanding the potential risk to marine mammals from collision with tidal turbines. International Journal of Marine Energy 19, 110–123. https://doi.org/10.1016/j.ijome.2017.07.004

Copping, A.E., Grear, M.E., 2018. Applying a simple model for estimating the likelihood of collision of marine mammals with tidal turbines. International Marine Energy Journal 1, 27–33. https://doi.org/10.36688/imej.1.27-33

Copping, A.E., Hemery, L.G., Overhus, D.M., Garavelli, L., Freeman, M.C., Whiting, J.M., Gorton, A.M., Farr, H.K., Rose, D.J., Tugade, L.G., 2020a. Potential environmental effects of marine renewable energy development—the state of the science. Journal of Marine Science and Engineering 8, 1–18. https://doi.org/10.3390/jmse8110879

Copping, A.E., Sather, N., Hannah, L., Whiting, J., Zydlewski, G., Staines, G., Gill, A., Hutchinson, I., A, O., Simas, T., Bald, J., Sparling, C., Wood, J., Masden, E., 2020b. 2020 State of the Science Report. State Sci. Rep. https://doi.org/10.2172/1632878

Copping, A.E., Sather, N.K., Hanna, L., Whiting, J., Zydlewski, G.B., Staines, G., Gill, G., Hutchison, I., O'Hagan, A.M., Simas, T., Bald, J., Sparling, C., Wood, J., Madsen, E., 2016. Annex IV 2016 State of the Science Report: Environmental effects of marine renewable energy development around the world. https://doi.org/10.1097/JNN.0b013e3182829024

David P. Wiggins, 2021. Xvfb.

Durand, N., Cornett, A., Bourban, S., 2008. 3D Modelling and Assessment of Tidal Current Energy Resources in the Bay of Fundy, in: 3rd International Conference on Ocean Energy, 6 October, Bilbao. pp. 2–7.

Easton, M.C., Woolf, D.K., Bowyer, P.A., 2012. The dynamics of an energetic tidal channel, the Pentland Firth, Scotland. Continental Shelf Research 48, 50–60. https://doi.org/10.1016/j.csr.2012.08.009

Eça, L., Hoekstra, M., 2014. A procedure for the estimation of the numerical uncertainty of CFD calculations based on grid refinement studies. Journal of Computational Physics 262, 104–130. https://doi.org/10.1016/j.jcp.2014.01.006

European Commission, 2007. Guidance document on the strict protection of animal species of Community interest under the Habitats Directive 92/43/EEC. Context 88.

European Marine Energy Centre, 2019. Tidal Devices, European Marine Energy Centre.

Felleman, F.L., Heimlich-Boran, J.R., Osborne, R.W., 1991. Feeding Ecology of the killer whale (Orcinus orca). In (KW Pryor and KS Norris, eds.) Dolphin Societies: Discoveries and Puzzles.

Fonoberova, M., Fonoberov, V.A., Mezić, I., 2013. Global sensitivity/uncertainty analysis for agent-based models. Reliability Engineering and System Safety 118, 8–17. https://doi.org/10.1016/j.ress.2013.04.004

Furness, R.W., Wade, H.M., Robbins, A.M.C., Masden, E.A., 2012. Assessing the sensitivity of seabird populations to adverse effects from tidal stream turbines and wave energy devices. ICES Journal of Marine Science 69, 1466–1479. https://doi.org/doi:10.1093/icesjms/fss131

Gabaldon, J., Turner, E.L., Johnson-Roberson, M., Barton, K., Johnson, M., Anderson, E.J., Alex Shorter, K., 2019. Integration, Calibration, and Experimental Verification of a Speed Sensor for Swimming Animals. IEEE Sensors Journal 19, 3616–3625. https://doi.org/10.1109/JSEN.2019.2895806

Gill, A.B., Bartlett, M., Thomsen, F., 2012. Potential interactions between diadromous fishes of U.K. conservation importance and the electromagnetic fields and subsea noise from marine renewable energy developments. Journal of Fish Biology 81, 664–695. https://doi.org/10.1111/j.1095-8649.2012.03374.x

Gillespie, D., Palmer, L., Macaulay, J., Sparling, C., Hastie, G., 2021. Harbour porpoises exhibit localized evasion of a tidal turbine. Aquatic Conservation: Marine and Freshwater Ecosystems 31, 2459–2468. https://doi.org/10.1002/aqc.3660

Gillespie, D., Palmer, L., Macaulay, J., Sparling, C., Hastie, G., 2020. Passive acoustic methods for tracking the 3D movements of small cetaceans around marine structures. PLoS ONE 15 (5). https://doi.org/https://doi.org/10.1371/journal.pone.0229058

GKinetic, 2021. GKinetic [WWW Document]. URL https://gkinetic.com/technology/

Glasson, J., Riki, T., Andrew, C., 2019. Introduction to environmental impact assessment, Routledge. https://doi.org/10.1080/07293682.2012.747551

Hammar, L., Andersson, S., Eggertsen, L., Haglund, J., Gullström, M., Ehnberg, J., Molander, S., 2013. Hydrokinetic turbine effects on fish swimming behaviour. PLoS ONE 8, 1–12. https://doi.org/10.1371/journal.pone.0084141

Hammar, L., Eggertsen, L., Andersson, S., Ehnberg, J., Arvidsson, R., Gullström, M., Molander, S., 2015. A probabilistic model for hydrokinetic turbine collision risks: Exploring impacts on fish. PLoS ONE 10, 1–25. https://doi.org/10.1371/journal.pone.0117756

Hastie, G.D., Bivins, M., Coram, A., Gordon, J., Jepp, P., MacAulay, J., Sparling, C., Gillespie, D., 2019a. Three-dimensional movements of harbour seals in a tidally energetic channel: Application of a novel sonar tracking system. Aquatic Conservation: Marine and Freshwater Ecosystems 29, 564–575. https://doi.org/10.1002/aqc.3017

Hastie, G.D., Russell, D.J.F., Benjamins, S., Moss, S., Wilson, B., Thompson, D., 2016. Dynamic habitat corridors for marine predators; intensive use of a coastal channel by harbour seals is modulated by tidal currents. Behavioral Ecology and Sociobiology 70, 2161–2174. https://doi.org/10.1007/s00265-016-2219-7

Hastie, G.D., Russell, D.J.F., Lepper, P., Elliott, J., Wilson, B., Benjamins, S., Thompson, D., 2018. Harbour seals avoid tidal turbine noise: Implications for collision risk. Journal of Applied Ecology 55, 684–693. https://doi.org/10.1111/1365-2664.12981

Hastie, G.D., Wu, G.M., Moss, S., Jepp, P., MacAulay, J., Lee, A., Sparling, C.E., Evers, C., Gillespie, D., 2019b. Automated detection and tracking of marine mammals: A novel sonar tool for monitoring effects of marine industry. Aquatic Conservation: Marine and Freshwater Ecosystems 29, 119–130. https://doi.org/10.1002/aqc.3103

Herman, J., Usher, W., 2017. SALib: an open-source Python library for sensitivity analysis. Journal of Open Source Software 2, 97.

Holmstrom, L., Hamer, T., Colclazier, E., Denis, N., Verschuyl, J., Ruché, D., 2011. Assessing avian-wind turbine collision risk: An approach angle dependent model. Wind Engineering 35, 289–312. https://doi.org/10.1260/0309-524X.35.3.289

Horne, N., Culloch, R., Schmitt, P., Kregting, L., 2019. Incorporating different tidal energy device designs into 4D collision risk simulations allowing increased flexibility for industry. Proceedings of the 13th European Wave and Tidal Energy Conference 12–13.

Horne, N., Culloch, R.M., Schmitt, P., Lieber, L., Wilson, B., Andrew, C., Dale, A.C., Houghton, J.D.R., Kregting, L.T., 2021a. Collision risk modelling for tidal energy devices: A flexible simulation-based approach. Journal of Environmental Management 278. https://doi.org/10.1016/j.jenvman.2020.111484

Horne, N., Schmitt, P., Culloch, R.M., Wilson, B., Dale, A.C., Houghton, J.D.R., Kregting, L.T., 2021b. Fast & Flexible : streamlining a simulation- based approach to collision risk assessments, in: European Wave and Tidal Energy Conference.

IPCC, 2014. Climate change 2014 Synthesis Report, Contribution of Working Groups I, II and III to the Fifth Assessment Report of the Intergovernmental Panel on Climate Change.

Joy, R., Wood, J.D., Sparling, C.E., Tollit, D.J., Copping, A.E., McConnell, B.J., 2018a. Empirical measures of harbor seal behavior and avoidance of an operational tidal turbine. Marine Pollution Bulletin 136, 92–106. https://doi.org/10.1016/j.marpolbul.2018.08.052

Joy, R., Wood, J.D., Sparling, C.E., Tollit, D.J., Copping, A.E., McConnell, B.J., 2018b. Empirical measures of harbor seal behavior and avoidance of an operational tidal turbine. Marine Pollution Bulletin 136, 92–106. https://doi.org/10.1016/j.marpolbul.2018.08.052

Juergen Riegel Werner Mayer, Y. van H., 2017. FreeCAD, Software.

Keenan, G., Sparling, C., Williams, H., Fortune, F., 2011. SeaGen Environmental Monitoring Programme Final Report.

Krahn, M.M., Wade, P.R., Kalinowski, S.T., Dahlheim, M.E., Taylor, B.L., Hanson, M.B., Ylitalo, G.M., Angliss, R.P., Stein, J.E., Waples, R.S., 2002. Status review of southern resident

killer whales (*Orcinus orca*) under the Endangered Species Act. U.S. Dept. Commer., NOAA Tech. Memo., NMFS-NWFSC-54. 159p.

Kregting, L., Elsaesser, B., Kennedy, R., Smyth, D., O'Carroll, J., Savidge, G., 2016. Do changes in current flow as a result of arrays of tidal turbines have an effect on benthic communities? PLoS ONE 11, 1–14. https://doi.org/10.1371/journal.pone.0161279

Kregting, L., Elsäßer, B., 2014. A hydrodynamic modelling framework for strangford lough part 1: Tidal model. Journal of Marine Science and Engineering 2, 46–65. https://doi.org/10.3390/jmse2010046

Levy, D.A., Cadenhead, A.D., 1995. Selective tidal stream transport of adult sockeye salmon (Oncorhynchus nerka) in the Fraser River Estuary. Canadian Journal of Fisheries and Aquatic Sciences 52, 1–12.

Lieber, L., Nimmo-Smith, W.A.M., Waggitt, J.J., Kregting, L., 2018. Fine-scale hydrodynamic metrics underlying predator occupancy patterns in tidal stream environments. Ecological Indicators 94, 397–408. https://doi.org/10.1016/j.ecolind.2018.06.071

Lieber, L., Williamson, B., Jones, C.S., Noble, L.R., Brierley, A., Miller, P., Scott, B.E., 2014. Introducing Novel Uses of Multibeam Sonar To Study Basking Sharks in the Light of Marine Renewable Energy Extraction 2–4.

Macaulay, J., Gordon, J., Gillespie, D., Malinka, C., Northridge, S., 2017. Passive acoustic methods for fine-scale tracking of harbour porpoises in tidal rapids. The Journal of the Acoustical Society of America 141, 1120–1132. https://doi.org/10.1121/1.4976077

Malinka, C.E., Gillespie, D.M., Macaulay, J.D.J., Joy, R., Sparling, C.E., 2018. First in situ passive acoustic monitoring for marine mammals during operation of a tidal turbine in Ramsey Sound, Wales. Marine Ecology Progress Series 590, 247–266. https://doi.org/10.3354/meps12467

Masden, E.A., Cook, A.S.C.P., 2016. Avian collision risk models for wind energy impact assessments. Environmental Impact Assessment Review 56, 43–49. https://doi.org/10.1016/j.eiar.2015.09.001

Masden, E.A., Foster, S., Jackson, A.C., 2013. Diving behaviour of Black Guillemots Cepphus grylle in the Pentland Firth, UK: Potential for interactions with tidal stream energy developments. Bird Study 60, 547–549. https://doi.org/10.1080/00063657.2013.842538

McCollum, D.L., Zhou, W., Bertram, C., De Boer, H.S., Bosetti, V., Busch, S., Després, J., Drouet, L., Emmerling, J., Fay, M., Fricko, O., Fujimori, S., Gidden, M., Harmsen, M., Huppmann, D., Iyer, G., Krey, V., Kriegler, E., Nicolas, C., Pachauri, S., Parkinson, S., Poblete-Cazenave, M., Rafaj, P., Rao, N., Rozenberg, J., Schmitz, A., Schoepp, W., Van Vuuren, D., Riahi, K., 2018. Energy investment needs for fulfilling the Paris Agreement and achieving the Sustainable Development Goals. Nature Energy 3, 589–599. https://doi.org/10.1038/s41560-018-0179-z

McKie, J., 2013. Marine Scotland - Meygen consent decision letter.

McKnight, J.C., Bennett, K.A., Bronkhorst, M., Russell, D.J.F., Balfour, S., Milne, R., Bivins, M., Moss, S.E.W., Colier, W., Hall, A.J., Thompson, D., 2019. Shining new light on mammalian

diving physiology using wearable near-infrared spectroscopy. PLoS Biology 17, 1–20. https://doi.org/10.1371/journal.pbio.3000306

Mcpherson, G., Pliatsikas, P., Roberts, R., Bain, N., Queiros, J., May, R., Humphries, S., Mcpherson, G., Forrest, S., Mcpherson, G., 2018. Nova Innovation Ltd 1–30.

MeyGen, 2014. MeyGen Tidal Energy Project Phase 1: Environmental Statement 43.

MeyGen, 2012. MeyGen Tidal Energy Project Phase 1 Environmental Statement.

Minesto, 2019a. Faroe Islands – tidal to go 100% renewable by 2030.

Minesto, 2019b. Minesto makes product development progress; sets DG100 wing specs.

Moura, A., Simas, T., Batty, R., Wilson, B., Thompson, D., Lonergan, M., Norris, J., Finn, M., Veron, G., Paillard, M., Abonnel, C., 2010. Scientific guidelines on Environmental Assessment : Equitable Testing and Evaluation of Marine Energy Extraction Devices in terms of Performance, Cost and Environmental Impact 24.

Nossent, J., Elsen, P., Bauwens, W., 2011. Sobol' sensitivity analysis of a complex environmental model. Environmental Modelling and Software 26, 1515–1525. https://doi.org/10.1016/j.envsoft.2011.08.010

Ocean Energy Europe, 2020. Ocean Energy Key trends and statistics, Ocean Energy Europe. https://doi.org/10.1007/978-1-4471-4385-7_11

Offshore Renewable Energy Catapult, 2016. Atlantis Resources' AR1500 at ORE Catapult Blyth.

Onoufriou, J., 2020. Harbour seals in a tidal stream environment: movement ecology and the effects of a renewable energy installation.

Onoufriou, J., Brownlow, A., Moss, S., Hastie, G., Thompson, D., 2019. Empirical determination of severe trauma in seals from collisions with tidal turbine blades. Journal of Applied Ecology. https://doi.org/10.1111/1365-2664.13388

Orbitat Marine, n.d. Orbital Marine [WWW Document]. URL https://orbitalmarine.com/

ORPC, 2016. Cobscook Bay Tidal Energy Project 2015 Environmental Monitoring Report.

Pebesma, E.J., 2004. Multivariable geostatistics in S: The gstat package. Computers and Geosciences 30, 683–691. https://doi.org/10.1016/j.cageo.2004.03.012

Polagye, B., Joslin, J., Murphy, P., Cotter, E., Scott, M., Gibbs, P., Bassett, C., Stewart, A., 2020. Adaptable monitoring package development and deployment: Lessons learned for integrated instrumentation at marine energy sites. Journal of Marine Science and Engineering 8. https://doi.org/10.3390/JMSE8080553

R Core Team, 2020. R: A Language and Environment for Statistical Computing.

R Core Team, 2009. R Data Import / Export. Network 1, 34. https://doi.org/10.1111/j.1365-2699.2008.01969.x

Rabitz, H., 2010. Global sensitivity analysis for systems with independent and/or correlated inputs. Procedia - Social and Behavioral Sciences 2, 7587–7589. https://doi.org/10.1016/j.sbspro.2010.05.131

Rossington, K., Benson, T., 2020. An agent-based model to predict fish collisions with tidal stream turbines. Renewable Energy 151, 1220–1229. https://doi.org/10.1016/j.renene.2019.11.127

Russell, D.J.F., 2016. Activity Budgets : Analysis of seal behaviour at sea (OESEA-15-66) Report for the Department of Business, Energy and Industrial Strategy.

Saltelli, A., Ratto, M., Andres, T., Campolongo, F., Cariboni, J., Gatelli, D., Saisana, M., Tarantola, S., 2008. Global sensitivity analysis: the primer. John Wiley \& Sons.

Schmitt, P., Culloch, R., Lieber, L., Molander, S., Hammar, L., Kregting, L., 2017. A tool for simulating collision probabilities of animals with marine renewable energy devices. PLoS ONE 12. https://doi.org/10.1371/journal.pone.0188780

Schuchert, P., Kregting, L., Pritchard, D., Savidge, G., Elsäßer, B., 2018. Using coupled hydrodynamic biogeochemical models to predict the effects of tidal turbine arrays on phytoplankton dynamics. Journal of Marine Science and Engineering 6, 1–18. https://doi.org/10.3390/jmse6020058

Scottish Natural Heritage, 2016. Assessing collision risk between underwater turbines and marine wildlife, SNH guidance note.

Shields, M.A., Woolf, D.K., Grist, E.P.M., Kerr, S.A., Jackson, A.C., Harris, R.E., Bell, M.C., Beharie, R., Want, A., Osalusi, E., Gibb, S.W., Side, J., 2011. Marine renewable energy: The ecological implications of altering the hydrodynamics of the marine environment. Ocean and Coastal Management 54, 2–9. https://doi.org/10.1016/j.ocecoaman.2010.10.036

Simas, T.C., Moura, a C., Patrício, S., Batty, R., 2009. Review and discussion of common environmental legislation for ocean energy schemes. Energy 1080–1088.

Simec Atlantis, 2019. MeyGen Update [Blog], Atlantis Resources, Simec Atlantis [WWW Document]. URL https://simecatlantis.com/2019/02/11/meygen-update-3/

Slingsby, J., Scott, B.E., Kregting, L., McIlvenny, J., Wilson, J., Couto, A., Roos, D., Yanez, M., Williamson, B.J., 2021. Surface Characterisation of Kolk-Boils within Tidal Stream Environments Using UAV Imagery. Journal of Marine Science and Engineering 9, 484. https://doi.org/10.3390/jmse9050484

Sparling, C., Lonergan, M., McConnell, B., 2018a. Harbour seals (Phoca vitulina) around an operational tidal turbine in Strangford Narrows: No barrier effect but small changes in transit behaviour. Aquatic Conservation: Marine and Freshwater Ecosystems 28, 194–204. https://doi.org/10.1002/aqc.2790

Sparling, C., Lonergan, M., McConnell, B., 2018b. Harbour seals (Phoca vitulina) around an operational tidal turbine in Strangford Narrows: No barrier effect but small changes in transit behaviour. Aquatic Conservation: Marine and Freshwater Ecosystems 28, 194–204. https://doi.org/10.1002/aqc.2790

Thompson, D., Brownlow, A., Onoufriou, J., Moss, S, E.W., 2015. Collision risk and impact study: Field tests of turbine blade-seal carcass collisions. Report to Scottish Government, no. MR 5 16.

Thompson, D., Duck, C.D., Morris, C.D., Russell, D.J.F., 2019. The status of harbour seals (Phoca vitulina) in the UK. Aquatic Conservation: Marine and Freshwater Ecosystems 29, 40–60. https://doi.org/10.1002/aqc.3110

Thompson, D., Onoufriou, J., Brownlow, A., Morris, C., 2016. Data based estimates of collision risk: an example based on harbour seal tracking data around a proposed tidal turbine array in the Pentland Firth. Scottish Natural Heritage Comissioned Report No. 900 41.

Tosin, M., Côrtes, A.M.A., Cunha, A., 2020. A Tutorial on Sobol' Global Sensitivity Analysis Applied to Biological Models 93–118. https://doi.org/10.1007/978-3-030-51862-2_6

UN, 2015. Transforming our world: The 2030 Agenda for Sustainable Development, Draft resolution referred to the United Nations summit for the adoption of the post-2015 development agenda by the General Assembly at its sixty-ninth session. UN Doc. A/70/L.1. https://doi.org/10.1201/b20466-7

Viehman, H., 2016. Hydroacoustic Analysis of the Effects of a Tidal Power Turbine on Fishes.

Waggitt, J.J., Dunn, H.K., Evans, P.G.H., Hiddink, J.G., Holmes, L.J., Keen, E., Murcott, B.D., Piano, M., Robins, P.E., Scott, B.E., Whitmore, J., Veneruso, G., 2018. Regional-scale patterns in harbour porpoise occupancy of tidal stream environments. ICES Journal of Marine Science 75, 701–710. https://doi.org/10.1093/icesjms/fsx164

Waggitt, J.J., Robbins, A.M.C., Wade, H.M., Masden, E.A., Furness, R.W., Jackson, A.C., Scott, B.E., 2017. Comparative studies reveal variability in the use of tidal stream environments by seabirds. Marine Policy 81, 143–152. https://doi.org/10.1016/j.marpol.2017.03.023

Wainwright, H.M., Finsterle, S., Jung, Y., Zhou, Q., Birkholzer, J.T., 2014. Making sense of global sensitivity analyses. Computers and Geosciences 65, 84–94. https://doi.org/10.1016/j.cageo.2013.06.006

Wickham, H., 2016. ggplot2: Elegant Graphics for Data Analysis.

Williams, R., O'Hara, P., 2010. Modelling ship strike risk to fin, humpback and killer whales in British Columbia, Canada. Journal of Cetacean Research and Management 11, 1–8.

Williamson, B.J., Fraser, S., Blondel, P., Bell, P.S., Waggitt, J.J., Scott, B.E., 2017. Multisensor Acoustic Tracking of Fish and Seabird Behavior Around Tidal Turbine Structures in Scotland. IEEE Journal of Oceanic Engineering 42, 948–965. https://doi.org/10.1109/JOE.2016.2637179

Wilson, B., Batty, R., Daunt, F., Carter, C., 2006. Collision risks between marine renewable energy devices and mammals, fish and diving birds Report to the Scottish Executive.

Wilson, B., Marmo, B., Lepper, P.A., Risch, D., Benjamins, S., Hastie, G., Carter, C., 2017. Good noise, bad noise: A tricky case of balancing risk of physical injury against acoustic disturbance for marine mammals and tidal energy devices. The Journal of the Acoustical Society of America 141, 3921–3921. https://doi.org/10.1121/1.4988861

Zambrano, C., 2016. Lessons learned from subsea tidal kite quarter scale ocean trials, in: WTE16—Second Workshop on Wave and Tidal Energy. Valdivia, Chile.

Zhang, X.Y., Trame, M.N., Lesko, L.J., Schmidt, S., 2015. Sobol sensitivity analysis: A tool to guide the development and evaluation of systems pharmacology models. CPT: Pharmacometrics and Systems Pharmacology 4, 69–79. https://doi.org/10.1002/psp4.6

Zhou, Z., Benbouzid, M., Charpentier, J.F., Scuiller, F., Tang, T., 2017. Developments in large marine current turbine technologies – A review. Renewable and Sustainable Energy Reviews 71, 852–858. https://doi.org/10.1016/j.rser.2016.12.113

Appendices

Appendix I: Supplementary material for Chapter 3

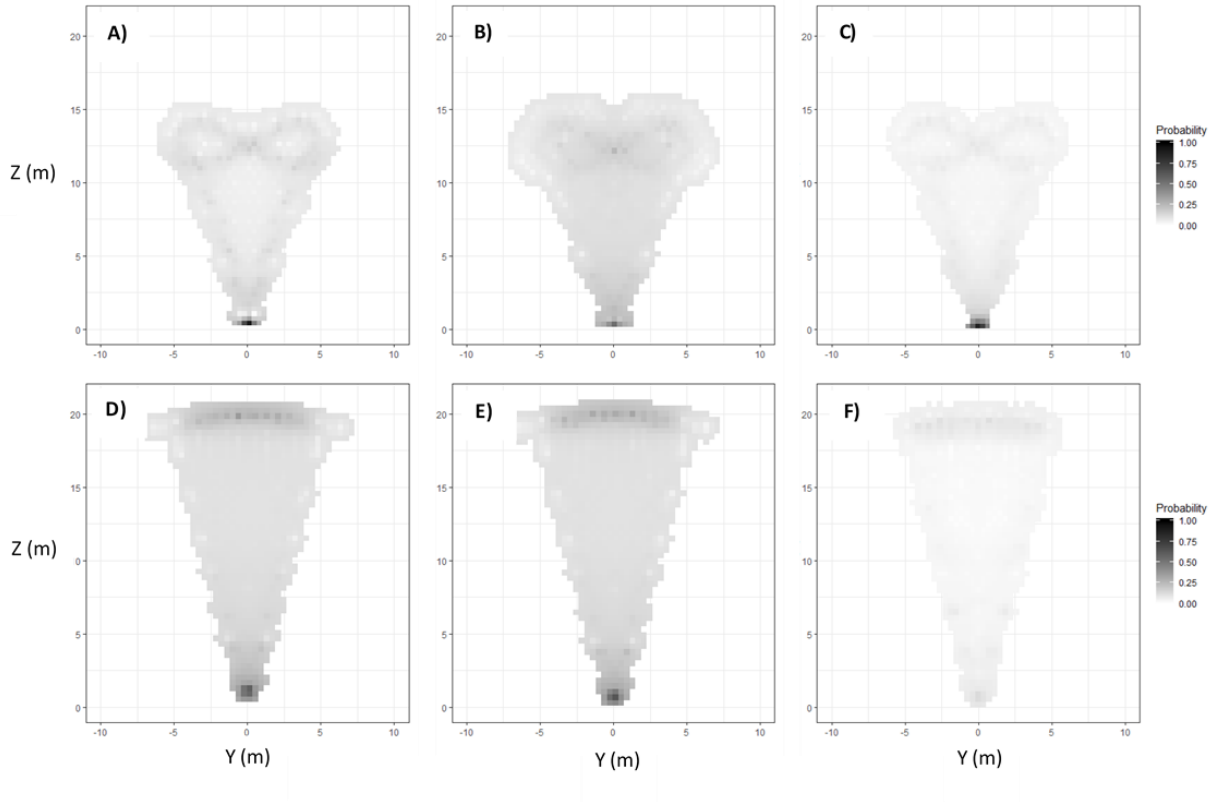

Figure 1. The 2D distribution of the probability of collisions for two of the eight scenarios tested **A)** Slow, Flat, Pup (SFP); **B)** Fast, Flat, Adult, (FFA); **C)** Fast, Flat, Pup (FFP); **D)** Slow, Downward, Pup (SDP); **E)** Fast, Downward, Adult, (FDA) and **F)** Fast, Downward, Pup, (FDP). The shading of the points relates to the probability of collision for that point (with darker shading indicating higher probability of collision).

Appendix II: Pilot study - Sensitivity testing of collision risk modelling for tidal energy convertors

Introduction

Previous chapters have focused on the development of a simulation-based approach (Chapters 2-5) that can alter potentially influential parameters, such as the angle of approach (Chapter 3), and it has been used to replicate outputs from a simple scenario that used the Band model for producing collision risk estimates for an environmental impact assessment (EIA) (Chapter 6). Moving forward, this tool can be used not only for assessment purposes but also for investigating which parameters are the most sensitive in the collision risk modelling process, i.e. which parameters, when varied within reasonable bounds, generate the greater variance and uncertainty in estimates. Based on these outputs, it would then be possible to target empirical data collection to address these knowledge gaps and to reduce the uncertainty in the collision risk model, producing a more refined estimate on collision and mortality risk.

Accurately quantifying the risk of collision between TECs and animals is a complex problem with numerous parameters that may influence the estimated risk (Hammar et al., 2015; Wilson et al., 2006). The parameters involved can be broadly split into three categories: device, animal, and environment (Fig. 1). Figure 1 outlines some of the parameters that can influence collision risk, this is not an exhaustive list and does not consider the interactions between parameters. For example, the noise output of the device may be linked to the density of animals in the vicinity of the device, as a loud device may reduce the number of animals within the immediate area of the device (Hastie et al., 2018). Also, the approach speed of animal and rotations per minute (RPM) of device depends on the tidal speed. Therefore, whilst it is important to understand the influence of each parameter on the results of the model separately, it is also important to investigate how they interact.

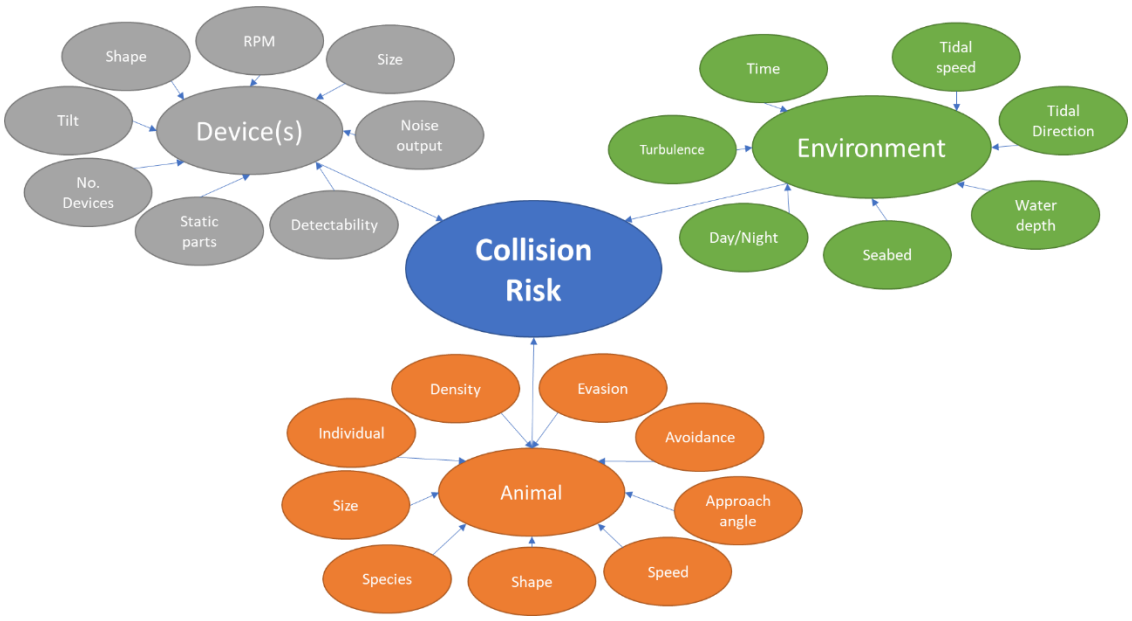

Figure 1. Some of the parameters that may affect collision risk between TECs and animals, grouped across the three broad categories.

As part of the EIA process, regulators may request data collection on some of these parameters to reduce knowledge gaps and better inform the collision risk modelling; these studies are often costly, in both time and money. For example, expensive animal-borne tags may be used to estimate density of animals in the area of planned installation (Joy et al., 2018b; Onoufriou, 2020). However, for several parameters, such as tidal speed and device shape, their data is essential information as part of any tidal development and therefore has no additional cost. In considering which knowledge gaps to focus data collection on, understanding the influence of each parameter on the model output is important. Some parameters may have larger effects on collision risk estimates, and therefore increase the uncertainty and ultimately reduce confidence in the outputs. Understanding these relationships can help stakeholders (e.g. regulators, advisors, industry) identify where resources (both time and money) can be better used to assess knowledge gaps in the most useful and proportionate manner.

Sensitivity analysis, which is a method that measures how sensitive a result is to variations in each of the model parameters, would improve our understanding of the influence of parameters in collision risk modelling. Specifically, in a given scenario, it can be used to identify which parameters are most influential on the estimates. There are two methods of sensitivity analysis, global and local. Local sensitivity analysis focuses on individual parameters. For example, a common method is one-at-a-time, where one parameter at a time is altered by a set amount (e.g. 10%) and the effect on model outputs is measured. This is a useful exercise for simple linear models however it does not account for non-linear relationships or relationships between parameters. For collision risk modelling, interactions between parameters, such as between animal speed and point of collision are likely to occur (Chapter 4) and non-linear trends are also likely to be present, such as those for angle of approach (Chapter 3). Therefore, global sensitivity analysis (GSA), which can assess these non-linear and interconnected relationships between parameters, would be a more robust and appropriate method. An additional benefit of GSA is that multiple parameters can be altered simultaneously.

The most appropriate GSA for the simulation-based collision risk model is the Sobol method as it uses variance-based measures to robustly quantify model sensitivities, including non-linear effects, which many alternative methods do not (Saltelli et al., 2008). The Sobol method assesses the sensitivity of the model output to the model inputs, put simply, to estimate sensitivities, the parameters being tested are varied, run through the model, and the variance of the results are analysed. The Sobol method has been used across many disciplines including pharmaceuticals (Zhang et al., 2015), environmental sciences (Nossent et al., 2011) and agent-based modelling (Fonoberova et al., 2013). It has been demonstrated to offer a more reliable and detailed assessment of sensitivities when compared to the more common one-at-a-time

approach (Saltelli et al., 2008). The Sobol method can quantify two different levels of effect; the first order effect, which is the influence a parameter has on the model results individually, and the second order effect, which is the combined effect that two parameters have on the model results. This method also provides the total effect of an input parameter, which is the sum of its first order effect and its contribution to all other second order effects.

The objective of this work is to demonstrate how a global sensitivity analysis method can be applied to the input and outputs of the simulation-based approach to collision risk modelling to better understand the influence that parameters have on the model estimates. For this preliminary work, a simple scenario investigating the influence of tidal speed and animal density on collision risk estimates were used. Tidal speed was chosen as this parameter can influence multiple parameters, including the approach speed of the animal and the rotational speed of the device. The animal density was chosen as this is an important parameter when considering collision risk modelling in the context of the impact at a population level, as would be required in an EIA, for example (Scottish Natural Heritage, 2016). The example uses a horizontal axis tidal turbine (HATT) and harbour seals (*Phoca vitulina*), taking values from the MeyGen Development EIA (MeyGen, 2014) and the Scottish Natural Heritage Guidance note (Scottish Natural Heritage, 2016).

Methods

The Sobol method for Global Sensitivity Analysis

The analysis was performed using the SALib package in python (Herman and Usher, 2017) investigating two parameters: tidal speed and animal density. The Sobol method is performed in three stages:

1. Produce randomised input values within a set upper and lower bound.
2. Run the simulation-based collision risk model for each of the randomised input values.
3. Analyse CRM results using the SALib.

To produce randomised input values the Saltelli sampler from the SAlib library was used (Herman and Usher, 2017). The Saltelli sampler uses quasi-randomised sequences to produce input values between the upper and lower bounds set. The number of samples is determined by the number of inputs (D) and the strength of the analysis (N) using Eq. 1:

(1) $$Number\ of\ Sample = N \times (2D + 2)$$

A higher N value increases the ability to analyse sensitivities more accurately. The samples produced are then used as the input values in the simulation-based collision risk model, where each input value will be used to produce a collision risk estimate.

All the collision risk estimates are extracted and are then analysed using the Sobol analysis function within the SALib package (Herman and Usher, 2017). Effect size, which is the amount of influence a parameter has on the output of the model, is calculated by analysing the variance in model outputs and attributing it to each input parameter.

Scenario and parameters

The scenario tested is the collision risk between a HATT and harbour seals, using values taken from the MeyGen EIA (MeyGen, 2014), and assessing the sensitivity of two parameters: tidal speed and animal density. Tidal speed will affect both the approach speed of the animal and the rotational speed of the device. In the example tested, the approach speed of the animal was set to match the tidal speed, which is the same method used in the Scottish Natural Heritage (SNH) guidance note (Scottish Natural Heritage, 2016). The rotational speed of the device is based on the operational conditions of the AR1500 HATT from the MeyGen Development (MeyGen, 2014). The TEC has a cut-in speed of 0.5ms^{-1} and the upper tidal speed for the Pentland Firth is 4.5ms^{-1} (Table 1). Where the device cut-in speed of 0.5ms^{-1} equates to 8RPM (rotations per minute) increasing to 14RPM, which is maintained when flow speed is between 3.4ms^{-1} and 4.5ms^{-1} (Fig. 2). The values for tidal speed were used to produce an equivalent rotational speed in RPM, which was then translated into radians per second (RPS) for use in the simulations using equation 1 in Chapter 4.

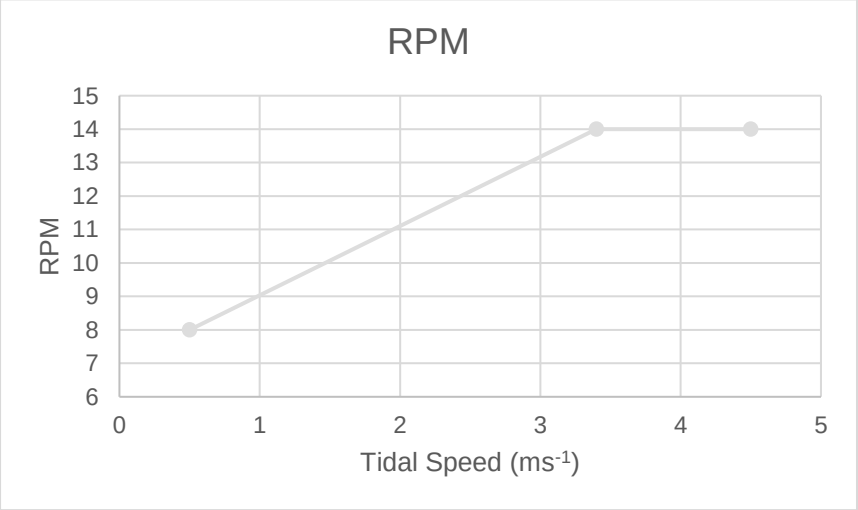

Figure 2. The RPM of the HATT based on the range of tidal speeds known to occur in the Pentland Firth.

The values for animal density are not used in the simulation element of the model, they are applied post processing. This is because the animal density is used to scale collision probabilities produced from simulations to a collision risk estimate at a population level (see Chapter 6). The values for animal density were taken from the MeyGen EIA, where a lower and upper value of 0.08 and 0.251 seals per km^2 respectively, was used (Table 1) (MeyGen, 2014).

Table 1. Inputs used in the collision risk model, their values and the source of the data, * indicates the parameters that were varied for the sensitivity analysis.

Input	**Value**	**Source**
Tidal Speed*	0.5-4.5ms^{-1}	(MeyGen, 2014)
Animal Density*	0.08-0.251 seals per km^2	(MeyGen, 2014)
Animal Length	1.41m	(Scottish Natural Heritage, 2016)
Animal Width	0.34m	(Scottish Natural Heritage, 2016)
Device	Horizontal axis tidal turbine (HATT)	(MeyGen, 2014)
Rotor radius	9m	(MeyGen, 2014)
Time period	1 year (3.154e+7 seconds)	(Scottish Natural Heritage, 2016)
Duration of dive	180 seconds	(Scottish Natural Heritage, 2016)
Surface time	39.5 seconds	(Scottish Natural Heritage, 2016)
Watch period	10 seconds	(Scottish Natural Heritage, 2016)
Water depth	31.5m	(MeyGen, 2014)

The lower and upper values for the two parameters investigated (Table 1) were then used to generate a sample of random input values using the Saltelli sampler process described above. The strength of analysis (i.e. N in Equation 1) was set to 100 for the two parameters, this produced a sample of 600 randomised input values for the two parameters.

In the 600 randomised input values there are 200 unique values for animal density and 200 unique values for tidal speed, which are repeated several times to create randomised unique pairings of the two input parameters. As the simulation-based element of the model does not

require animal density only the 200 unique values for tidal speed were run in simulations; therefore, saving computational time as less simulations were required. The collision probabilities produced were then matched to the full list of 600 input files using the corresponding tidal speeds. Collision risk estimates for all 600 input values were then produced using the inputs outlined in Table 1 and the methods outlined in Chapter 6.

Simulation Model

Simulations

Time lags per starting position were set to 100 in a 1m-by-1m grid that covered the swept area of the 18m diameter HATT rotor, meaning there were 361 starting positions. This meant, for each of the 200 tidal speeds, 36,100 simulations had to be run. This equated to a total of 7,220,000 simulations which took approximate 120 hours total runtime using the high-performance computer setup outlined in Chapter 5. Upon completion of the simulations, the results were analysed to produce collision probabilities for each of the tidal speeds tested (see Chapters 3 and 4 for further details).

Collision risk estimate

To produce a collision risk estimate, the methods outlined in Chapter 6 were used. However, the density estimates first had to be scaled from seals per km^2 in the vicinity of the device to the number of seals per m^3 in the depths covered by the swept area of the device, using equations in the Scottish Natural Heritage guidance note (Scottish Natural Heritage, 2016). Scottish Natural Heritage recommendations based on seal diving behaviour was used which took the density in km^3 and divided it by 1,000,000 to produce a value in m^2. This value was then scaled to the adjusted at sea density by dividing it by the proportion of seals visible at the surface (Scottish Natural Heritage, 2016). The proportion visible at the surface is calculated using Eq. 2 where t_u is the mean underwater duration of a dive, t_s is the mean surface time, and t_w is the time taken for a watch during the marine mammal survey.

(2) $$Proportion\ visible\ at\ surface = 1 - \left(\frac{1}{t_u + t_s}\right) \times \max\left(0, t_u - t_w\right)$$

The at sea density was then used to calculate the proportion at risk depth, which is based on the proportion of time seals spent at various depths depending on the depth of the device and where in the water column the device rotor is situated (Scottish Natural Heritage, 2016). The values used to calculate the time seals spent at depth (Table 2) were based on the SNH guidance. The values for the device location were for a HATT at 31.5m depth with the highest reach of the blade tip of 8m depth and the lowest reach of the blades at 26m. The resulting calculation was 38.2% of time at risk depth, which is then used in Eq. 3 to produce the density at risk depth, where the density at risk depth (D) is produced by multiplying the adjusted at sea density (D_A) by the proportion of time at risk depth (P) divided by the diameter of the rotor ($2R$).

(3) $$D = D_A \times P/2R$$

After calculating the density at risk depth, the equations 1 and 2 from Chapter 6, were used to calculate the collision risk estimates for the 600 inputs tested. Summarised, the equations scaled the collision probability by density at risk depth and animal speed which produced the number of collisions predicted per second. The collisions per second were then multiplied by the amount of time the device is typically in operation, which was estimated at 12.4% based on the Scottish Natural Heritage Guidance. This is then scaled up to produce a predicted number of seals colliding per year.

Table 2. Proportion of time spent at each depth interval for harbour seals for depths between 0-35m from the SNH guidance note (Scottish Natural Heritage, 2016).

Depth	Proportion of time
0	0.22
0-5	0.04
5-10	0.11
10-15	0.14
15-20	0.09
20-25	0.07
25-30	0.19
30-35	0.12

Analysis

The results containing the collision risk estimates in seals per year were then imported to python and analysed using the SAlib package. The 600 values from these estimates were input to the Sobol analyse function to produce first order, second order and total effect size. 95% confidence intervals for each result were also produced from bootstrapping of results.

Results

The results from this study were inconclusive. The first order effects showed a higher effect size for animal density (0.215) over tidal speed (0.169) (Table 3), however the confidence intervals around this were large and showed overlap for the two parameters (Table 3, Fig. 4; left). The collision risk estimates used in the analysis showed a clear positive relationship for both tidal speed and animal density (Fig. 3). The second order effects produced a negative result indicating

an error with the calculation, which is often due to an insufficient strength of analysis (N) (Saltelli et al., 2008). The total effect size was higher for animal density, but this was above 1 (Table 3), which also indicates an issue with the results, as the effect size should be between 0 and 1 (Saltelli et al., 2008), however, there can be positive correlation between parameters causing some variance to be counted twice in total effect calculations to produce an effect size above 1 (Rabitz, 2010).

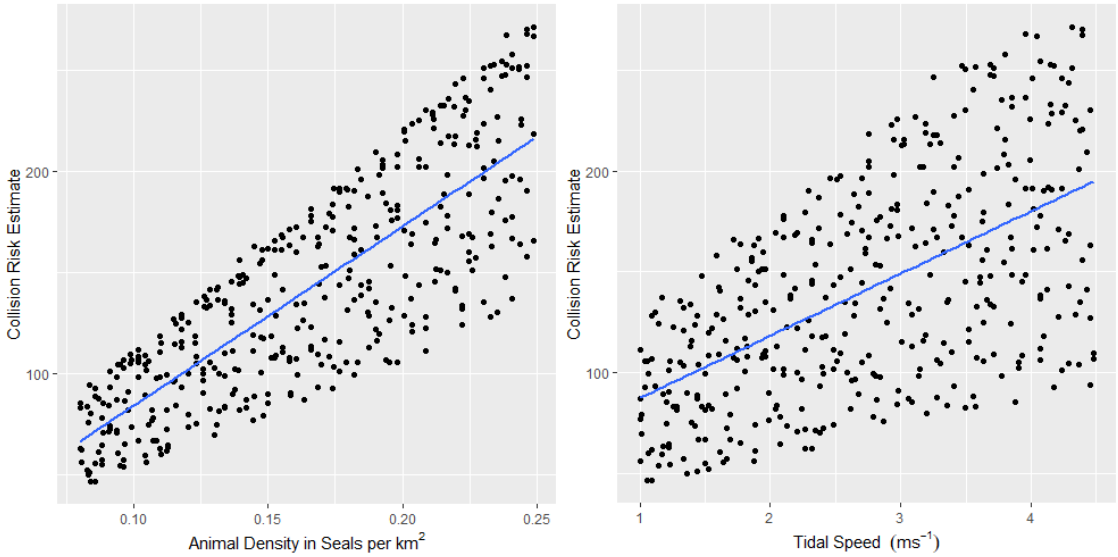

Figure 3. Collision risk estimates (black dots) for animal density (left) and tidal speed (right) with a fitted linear model (blue line).

Table 3. Results from the Sobol analysis for the two inputs animal density and tidal speed. Note that the 2nd order effects are the same as they are the combined effects of the two parameters.

Parameter	1st Order Effect	1st CI	2nd Order	2nd CI	Total Effect	Total CI
Animal Density	0.215006	0.333010	*-0.210508*	*0.402388*	1.136543	0.225466
Tidal Speed	0.169243	0.215820			0.717985	0.239359

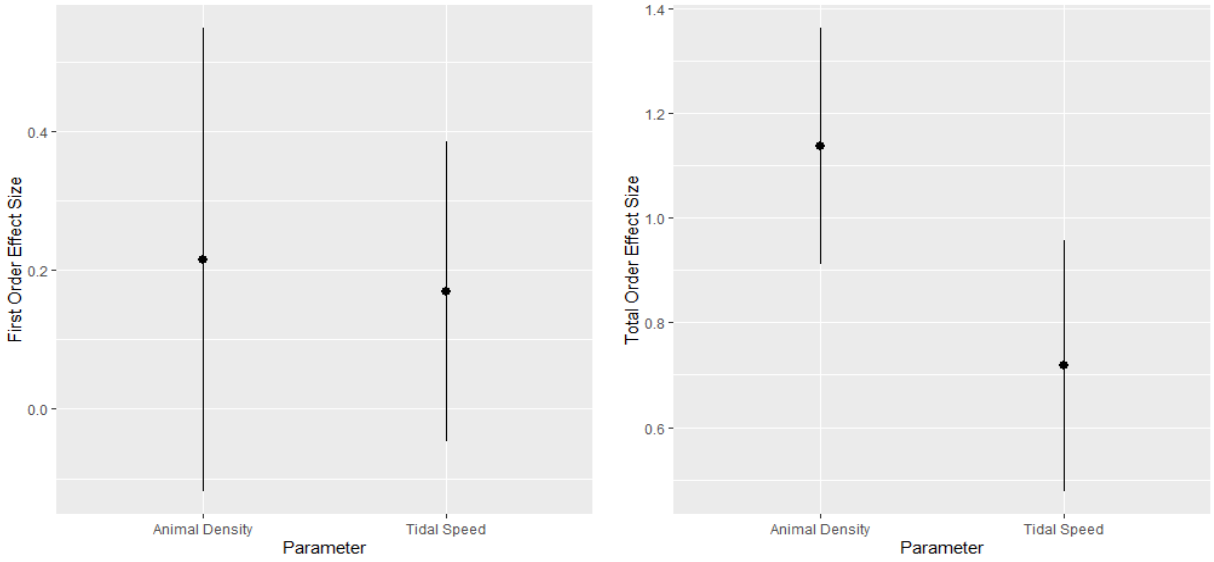

Figure 4. The effect size for first order effects (left) and total effect size (right) for animal density and tidal speed. The point is the effect size, and the lines display the 95% confidence intervals.

Discussion

This study aimed to perform a simplified global sensitivity analysis to estimate the influence of tidal speed and animal density on collision risk estimates, however, the results were inconclusive. The first order effects did indicate that animal density may be more influential however the confidence intervals around these estimates were broad and overlapped. Also, the results for second order and total order effect had errors. These issues could be due to a low strength of analysis (N) and therefore further, higher strength, investigation may be required. This will be more computationally demanding, potentially taking months to run the simulations. Despite the issues the Sobol method does show promise as a useful tool in investigating collision risk as it has been used widely (Fonoberova et al., 2013; Nossent et al., 2011; Zhang et al., 2015) and can be performed using the simulation-based approach.

Further work to investigate the influence of various parameters on collision risk models will be useful. If performed with more parameters and with a higher strength of analysis the results could indicate some of the more influential parameters. One of the issues with the analysis in this study could be due to only testing two parameters. There are many parameters that are fixed in this analysis (Table 1) and it is possible that fixed parameters can still influence the results of a model (Saltelli et al., 2008). Results from previous Chapters 3 & 4 have indicated possible non-linear relationships between input parameters and the results of the model. It is also possible that input parameters have a joint influence on the results of a model, e.g. second order effect. Therefore, as one input parameter is varied, its combined influence with a fixed parameter may change therefore that effect may be responsible for some of the variance in this study and, as there are many fixed parameters, the effect could make up a significant portion of the variance. Therefore, when further investigation is performed using this method, more parameters should be tested to

investigate their influence, especially those likely to have non-linear effects, such as angle of approach.

The Sobol method has been used widely (Nossent et al., 2011; Wainwright et al., 2014; Zhang et al., 2015) and offers a comprehensive approach that can quantify both individual and combined effects from parameters (Tosin et al., 2020). Expansion of this method to incorporate more inputs will provide further understanding of the sensitivities surrounding collision risk modelling. Also, methods in which parameters are used within a model can be examined, for example, information on dive behaviour of animals could be incorporated into the outputs from the simulation-based element of the model, as demonstrated in chapter 3, where the probability of being at depth was multiplied by collision probably at that depth. However, in this chapter, and in many EIAs (MeyGen, 2014; Scottish Natural Heritage, 2016), probability at risk depth is used to scale animal density. These two techniques could be compared side-by-side using a sensitivity analysis to see which has the greatest influence. Furthermore, the data used to produce input values may be different for each parameter, for example here the upper and lower values for animal density make use of the confidence intervals around estimates from surveys whereas the tidal speed values are more definitive values for upper and lower speeds that occur in the area. The differences in how values are obtained must also be considered when performing sensitivity analysis to form a coherent understanding of collision risk modelling.

A robust and comprehensive sensitivity analysis could guide future data collection efforts for collision risk assessments by identifying those parameters that have the greatest influence on estimates. An important consideration in guiding data collection will be the more than just the influence of parameters but also costs (time and money) of collecting the data to produce the various inputs, and that requests on developers are proportionate to the risk. A wider cost-benefit analysis approach may be useful in combining the results of a sensitivity analysis with the logistical aspects of data collection. For example, a highly influential effect on collision risk estimates has been avoidance, where a 98% avoidance rate has been used previously (Mcpherson et al., 2018) and takes the no avoidance collision estimate and reduces it by 98%. However, this avoidance rate is based on expert advice guided by data and not solely on empirical data. If empirical data are required to produce an avoidance rate, this may have a large effect on collision risk estimates but will still require expensive data collection methods such as passive acoustic monitoring (Gillespie et al., 2020), active sonar (Gillespie et al., 2020) and/or animal tagging (Thompson et al., 2016). Other parameters, such as tidal speed and device shape, are gathered as part of the device development and installation and therefore have no additional cost. Even though they may have a small effect on collision risk estimates, they may improve estimates in combination and therefore will be worth including. To aid data collection for future collision risk assessments a sensitivity analysis that makes use of the data from multiple different assessments could be used to indicate which data may be suitable to be used across

developments and which data should be the focus of site-specific data collection. Some information may vary greatly between sites, but have little effect, or, conversely, some data may vary little across sites, but have a greater effect. Furthermore, several important considerations must be made when recommending data collection for collision risk modelling. These include the influence of parameters on estimate (i.e. the results of sensitivity analysis), the financial cost of obtaining data, the time required to gather sufficient information, and the risk of obtaining the data (i.e. are the methods guaranteed to obtain the desired parameters), and all things considered, if the request for more data is proportionate to the risk.

Collision risk modelling will continue to have an important role in the consenting of devices, and sensitivity analysis can be a useful addition to assist in identifying parameters that have the most influence on estimates in a given scenario. Refinements have been attempted with other modelling approaches such as the Band model (Scottish Natural Heritage, 2016) however, as demonstrated in previous chapters, the simulation-based approach has clear advantages, such as the ability to estimate risk for novel device designs (Chapter 2), alter ecological parameters (Chapter 3) and estimate mortality (Chapter 4). As these methods are developed with a more detailed investigation into the sensitivities of risk and they can be used to identify important parameters to guide data collection in order to improve estimates and better inform regulators.

References

375 Designs, 2014. Tidal Stream Turbine.

Alistair, J., Onoufriou, R., 2019. Harbour Seals (Phoca vitulina) in a Tidal Stream Environment: Movement Ecology and the Effects of a Renewable Energy Installation.

Allegue, H., 2017. Variability of harbour seal (Phoca vitulina) foraging behaviour during out-migrations of salmon smolts.

Atlantis Resources, 2016. AR1500 Tidal Turbine Brochure [WWW Document]. URL https://simecatlantis.com/wp/wp-content/uploads/2016/08/AR1500-Brochure-Final-1.pdf

Bachant, P., Wosnik, M., 2015. Characterising the near-wake of a cross-flow turbine. Journal of Turbulence 16, 392–410. https://doi.org/10.1080/14685248.2014.1001852

Band, B., 2000. Windfarms and birds: Calculating a theoretical collision risk assuming no avoiding action, Guidance Note Series, Scottish Natural Heritage.

Band, B., Sparling, C., Thompson, D., Onoufriou, J., Martin, E.S., West, N., 2016. Refining estimates of collision risk for harbour seals and tidal turbines. Scottish Marine and Freshwater Science 7, 133. https://doi.org/10.7489/1786-1

Batty, R.S., Wilson, B., 2010. Predicting the abilities of marine vertebrates to evade collision with tidal stream turbines . 3rd International Conference on Ocean Energy, 6 October, Bilbao 3–6.

Benjamins, S., Dale, A., van Geel, N., Wilson, B., 2016. Riding the tide: Use of a moving tidal-stream habitat by harbour porpoises. Marine Ecology Progress Series 549, 275–288. https://doi.org/10.3354/meps11677

Benjamins, S., Dale, A.C., Hastie, G., Waggitt, J.J., Lea, M.A., Scott, B., Wilson, B., 2015. Confusion reigns? A review of marine megafauna interactions with tidal-stream environments. Oceanography and Marine Biology: An Annual Review 53, 1–54. https://doi.org/10.1201/b18733

Benjamins, S., van Geel, N., Hastie, G., Elliott, J., Wilson, B., 2017. Harbour porpoise distribution can vary at small spatiotemporal scales in energetic habitats. Deep-Sea Research Part II: Topical Studies in Oceanography 141, 191–202. https://doi.org/10.1016/j.dsr2.2016.07.002

Blender Online Commuinity, 2018. Blender - a 3D modelling and rendering package.

Booth, C., Sparling, C., Wood, J., Tollitt, D., Scott-Heyward, L., Rexstad, E., Hultgren, Y., Johnsson, M., Knutzen, E., 2015. Advancing a key consenting risk for tidal energy: The risk of marine mammal collision for in-stream tidal energy, in: Proceedings of the 3rd Marine Energy Technology Symposium METS2015 April 27-29, 2015, Washington, D.C. p. 4.

Borthwick, A.G.L., 2016. Marine Renewable Energy Seascape. Engineering 2, 69–78. https://doi.org/10.1016/J.ENG.2016.01.011

BP, 2020. Statistical Review of World Energy.

Byrne, S., 1983. Bird Movements and Collision Mortality at a large horizontal axis wind turbine. Cal-Neva Wildlife Transactions 76–83.

Carlson, T., Elster, J., Copping, A.E., Jones, M., Watkins, M., Jepsen, R., Metzinge, K., Watson, B.E., 2012. Assessment of Strike of Adult Killer Whales by an OpenHydro Tidal Turbine Blade. Prepared for the U.S. Department of Energy by Pacific Northwest National Laboratory.

CG Trader, 2014. The-brandals, GORLOV Wind Turbine Free 3D model.

Chudzinska, M., Nabe-Nielsen, J., Smout, S., Aarts, G., Brasseur, S., Graham, I., Thompson, P., McConnell, B., 2021. AgentSeal: Agent-based model describing movement of marine central-place foragers. Ecological Modelling 440. https://doi.org/10.1016/j.ecolmodel.2020.109397

Copping, A.E., Grear, M., Jepsen, R., Chartrand, C., Gorton, A., 2017. Understanding the potential risk to marine mammals from collision with tidal turbines. International Journal of Marine Energy 19, 110–123. https://doi.org/10.1016/j.ijome.2017.07.004

Copping, A.E., Grear, M.E., 2018. Applying a simple model for estimating the likelihood of collision of marine mammals with tidal turbines. International Marine Energy Journal 1, 27–33. https://doi.org/10.36688/imej.1.27-33

Copping, A.E., Hemery, L.G., Overhus, D.M., Garavelli, L., Freeman, M.C., Whiting, J.M., Gorton, A.M., Farr, H.K., Rose, D.J., Tugade, L.G., 2020a. Potential environmental effects of marine renewable energy development—the state of the science. Journal of Marine Science and Engineering 8, 1–18. https://doi.org/10.3390/jmse8110879

Copping, A.E., Sather, N., Hannah, L., Whiting, J., Zydlewski, G., Staines, G., Gill, A., Hutchinson, I., A, O., Simas, T., Bald, J., Sparling, C., Wood, J., Masden, E., 2020b. 2020 State of the Science Report. State Sci. Rep. https://doi.org/10.2172/1632878

Copping, A.E., Sather, N.K., Hanna, L., Whiting, J., Zydlewski, G.B., Staines, G., Gill, G., Hutchison, I., O'Hagan, A.M., Simas, T., Bald, J., Sparling, C., Wood, J., Madsen, E., 2016. Annex IV 2016 State of the Science Report: Environmental effects of marine renewable energy development around the world. https://doi.org/10.1097/JNN.0b013e3182829024

David P. Wiggins, 2021. Xvfb.

Durand, N., Cornett, A., Bourban, S., 2008. 3D Modelling and Assessment of Tidal Current Energy Resources in the Bay of Fundy, in: 3rd International Conference on Ocean Energy, 6 October, Bilbao. pp. 2–7.

Easton, M.C., Woolf, D.K., Bowyer, P.A., 2012. The dynamics of an energetic tidal channel, the Pentland Firth, Scotland. Continental Shelf Research 48, 50–60. https://doi.org/10.1016/j.csr.2012.08.009

Eça, L., Hoekstra, M., 2014. A procedure for the estimation of the numerical uncertainty of CFD calculations based on grid refinement studies. Journal of Computational Physics 262, 104–130. https://doi.org/10.1016/j.jcp.2014.01.006

European Commission, 2007. Guidance document on the strict protection of animal species of Community interest under the Habitats Directive 92/43/EEC. Context 88.

European Marine Energy Centre, 2019. Tidal Devices, European Marine Energy Centre.

Felleman, F.L., Heimlich-Boran, J.R., Osborne, R.W., 1991. Feeding Ecology of the killer whale (Orcinus orca). In (KW Pryor and KS Norris, eds.) Dolphin Societies: Discoveries and Puzzles.

Fonoberova, M., Fonoberov, V.A., Mezić, I., 2013. Global sensitivity/uncertainty analysis for agent-based models. Reliability Engineering and System Safety 118, 8–17. https://doi.org/10.1016/j.ress.2013.04.004

Furness, R.W., Wade, H.M., Robbins, A.M.C., Masden, E.A., 2012. Assessing the sensitivity of seabird populations to adverse effects from tidal stream turbines and wave energy devices. ICES Journal of Marine Science 69, 1466–1479. https://doi.org/doi:10.1093/icesjms/fss131

Gabaldon, J., Turner, E.L., Johnson-Roberson, M., Barton, K., Johnson, M., Anderson, E.J., Alex Shorter, K., 2019. Integration, Calibration, and Experimental Verification of a Speed Sensor for Swimming Animals. IEEE Sensors Journal 19, 3616–3625. https://doi.org/10.1109/JSEN.2019.2895806

Gill, A.B., Bartlett, M., Thomsen, F., 2012. Potential interactions between diadromous fishes of U.K. conservation importance and the electromagnetic fields and subsea noise from marine renewable energy developments. Journal of Fish Biology 81, 664–695. https://doi.org/10.1111/j.1095-8649.2012.03374.x

Gillespie, D., Palmer, L., Macaulay, J., Sparling, C., Hastie, G., 2021. Harbour porpoises exhibit localized evasion of a tidal turbine. Aquatic Conservation: Marine and Freshwater Ecosystems 31, 2459–2468. https://doi.org/10.1002/aqc.3660

Gillespie, D., Palmer, L., Macaulay, J., Sparling, C., Hastie, G., 2020. Passive acoustic methods for tracking the 3D movements of small cetaceans around marine structures. PLoS ONE 15 (5). https://doi.org/https://doi.org/10.1371/journal.pone.0229058

GKinetic, 2021. GKinetic [WWW Document]. URL https://gkinetic.com/technology/

Glasson, J., Riki, T., Andrew, C., 2019. Introduction to environmental impact assessment, Routledge. https://doi.org/10.1080/07293682.2012.747551

Hammar, L., Andersson, S., Eggertsen, L., Haglund, J., Gullström, M., Ehnberg, J., Molander, S., 2013. Hydrokinetic turbine effects on fish swimming behaviour. PLoS ONE 8, 1–12. https://doi.org/10.1371/journal.pone.0084141

Hammar, L., Eggertsen, L., Andersson, S., Ehnberg, J., Arvidsson, R., Gullström, M., Molander, S., 2015. A probabilistic model for hydrokinetic turbine collision risks: Exploring impacts on fish. PLoS ONE 10, 1–25. https://doi.org/10.1371/journal.pone.0117756

Hastie, G.D., Bivins, M., Coram, A., Gordon, J., Jepp, P., MacAulay, J., Sparling, C., Gillespie, D., 2019a. Three-dimensional movements of harbour seals in a tidally energetic channel: Application of a novel sonar tracking system. Aquatic Conservation: Marine and Freshwater Ecosystems 29, 564–575. https://doi.org/10.1002/aqc.3017

Hastie, G.D., Russell, D.J.F., Benjamins, S., Moss, S., Wilson, B., Thompson, D., 2016. Dynamic habitat corridors for marine predators; intensive use of a coastal channel by harbour seals is modulated by tidal currents. Behavioral Ecology and Sociobiology 70, 2161–2174. https://doi.org/10.1007/s00265-016-2219-7

Hastie, G.D., Russell, D.J.F., Lepper, P., Elliott, J., Wilson, B., Benjamins, S., Thompson, D., 2018. Harbour seals avoid tidal turbine noise: Implications for collision risk. Journal of Applied Ecology 55, 684–693. https://doi.org/10.1111/1365-2664.12981

Hastie, G.D., Wu, G.M., Moss, S., Jepp, P., MacAulay, J., Lee, A., Sparling, C.E., Evers, C., Gillespie, D., 2019b. Automated detection and tracking of marine mammals: A novel sonar tool for monitoring effects of marine industry. Aquatic Conservation: Marine and Freshwater Ecosystems 29, 119–130. https://doi.org/10.1002/aqc.3103

Herman, J., Usher, W., 2017. SALib: an open-source Python library for sensitivity analysis. Journal of Open Source Software 2, 97.

Holmstrom, L., Hamer, T., Colclazier, E., Denis, N., Verschuyl, J., Ruché, D., 2011. Assessing avian-wind turbine collision risk: An approach angle dependent model. Wind Engineering 35, 289–312. https://doi.org/10.1260/0309-524X.35.3.289

Horne, N., Culloch, R., Schmitt, P., Kregting, L., 2019. Incorporating different tidal energy device designs into 4D collision risk simulations allowing increased flexibility for industry. Proceedings of the 13th European Wave and Tidal Energy Conference 12–13.

Horne, N., Culloch, R.M., Schmitt, P., Lieber, L., Wilson, B., Andrew, C., Dale, A.C., Houghton, J.D.R., Kregting, L.T., 2021a. Collision risk modelling for tidal energy devices: A flexible simulation-based approach. Journal of Environmental Management 278. https://doi.org/10.1016/j.jenvman.2020.111484

Horne, N., Schmitt, P., Culloch, R.M., Wilson, B., Dale, A.C., Houghton, J.D.R., Kregting, L.T., 2021b. Fast & Flexible : streamlining a simulation- based approach to collision risk assessments, in: European Wave and Tidal Energy Conference.

IPCC, 2014. Climate change 2014 Synthesis Report, Contribution of Working Groups I, II and III to the Fifth Assessment Report of the Intergovernmental Panel on Climate Change.

Joy, R., Wood, J.D., Sparling, C.E., Tollit, D.J., Copping, A.E., McConnell, B.J., 2018a. Empirical measures of harbor seal behavior and avoidance of an operational tidal turbine. Marine Pollution Bulletin 136, 92–106. https://doi.org/10.1016/j.marpolbul.2018.08.052

Joy, R., Wood, J.D., Sparling, C.E., Tollit, D.J., Copping, A.E., McConnell, B.J., 2018b. Empirical measures of harbor seal behavior and avoidance of an operational tidal turbine. Marine Pollution Bulletin 136, 92–106. https://doi.org/10.1016/j.marpolbul.2018.08.052

Juergen Riegel Werner Mayer, Y. van H., 2017. FreeCAD, Software.

Keenan, G., Sparling, C., Williams, H., Fortune, F., 2011. SeaGen Environmental Monitoring Programme Final Report.

Krahn, M.M., Wade, P.R., Kalinowski, S.T., Dahlheim, M.E., Taylor, B.L., Hanson, M.B., Ylitalo, G.M., Angliss, R.P., Stein, J.E., Waples, R.S., 2002. Status review of southern resident killer whales (*Orcinus orca*) under the Endangered Species Act. U.S. Dept. Commer., NOAA Tech. Memo., NMFS-NWFSC-54. 159p.

Kregting, L., Elsaesser, B., Kennedy, R., Smyth, D., O'Carroll, J., Savidge, G., 2016. Do changes in current flow as a result of arrays of tidal turbines have an effect on benthic communities? PLoS ONE 11, 1–14. https://doi.org/10.1371/journal.pone.0161279

Kregting, L., Elsäßer, B., 2014. A hydrodynamic modelling framework for strangford lough part 1: Tidal model. Journal of Marine Science and Engineering 2, 46–65. https://doi.org/10.3390/jmse2010046

Levy, D.A., Cadenhead, A.D., 1995. Selective tidal stream transport of adult sockeye salmon (Oncorhynchus nerka) in the Fraser River Estuary. Canadian Journal of Fisheries and Aquatic Sciences 52, 1–12.

Lieber, L., Nimmo-Smith, W.A.M., Waggitt, J.J., Kregting, L., 2018. Fine-scale hydrodynamic metrics underlying predator occupancy patterns in tidal stream environments. Ecological Indicators 94, 397–408. https://doi.org/10.1016/j.ecolind.2018.06.071

Lieber, L., Williamson, B., Jones, C.S., Noble, L.R., Brierley, A., Miller, P., Scott, B.E., 2014. Introducing Novel Uses of Multibeam Sonar To Study Basking Sharks in the Light of Marine Renewable Energy Extraction 2–4.

Macaulay, J., Gordon, J., Gillespie, D., Malinka, C., Northridge, S., 2017. Passive acoustic methods for fine-scale tracking of harbour porpoises in tidal rapids. The Journal of the Acoustical Society of America 141, 1120–1132. https://doi.org/10.1121/1.4976077

Malinka, C.E., Gillespie, D.M., Macaulay, J.D.J., Joy, R., Sparling, C.E., 2018. First in situ passive acoustic monitoring for marine mammals during operation of a tidal turbine in Ramsey Sound, Wales. Marine Ecology Progress Series 590, 247–266. https://doi.org/10.3354/meps12467

Masden, E.A., Cook, A.S.C.P., 2016. Avian collision risk models for wind energy impact assessments. Environmental Impact Assessment Review 56, 43–49. https://doi.org/10.1016/j.eiar.2015.09.001

Masden, E.A., Foster, S., Jackson, A.C., 2013. Diving behaviour of Black Guillemots Cepphus grylle in the Pentland Firth, UK: Potential for interactions with tidal stream energy developments. Bird Study 60, 547–549. https://doi.org/10.1080/00063657.2013.842538

McCollum, D.L., Zhou, W., Bertram, C., De Boer, H.S., Bosetti, V., Busch, S., Després, J., Drouet, L., Emmerling, J., Fay, M., Fricko, O., Fujimori, S., Gidden, M., Harmsen, M., Huppmann, D., Iyer, G., Krey, V., Kriegler, E., Nicolas, C., Pachauri, S., Parkinson, S., Poblete-Cazenave, M., Rafaj, P., Rao, N., Rozenberg, J., Schmitz, A., Schoepp, W., Van Vuuren, D., Riahi, K., 2018. Energy investment needs for fulfilling the Paris Agreement and achieving the Sustainable Development Goals. Nature Energy 3, 589–599. https://doi.org/10.1038/s41560-018-0179-z

McKie, J., 2013. Marine Scotland - Meygen consent decision letter.

McKnight, J.C., Bennett, K.A., Bronkhorst, M., Russell, D.J.F., Balfour, S., Milne, R., Bivins, M., Moss, S.E.W., Colier, W., Hall, A.J., Thompson, D., 2019. Shining new light on mammalian diving physiology using wearable near-infrared spectroscopy. PLoS Biology 17, 1–20. https://doi.org/10.1371/journal.pbio.3000306

Mcpherson, G., Pliatsikas, P., Roberts, R., Bain, N., Queiros, J., May, R., Humphries, S., Mcpherson, G., Forrest, S., Mcpherson, G., 2018. Nova Innovation Ltd 1–30.

MeyGen, 2014. MeyGen Tidal Energy Project Phase 1: Environmental Statement 43.

MeyGen, 2012. MeyGen Tidal Energy Project Phase 1 Environmental Statement.

Minesto, 2019a. Faroe Islands – tidal to go 100% renewable by 2030.

Minesto, 2019b. Minesto makes product development progress; sets DG100 wing specs.

Moura, A., Simas, T., Batty, R., Wilson, B., Thompson, D., Lonergan, M., Norris, J., Finn, M., Veron, G., Paillard, M., Abonnel, C., 2010. Scientific guidelines on Environmental Assessment : Equitable Testing and Evaluation of Marine Energy Extraction Devices in terms of Performance, Cost and Environmental Impact 24.

Nossent, J., Elsen, P., Bauwens, W., 2011. Sobol' sensitivity analysis of a complex environmental model. Environmental Modelling and Software 26, 1515–1525. https://doi.org/10.1016/j.envsoft.2011.08.010

Ocean Energy Europe, 2020. Ocean Energy Key trends and statistics, Ocean Energy Europe. https://doi.org/10.1007/978-1-4471-4385-7_11

Offshore Renewable Energy Catapult, 2016. Atlantis Resources' AR1500 at ORE Catapult Blyth.

Onoufriou, J., 2020. Harbour seals in a tidal stream environment: movement ecology and the effects of a renewable energy installation.

Onoufriou, J., Brownlow, A., Moss, S., Hastie, G., Thompson, D., 2019. Empirical determination of severe trauma in seals from collisions with tidal turbine blades. Journal of Applied Ecology. https://doi.org/10.1111/1365-2664.13388

Orbitat Marine, n.d. Orbital Marine [WWW Document]. URL https://orbitalmarine.com/

ORPC, 2016. Cobscook Bay Tidal Energy Project 2015 Environmental Monitoring Report.

Pebesma, E.J., 2004. Multivariable geostatistics in S: The gstat package. Computers and Geosciences 30, 683–691. https://doi.org/10.1016/j.cageo.2004.03.012

Polagye, B., Joslin, J., Murphy, P., Cotter, E., Scott, M., Gibbs, P., Bassett, C., Stewart, A., 2020. Adaptable monitoring package development and deployment: Lessons learned for integrated instrumentation at marine energy sites. Journal of Marine Science and Engineering 8. https://doi.org/10.3390/JMSE8080553

R Core Team, 2020. R: A Language and Environment for Statistical Computing.

R Core Team, 2009. R Data Import / Export. Network 1, 34. https://doi.org/10.1111/j.1365-2699.2008.01969.x

Rabitz, H., 2010. Global sensitivity analysis for systems with independent and/or correlated inputs. Procedia - Social and Behavioral Sciences 2, 7587–7589. https://doi.org/10.1016/j.sbspro.2010.05.131

Rossington, K., Benson, T., 2020. An agent-based model to predict fish collisions with tidal stream turbines. Renewable Energy 151, 1220–1229. https://doi.org/10.1016/j.renene.2019.11.127

Russell, D.J.F., 2016. Activity Budgets : Analysis of seal behaviour at sea (OESEA-15-66) Report for the Department of Business, Energy and Industrial Strategy.

Saltelli, A., Ratto, M., Andres, T., Campolongo, F., Cariboni, J., Gatelli, D., Saisana, M., Tarantola, S., 2008. Global sensitivity analysis: the primer. John Wiley \& Sons.

Schmitt, P., Culloch, R., Lieber, L., Molander, S., Hammar, L., Kregting, L., 2017. A tool for simulating collision probabilities of animals with marine renewable energy devices. PLoS ONE 12. https://doi.org/10.1371/journal.pone.0188780

Schuchert, P., Kregting, L., Pritchard, D., Savidge, G., Elsäßer, B., 2018. Using coupled hydrodynamic biogeochemical models to predict the effects of tidal turbine arrays on phytoplankton dynamics. Journal of Marine Science and Engineering 6, 1–18. https://doi.org/10.3390/jmse6020058

Scottish Natural Heritage, 2016. Assessing collision risk between underwater turbines and marine wildlife, SNH guidance note.

Shields, M.A., Woolf, D.K., Grist, E.P.M., Kerr, S.A., Jackson, A.C., Harris, R.E., Bell, M.C., Beharie, R., Want, A., Osalusi, E., Gibb, S.W., Side, J., 2011. Marine renewable energy: The ecological implications of altering the hydrodynamics of the marine environment. Ocean and Coastal Management 54, 2–9. https://doi.org/10.1016/j.ocecoaman.2010.10.036

Simas, T.C., Moura, a C., Patrício, S., Batty, R., 2009. Review and discussion of common environmental legislation for ocean energy schemes. Energy 1080–1088.

Simec Atlantis, 2019. MeyGen Update [Blog], Atlantis Resources, Simec Atlantis [WWW Document]. URL https://simecatlantis.com/2019/02/11/meygen-update-3/

Slingsby, J., Scott, B.E., Kregting, L., McIlvenny, J., Wilson, J., Couto, A., Roos, D., Yanez, M., Williamson, B.J., 2021. Surface Characterisation of Kolk-Boils within Tidal Stream Environments Using UAV Imagery. Journal of Marine Science and Engineering 9, 484. https://doi.org/10.3390/jmse9050484

Sparling, C., Lonergan, M., McConnell, B., 2018a. Harbour seals (Phoca vitulina) around an operational tidal turbine in Strangford Narrows: No barrier effect but small changes in transit behaviour. Aquatic Conservation: Marine and Freshwater Ecosystems 28, 194–204. https://doi.org/10.1002/aqc.2790

Sparling, C., Lonergan, M., McConnell, B., 2018b. Harbour seals (Phoca vitulina) around an operational tidal turbine in Strangford Narrows: No barrier effect but small changes in transit behaviour. Aquatic Conservation: Marine and Freshwater Ecosystems 28, 194–204. https://doi.org/10.1002/aqc.2790

Thompson, D., Brownlow, A., Onoufriou, J., Moss, S, E.W., 2015. Collision risk and impact study: Field tests of turbine blade-seal carcass collisions. Report to Scottish Government, no. MR 5 16.

Thompson, D., Duck, C.D., Morris, C.D., Russell, D.J.F., 2019. The status of harbour seals (Phoca vitulina) in the UK. Aquatic Conservation: Marine and Freshwater Ecosystems 29, 40–60. https://doi.org/10.1002/aqc.3110

Thompson, D., Onoufriou, J., Brownlow, A., Morris, C., 2016. Data based estimates of collision risk: an example based on harbour seal tracking data around a proposed tidal turbine array in the Pentland Firth. Scottish Natural Heritage Comissioned Report No. 900 41.

Tosin, M., Côrtes, A.M.A., Cunha, A., 2020. A Tutorial on Sobol' Global Sensitivity Analysis Applied to Biological Models 93–118. https://doi.org/10.1007/978-3-030-51862-2_6

UN, 2015. Transforming our world: The 2030 Agenda for Sustainable Development, Draft resolution referred to the United Nations summit for the adoption of the post-2015 development agenda by the General Assembly at its sixty-ninth session. UN Doc. A/70/L.1. https://doi.org/10.1201/b20466-7

Viehman, H., 2016. Hydroacoustic Analysis of the Effects of a Tidal Power Turbine on Fishes.

Waggitt, J.J., Dunn, H.K., Evans, P.G.H., Hiddink, J.G., Holmes, L.J., Keen, E., Murcott, B.D., Piano, M., Robins, P.E., Scott, B.E., Whitmore, J., Veneruso, G., 2018. Regional-scale patterns in harbour porpoise occupancy of tidal stream environments. ICES Journal of Marine Science 75, 701–710. https://doi.org/10.1093/icesjms/fsx164

Waggitt, J.J., Robbins, A.M.C., Wade, H.M., Masden, E.A., Furness, R.W., Jackson, A.C., Scott, B.E., 2017. Comparative studies reveal variability in the use of tidal stream environments by seabirds. Marine Policy 81, 143–152. https://doi.org/10.1016/j.marpol.2017.03.023

Wainwright, H.M., Finsterle, S., Jung, Y., Zhou, Q., Birkholzer, J.T., 2014. Making sense of global sensitivity analyses. Computers and Geosciences 65, 84–94. https://doi.org/10.1016/j.cageo.2013.06.006

Wickham, H., 2016. ggplot2: Elegant Graphics for Data Analysis.

Williams, R., O'Hara, P., 2010. Modelling ship strike risk to fin, humpback and killer whales in British Columbia, Canada. Journal of Cetacean Research and Management 11, 1–8.

Williamson, B.J., Fraser, S., Blondel, P., Bell, P.S., Waggitt, J.J., Scott, B.E., 2017. Multisensor Acoustic Tracking of Fish and Seabird Behavior Around Tidal Turbine Structures in Scotland. IEEE Journal of Oceanic Engineering 42, 948–965. https://doi.org/10.1109/JOE.2016.2637179

Wilson, B., Batty, R., Daunt, F., Carter, C., 2006. Collision risks between marine renewable energy devices and mammals, fish and diving birds Report to the Scottish Executive.

Wilson, B., Marmo, B., Lepper, P.A., Risch, D., Benjamins, S., Hastie, G., Carter, C., 2017. Good noise, bad noise: A tricky case of balancing risk of physical injury against acoustic disturbance for marine mammals and tidal energy devices. The Journal of the Acoustical Society of America 141, 3921–3921. https://doi.org/10.1121/1.4988861

Zambrano, C., 2016. Lessons learned from subsea tidal kite quarter scale ocean trials, in: WTE16—Second Workshop on Wave and Tidal Energy. Valdivia, Chile.

Zhang, X.Y., Trame, M.N., Lesko, L.J., Schmidt, S., 2015. Sobol sensitivity analysis: A tool to guide the development and evaluation of systems pharmacology models. CPT: Pharmacometrics and Systems Pharmacology 4, 69–79. https://doi.org/10.1002/psp4.6

Zhou, Z., Benbouzid, M., Charpentier, J.F., Scuiller, F., Tang, T., 2017. Developments in large marine current turbine technologies – A review. Renewable and Sustainable Energy Reviews 71, 852–858. https://doi.org/10.1016/j.rser.2016.12.113

Appendix III: A review of Northern Ireland seal count data 1992-2017: Investigating population trends and recommendations for future monitoring

Ross Culloch, Nicholas Horne & Louise Kregting

Executive Summary

Background

The Department of Agriculture, Environment and Rural Affairs (DAERA) coordinate the Northern Ireland seal counts and have requested are view of these data (from 1992 – 2017) to determine whether the methods employed have produced sufficient data to inform trends in seal populations over time. In addition, DAERA wanted to determine whether the methods employed are fit for future monitoring and if the count programme can be rationalised to better fit currently available resources.

Methods

The database was first summarised by columns to review available data. Maximum counts for each year and for each month were extracted from the database for: 1) harbour seal adults and juveniles combined, 2) harbour seal pups, 3) grey seal adults and juveniles combined, 4) grey seal pups, using counts from hauled out seals only. These were compared to proxies of effort (including: number of unique Seal Count IDs, number of surveys and number of Area IDs surveyed). A regression analysis was undertaken to assess what the percentage of annual change was, for each of the four species/age class datasets. This was done for Northern Ireland as a whole and for two individual areas separately; Strangford Lough and Murlough, both of which are ASSIs and SACs with harbour seals listed as a qualifying feature.

Results

Large numbers of missing values for environmental and observational data meant that these could not be included in the analysis, which resulted in a limited dataset to work from. Highest counts of adult harbour seals were in August and September, corresponding with the moult. The highest counts of harbour seal pups were in July, corresponding to the breeding season. For grey seals, the highest counts for adults were in August and September, with higher counts for pups in October; which corresponds to the breeding season. Comparing maximum counts with proxies for survey effort suggested that the harbour seal breeding season and moult were targeted, rather than the grey seal breeding season.

It is highly likely that varying effort across years and areas has played an influential role in the trends identified. In general, there has been lower effort in the earlier and the most recent years. If these data are omitted (using data from 1995 – 2014, inclusive), then, for the whole of Northern Ireland, there was a 0.1% and 0.88% annual increase in adult harbour seals and pups, respectively; and for grey seals, there was a 1.24% and a 4.91% annual increase in adults and pups, respectively.

Using the same approach in Strangford Lough, there was a 2.01% and a 1.31% annual decrease in harbour seal adults and pups, respectively; and for grey seals there was a 2.8% and a 5.21% annual increase in adults and pups, respectively. For Murlough, there was a 2.05% and a 4.41%

annual increase in harbour seal adults and pups, respectively. Grey seals occurred in lower numbers at Murlough and were not assessed quantitatively, but it did appear that counts in recent years were yielding higher numbers. With respect to conservation objectives for the respective ASSIs and SACs, it appears that Murlough is successfully meeting the objective relating to maintaining a minimum population size of 84 harbour seals. However, for Strangford Lough, this may not be the case, as the population should be at least 200 adults, with at least 25% of the population being pups. The most recent year that had any notable survey effort was 2014, where the maximum count was 87 adults and 34 pups, which equates to pups making up approximately 28% of the population. Applying a correction factor to account for seals at sea during the count would provide a maximum population estimate of 145 adults.

The variability in results based on the subsets of data analysed does demonstrate the issues associated with variable survey effort over time and space. As such, it is strongly recommended that these results are interpreted with caution. For example, it was not possible to identify, with confidence, whether low maximum counts were attributable to incomplete surveys of areas or were a true representation of a decreasing population.

Recommendations

- The errors in the database identified in this report should be cross-referenced with the datasheets from the field in an effort to maximise the volume of data for future analysis.
- Every effort should be made to ensure that the database is up-to-date and the analyses presented herein should be replicated with the complete counts in order to re-assess population trends.
- A minimum of two counts for each targeted species/demographic should be maintained. Specifically, these are: 1) harbour seal adults during the moult, 2) harbour seal pups during the breeding seasonand3) grey seal adults and pups during the breeding season.
- Surveys should be undertaken in the best possible environmental conditions to allow for the maximum seal count. The most important factors in this respect are to ensure that surveys are undertaken +/- 2 hours from low tide and avoid periods of medium to heavy or prolonged rain.
- Restructuring the database to make it more streamlined and easier to manage would be extremely advantageous for future analysis and would likely result in fewer errors being entered into the database. Specific examples are provided in more detail within the report.
- It is strongly recommended that Northern Ireland provides representation at the Special Committeee on Seals (SCOS), where scientific advice to government on matters relating to seal populations are discussed.

Full report
https://pureadmin.qub.ac.uk/ws/portalfiles/portal/162797935/AE1_18_772548_NI_Seal_Report_Final_2017.pdf